Graduate Theses and Dissertations — Graduate School

January 2013

Multidimensional Signal Analysis for Wireless Communications Systems

Ali Gorcin
University of South Florida, agorcin@mail.usf.edu

Multidimensional Signal Analysis for Wireless Communications Systems

by

Ali Görçin

A dissertation submitted in partial fulfillment
of the requirements for the degree of
Doctor of Philosophy
Department of Electrical Engineering
College of Engineering
University of South Florida

Major Professor: Hüseyin Arslan, Ph.D.
Richard D. Gitlin, Sc.D.
Chris P. Tsokos, Ph.D.
Dmitry B. Goldgof, Ph.D.
Wilfrido Moreno, Ph.D.

Date of Approval:
June 28, 2013

Keywords: Wireless Multidimensional Hyperspace, Elecrospace, Dynamic Spectrum Access, Spectrum Sensing, Signal Identification, Direction of Arrival Estimation, Signal Detection and Estimation, Spectrum Allocation Prediction, Cognitive Radios

DEDICATION

To my family

ACKNOWLEDGMENTS

I would like to thank the committee members for their guidance and help on the development of the dissertation. I would also like to thank to my colleagues at USF who we shared a window of time with me here, to the current and past members of wireless communications and signal processing group at Electrical Engineering Department at USF, and to the staff members of the Electrical Engineering Department at USF for their help and guidance through the time that I've had at USF. During my time in Tampa Bay area, I also had the chance to develop very strong friendship bonds. I would like to express my very warm appreciation and gratitude to them.

TABLE OF CONTENTS

LIST OF FIGURES

ABSTRACT

Wireless communications systems underwent an evolution as the voice oriented applications evolved to data and multimedia based services. Furthermore, current wireless technologies, regulations and the understanding of the technology are insufficient for the requirements of future wireless systems. Along with the rapid rise at the number of users, increasing demand for more communications capacity to deploy multimedia applications entail effective utilization of communications resources. Therefore, there is a need for effective spectrum allocation, adaptive and complex modulation, error recovery, channel estimation, diversity and code design techniques to allow high data rates while maintaining desired quality of service, and reconfigurable and flexible air interface technologies for better interference and fading management. However, traditional communications system design is based on allocating fixed amounts of resources to the user and does not consider adaptive spectrum utilization.

Technologies which will lead to adaptive, intelligent, and aware wireless communications systems are expected to come up with consistent methodologies to provide solutions for the capacity, interference, and reliability problems of the wireless networks. Spectrum sensing feature of cognitive radio systems are a step forward to better recognize the problems and to achieve efficient spectrum allocation. On the other hand, even though spectrum sensing can constitute a solid base to achieve the reconfigurability and awareness goals of next generation networks, a new perspective is required to benefit from the whole dimensions of the available electro hyperspace. Therefore, spectrum sensing should evolve to a more general and comprehensive awareness providing a mechanism, not only as a part of CR systems which provide channel occupancy information but also as a communication environment awareness component of dynamic spectrum access paradigm which can adapt sensing parameters autonomously to ensure robust identification and parameter estimation for the signals over the monitored spectrum. Such an approach will lead to recognition of communications opportunities in different dimensions of spectrum hyperspace, and provide necessary information about the air interfaces, access techniques and waveforms that are deployed over the monitored spectrum to accomplish adaptive resource management and spectrum access.

We define multidimensional signal analysis as a methodology, which not only provides the information that the spectrum hyperspace dimension in interest is occupied or not, but also reveals the underlaying information regarding to the parameters, such as employed channel access methods, duplexing techniques and other parameters related to the air interfaces of the signals accessing to the monitored channels and more. To achieve multidimensional signal analysis, a comprehensive sensing, classification, and a detection approach is required at the initial stage. In this thesis, we propose the multidimensional signal analysis procedures under signal identification algorithms in time, frequency. Moreover, an angle of arrival estimation system for wireless signals, and a spectrum usage modeling and prediction method are proposed as multidimensional signal analysis functionalities.

CHAPTER 1

INTRODUCTION

Wireless communications systems underwent an evolution as the voice oriented applications evolved to data and multimedia based services. Eventually, the progress of wireless technologies and standards from the first generation through the fourth and beyond led to the prevalence of wireless services among daily users triggering an extensive growth on the demand for wireless communications services. Along with the rapid rise at the number of users, increasing demand for more communications capacity to deploy multimedia applications entail effective utilization of communications resources. As a matter of fact, this is a requirement which stems from the limited resources *e.g.*, frequency spectrum, physical limits on communications, *e.g.*, data transmission limitations indicated by Shannon - Hartley Theorem and the characteristics of wireless channel itself. When the current state of the wireless technologies is considered, improvements can be achieved in terms of

- effective spectrum allocation,

- adaptive and complex modulation, error recovery, channel estimation, diversity and code design techniques to allow high data rates while maintaining desired quality of service (QoS),

- reconfigurable and flexible air interface technologies for better interference and fading management, and

- cooperation of these concepts in an environment that they exist along with the present wireless technologies.

Traditional communications system design is based on allocating fixed amounts of resources to the user and does not consider adaptive spectrum utilization. Therefore, when the first item is considered from this point of view, Federal Communications Commission (FCC) frequency allocation chart indicates the scarcity of frequency bands, especially at the Ultra-high frequency (UHF) range for the United States of America and new spectrum allocation auctions can be seen as a straightforward answer to the problem. However, this will be a temporarily solution and the scarcity problems will reemerge by the time as the

1

user numbers grow. Adaptive design methodologies, on the other hand, identify the requirements of the user constantly, and then allocate just enough resources, thus enabling more efficient utilization of the system resources and consequently improve the total capacity utilization. When the spectrum allocations are considered from this point of view, it can be seen that in reality, dynamic usage of the spectrum must be distinguished from the static usage because while the static transmitters such as digital tv signals continuously occupy the spectrum, the dynamic users do not transmit consistently. Therefore, the intermittent utilization of the dynamic users leads to new *communications opportunities*, and can be exploited to access the spectrum. This dynamic spectrum access (DSA) paradigm is one of the main improvement points to achieve efficient frequency spectrum utilization.

Beyond the studies and definitions on radio systems which are computationally intelligent to choose and support multiple variations of wireless communications systems [1], widely accepted terminology to achieve efficient frequency spectrum utilization is introduced through software defined radios (SDR) and later on cognitive radios (CR) by Joseph Mitola III [2]. Cognitive radio technology introduces secondary users to the wireless spectrum for opportunistic spectrum access (OSA) and allocation of secondary users should be conducted in such a reliable and flexible way that the communication of licensed (primary) users will not be effected or there will be no loss at the quality of the service due to secondary access. Therefore, spectrum sensing feature of CRs achieves the detection of licensed or primary users (PUs) via digital signal processing methods such as energy detection, matched filtering, covariance matrix based algorithms, cyclostationary feature detection, and multi-taper spectral estimation [3].

In the literature, spectrum sensing concept of CR is taken into consideration only from the aspect of efficient spectrum usage. This approach limits the possibilities only into time, frequency, and space domains. Conventional single dimension analysis tools working in these domains can provide limited characteristics of the analyzed signal. However, multidimensional analysis approach of signal intelligence investigates multiple signal attributes in once by using projection onto different domains. For instance, time-frequency representation (TFR) provides the details about the temporal spectral components of the signal contents. On the other hand, there are other dimensions that need to be explored further for spectrum opportunity. For example, the code dimension of the spectrum space has not been explored well in the literature. Therefore, the conventional spectrum sensing algorithms do not know how to deal with signals that use spread spectrum and time or frequency hopping. Similarly, angle dimension has not been exploited well enough for spectrum opportunity. It is assumed that the users are transmitting in all directions. However, with the recent advances in multi-antenna technologies, e.g. beam forming; multiple users can be multiplexed into the same channel

2

at the same time in the same geographical area. This also creates new opportunities for spectral estimation, where not only the frequency spectrum but also the angle of arrivals might need to be estimated. With these new dimensions, sensing only the frequency spectrum usage falls short. The radio space with the introduced dimensions can be defined as "a theoretical hyperspace occupied by radio signals, which has dimensions of location, angle-of-arrival, frequency, time, and possibly others" [133]. This hyperspace is called electrospace, transmission hyperspace, radio spectrum space, or simply spectrum space by various authors, and it can be used to describe how radio environment can be shared among multiple (primary and/or secondary) systems [6]. An immediate consequence of introducing multidimensionality into wireless communications is to unveil different characteristics of radio signals. Thus, the knowledge that could be obtained from the received signal can be increased through multidimensionality. As in illustrated in Figure 2, multidimensionality allows one to see further details of the electrospace. As a consequence, additional dimensions can be used in distinguishing signals which cannot be separated from each other through the use of methods operating in already existing dimensions. One of the very well-known examples is spread spectrum technology. By introducing code as a new dimension, users who use the same portion of the spectrum at the same time can still be separated from each other.

1.1 Motivation

Spectrum sensing is perceived as a feature that solely provides whether the primary user exists in a communication channel or not in time or frequency domains due to its initial definition of scope as an information provider about the channel[1] access status of primary users to enable secondary access [4]. Extension of sensing to the wideband scenarios and the final decision stage outputs of the current wideband sensing techniques [34] also prove this perception. However, FCC Spectrum Policy Task Force (SPTF) report [5] recommends the improvement of wireless throughput by achieving signal orthogonality over a range of dimensions grouped under a domain called as *spectrum hyperspace* [6]. Spectrum hyperspace includes but not limited to frequency, time, space, power, polarization, angle of arrival, and code dimensions. Secondary access can be extended to these dimensions as some of the other communications opportunities are illustrated in Fig. 1.1. Moreover, Multi-dimensional signal analysis can provide powerful signal processing tools for CR and SDR signal analysis including waveform awareness and feature extraction applications. Signal processing methodologies can offer many new aspects of analyzed signal, channel and transceiver.

[1]channel term here refers to a frequency band of a certain bandwidth as defined in [4].
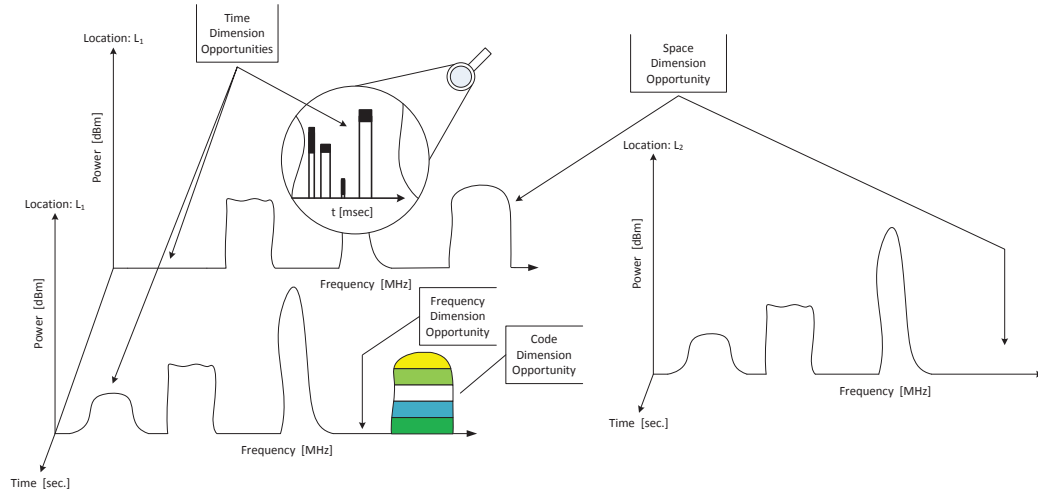
Figure 1.1: Spectrum hyperspace opportunities

Utilization of the dimensions of the hyperspace, to improve the throughput, not only requires the spectrum sensing methods to decide whether primary users exist in the channel or not but also to identify the primary user waveforms (*e.g.*, the air interface parameters, burst structures, chip rates etc.) and the employed radio access techniques without going to the demodulation stage [7, 8]. In fact, International Telecommunication Union Radiocommunication Sector (ITU-R) report [9] on definitions of SDR and CR indicates that CR should "dynamically and autonomously adjust its operational parameters and protocols according to its obtained knowledge in order to achieve predefined objectives". Moreover, ITU-R reports on cognitive radio systems in the land mobile services and CR systems specific for IMT systems indicate use of CR technology to improve the management of assigned spectrum resources, consider CR as the enabler of OSA amongst wireless network operators without any prior agreements, and propose CR as the controller of the terminal reconfiguration in heterogeneous networks [10, 11]. One example that will benefit from these definitions is the channel usage prediction methods such as time domain opportunistic channel allocation method which achieve DSA by exploiting the idle periods between bursty transmissions based on the signal identification information [12]. Another case is the maximum likelihood (ML) signal direction of arrival estimators. Instead of being unknown stochastic processes, if the incident signals are known, useful DOA estimation properties can be derived peculiar to ML estimators [13]. Therefore, CR should be aware of the communications environment as much as possible also to achieve the rest of the goals itemized above. To this end, sensing procedures should provide the information about the wireless signals in the communications medium for CR to adjust the transmission parameters adaptively [14].

4

Reconfigurability and awareness issues are also addressed in the context of the transparently reconfigurable ubiquitous terminal (TRUST) project, and a mode identification and switching concept is introduced. Mode identification can be conducted blindly only by the radio itself or in an assisted manner in which some information is available [15]. The mode identification concept defined in the TRUST project later on extended to initial mode identification and alternative mode monitoring methods in [16] and identification of radio access technologies (RATs) is achieved based on received signal strength indicators. On the other hand, a configurable receiver architecture that classify the wireless signals based on bandwidth estimation with the radial basis function neural networks is proposed in [17]. Classification of overlapping air interfaces based on a distributed approach and implementation of pattern recognition techniques is achieved in [18]. An air interface identification approach based on cyclostationary feature detection is proposed in [19]. Pattern classification and machine learning methods are combined to classify wireless signals based on their characteristics such as burst size, hopping pattern, and carrier number i n [20]. The proposed methodology introduces learning and prediction functionalities therefore, it is possible to classify new signals and extend the communications capability of the proposed CR based system. Machine learning techniques are also employed for RAT recognition in [14]. Spectrum power measurements with low temporal resolution are utilized to achieve supervised classification of the RATs.

Whether under the concept of CR or not, instead of providing a comprehensive and unifying approach, the research on extracting more information from the communications medium focuses on some different and specific aspects of adaptiveness and awareness requirements. On the other hand, even though spectrum sensing can constitute a solid base to achieve the reconfigurability and awareness goals described, current technical level of sensing cannot satisfy the requirements [7, 21]. Therefore, based on the defined scope of more adaptive, aware and intelligent communications systems, spectrum sensing should evolve to a more general and comprehensive awareness providing mechanism, not only as a part of CR systems which provide channel occupancy information but also as a communication environment awareness component of DSA paradigm which can adapt sensing parameters autonomously to ensure robust identification of the signals over the monitored spectrum. Such a perspective will lead to recognition of communications opportunities in different dimensions of spectrum hyperspace, and provide necessary information about the air interfaces, access techniques and waveforms that are deployed over the monitored spectrum to accomplish adaptive resource management and spectrum access. Therefore, one main part of the thesis will deal with the signal identification feature of that is defined under the dynamic spectrum access concept for efficient spectral utilization.

5

1.2 Signal Identification for Dynamic Spectrum Access

We define signal identification as a procedure, which not only provides the information that the spectrum hyperspace dimension in interest is occupied or not, but also reveals the underlaying information regarding to the parameters, such as employed channel access methods, duplexing techniques and other parameters related to the air interfaces of the signals accessing to the monitored channels. To achieve signal identification, a comprehensive sensing, classification, and detection approach is required and in this thesis, we propose the signal identification block diagram given in Fig. 1.2. along with signal identification algorithms in time, frequency, angle of arrival domains and a spectrum usage prediction method to satisfy these requirements.
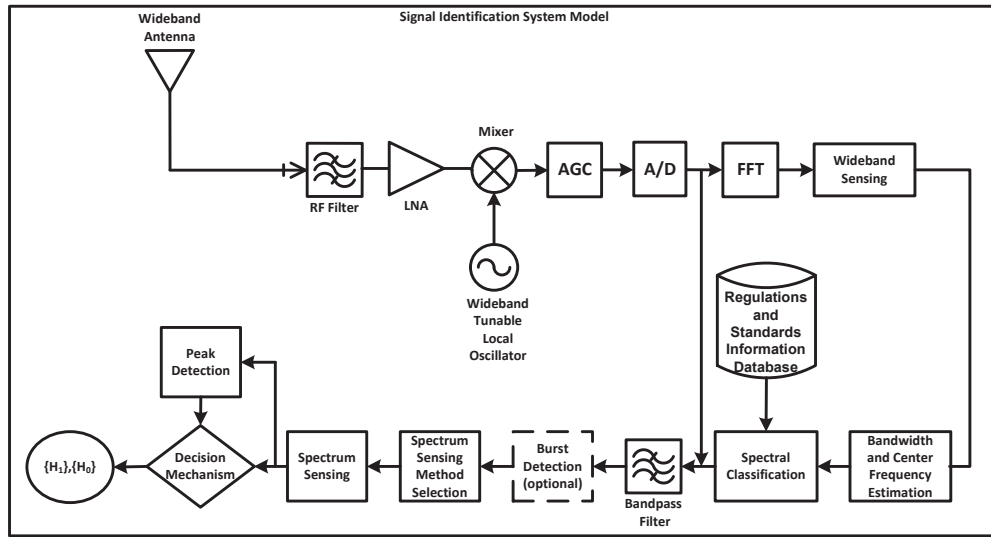
Figure 1.2: Signal identification block diagram

The features of the analog to digital converter following the wideband radio frequency (RF) front-end in Fig. 1.2, have crucial importance for the performance of the signal identification procedure. Signals that have high power levels are mixed with very low power signals in the spectrum. Therefore, digitization process should have the capability to represent a wide dynamic range in the digital domain. This requirement can be satisfied by the employment of high resolution ADC circuity such as 12 and 16 bit converters proposed in the literature [22, 34], but the wideband nature of the conversion also demands high sampling rates. To overcome the difficulty of balancing the resolution and speed requirements, implementation of notch filters at the RF front-end to isolate high-power signals and sampling sub-Nyquist rates are proposed. Both approaches

assume certain information such as frequency bands of high power signals and spectral occupation rate are available beforehand. In our work, we assume that a wide dynamic range is available at the mixer input to achieve high level input power sensitivity, but also on the other hand, an automatic gain control (AGC) block is allocated before the ADC block to enable to the resolution adjustment of the conversion block. Therefore, balance between resolution and speed can be achieved in an adaptive manner.

The received wideband signal is composed of noise and various signals which employ different access techniques and comprise unique characteristics inherited from the definition of their technologies *e.g.*, standards, air interfaces. These features have projections over the dimensions of the spectrum hyperspace and can be used to identify these signals however, a certain level of abstraction is required forehand to achieve efficient detection and identification. When the dimensions listed in the context of hyperspace considered, both channel assignments over the wireless spectrum which is managed by the regulatory organizations and standard based carrier spacings imply the frequency as the initial dimension to start the separation of the signals. Therefore, frequency domain representation of the wideband signal is obtained through fast Fourier transform (FFT) at the next stage of the signal identification procedure. It should be noted that, FFT is also the initial block of wideband sensing algorithms such as multiband joint detection and wavelet detection. Thus, based on the selected wideband sensing algorithm at the next stage, FFT block shown in Fig. 1.2 can be assumed as a part of the wideband sensing process.

Wideband sensing stage provides the information of the channels which have activity over the wideband spectrum, however, the binary decision process behind wideband sensing does not provide any further information about the nature of the activity. For instance, while multiple users can access to a single channel with burst transmission, there can be an only one user in a given channel using direct-sequence spread spectrum (DSSS) modulation or a single user can access multiple channels. Moreover, wireless signals can overlap in frequency, in time or in both dimensions leading to interference as shown in Fig. 1.3. Therefore, before starting any identification procedure a certain level of signal separation should be achieved. Bandwidth and center frequency estimation, bandpass filter and the following optional burst detection blocks aim to conduct this separation operation. For instance, if the signals are overlapped in time, the bandwidth and center frequency estimation block, along with the bandpass filter that operate over the estimated band of interest lead to elimination of the time-domain components of other channels. If there are still multiple users or techniques accessing the channel, before the selection and the execution of the spectrum sensing method, burst detection can be applied to the filtered data. On the other hand, if the sensing procedure will be effected from spectral overlap, filtering and the burst detection procedures can provide spectral distinction.

7
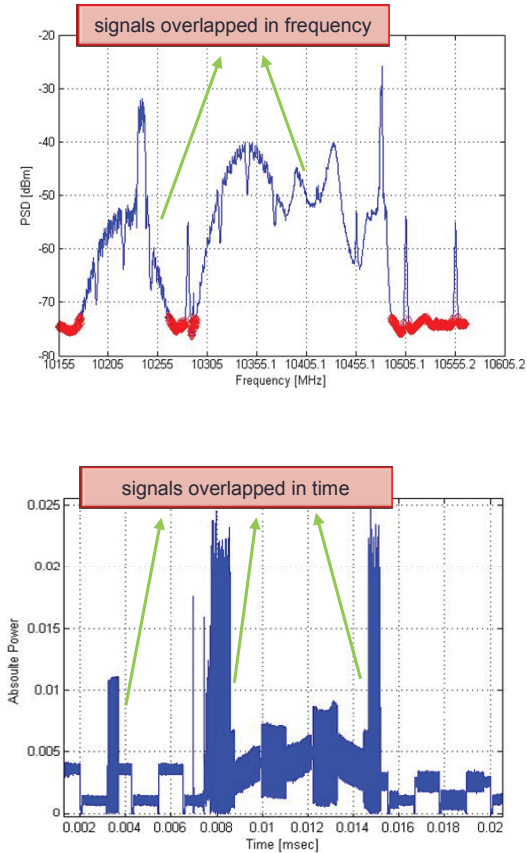
Figure 1.3: Interference in frequency and time

Spectral classification block, in between the signal processing blocks simply compares the estimated spectral information with the regulatory and wireless standard based information to decide the candidate signals which can be utilizing the channel that the communications activity is detected by the wideband sensing stage. This comparison process has vital importance for the signal identification procedure, because it leads to the selection of a method from a set of spectrum sensing applications which will lead to direct identification of the signal or the signals accessing to the channel.

One classification of the spectrum sensing methods considers the signal parameters that are involved in the sensing process and classifies the spectrum sensing methods as either coherent or non-coherent [22]. For instance, between matched filtering, cyclostationary feature detection, and energy detection, first two are coherent detection methods with better detection probability than non-coherent energy detection. However, the coherent detectors require a priori information. Matched filter provides optimal detection by maximizing signal to noise ratio (SNR) but requires demodulation parameters. Cyclostationary feature detection can

detect random signals depending on their cyclic features even if the signal is in the background of noise but it requires information about the cyclic characteristics. But more importantly, while non-coherent methods such as energy detection is applied by setting a threshold for solely detecting the existence of the signal, coherent sensing methods can lead to signal identification.

Table 1.1: Identification capabilities of spectrum sensing techniques

Sensing Method	Dimension	Sensing Parameter	Result
Energy Detection	time/frequency	signal energy	Detection Only
Matched Filter	time	time-domain signal structure and characteristics *e.g.*, pulse shape, package format, guard time, burst duration	Detection and Identification
Cyclostationary Feature Detection	frequency/code	chip rate,data rate,cp size, symbol duration, modulation type, carrier spacing and number	Detection and Identification
Statistical Tests	time	signal distribution	Detection Only
Entropy Based	frequency	signal entropy	Detection Only
Eigenvalue Based	time/ angle	signal eigenvalues direction of arrival	Detection Only
Autocorrelation	time	cyclic prefix, midamble preamble, pn sequence, and others	Detection and Identification
Multitaper Based	frequency	signal energy	Detection Only
Wavelet	frequency	signal energy	Detection Only
Multiband Joint Detection	frequency	signal energy	Detection Only

Table 1.1 provides an extensive set of sensing methods classified based on and ability of identification. Therefore, the introduced signal identification procedure can select the sensing method which will lead to identification of the signals in the given spectrum depending on the information acquired from the wideband signal received. For example, if the spectral classification indicates the probability of DSSS signals in the given channel, cyclostationary feature detection can be employed for identification purposes and in this case, peak detection algorithm will search for a certain range of frequencies to make a decision. In fact, in a specific scenario, if only the channel occupancy information is extremely important, proposed procedure can be operated with a non-coherent sensing method to guarantee detection as much as possible.

The statistical tests listed in Table 1.1 include but not limited to Anderson-Darling test, student's t-test, Kolmogorov-Smirnov test, and tests are based on statistical covariances. The last two items are also wideband sensing techniques which provide sensing decision directly in contrary to the sweep tune and filter bank based wideband sensing techniques which require another sensing method at the final stage. Modulation

classification is kept out of scope of this study because same modulation type and order can be employed by different wireless signals in the spectrum. Therefore, identification in the modulation dimension introduces its own challenges. An example signal identification scenario based on single carrier and multi-carrier distinction and identification which also leads to parameter estimation for multi-carrier systems is illustrated in Fig.
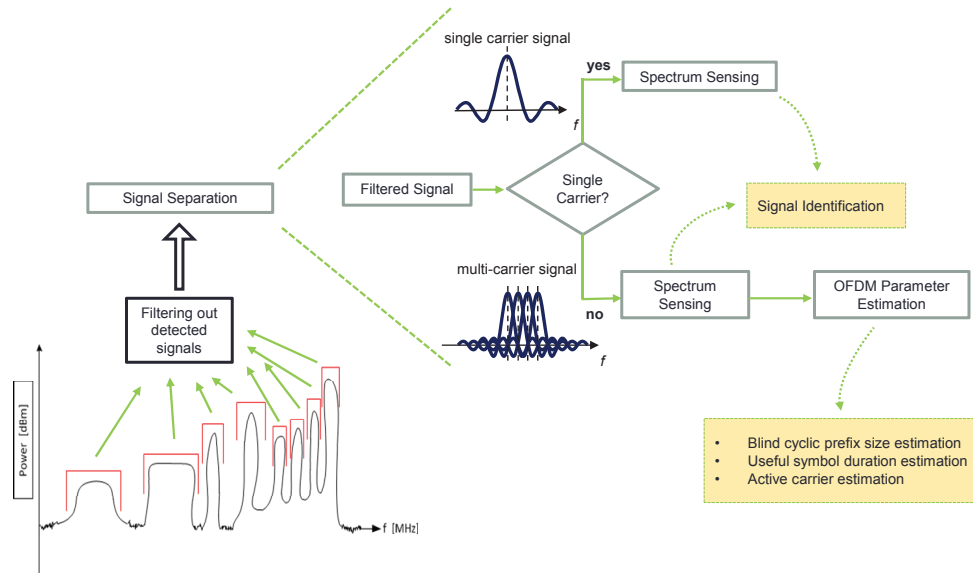
Figure 1.4: Signal identification scenario
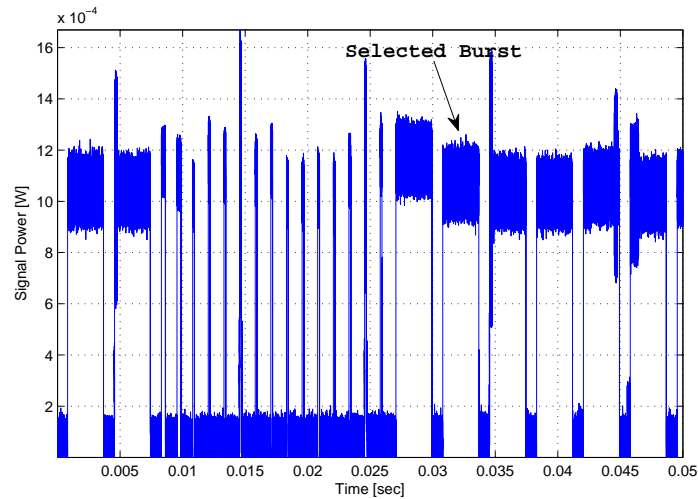
Figure 1.5: Recorded ISM band (time signal)

One alternative approach to the proposed signal identification procedure could be considering the procedures in time domain and designing the blocks after the ADC assuming burst transmission in the moni-

10

tored channels. Under these assumptions, we conducted Bluetooth based communications beside the ongoing communications activity and recorded the whole 80 MHz band from 2.4 GHz to 2.48 GHz with the wideband receiver available in our laboratory. Fig. 1.5 shows the time domain data of 50 milliseconds of recording. When the PSD of the burst marked in the figure is plotted, it is identified as a Bluetooth signal centered around 40 MHz. The 54 bits fixed header of the Bluetooth signals makes it suitable for data rate estimation via cyclostationary feature detection. However, the resulting cyclic spectrum of the selected burst is given in Fig. 1.6 and does not reveal the data rate information expected. On the other hand, when the spectral parameters are estimated in the first place, and the bandpass filter is applied to leave only the time domain components unique to estimated frequency range, final sensing process based on cyclostationary feature detection leads to the dominant peak indicating data rate of Bluetooth signal as shown in Fig. 1.7. Therefore, in a wideband sensing scenario, if the burst detection is conducted without filtering each signal, some other dominant frequencies over the detected burst may overshadow the features of the signal that would normally lead identification.
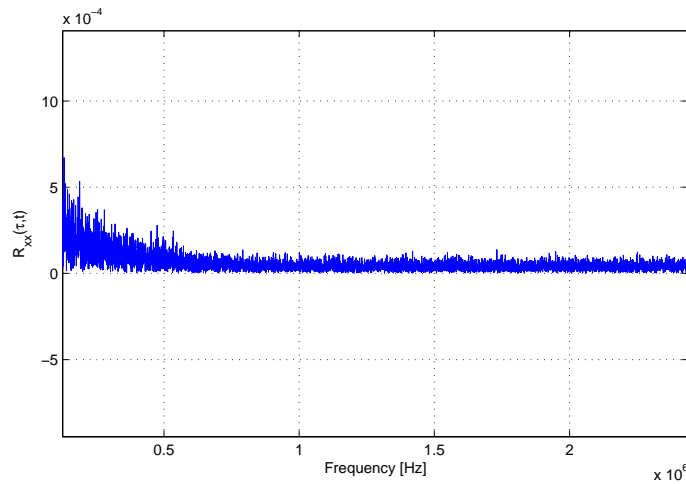
Figure 1.6: Cyclic autocorrelation of detected burst

It is clear that contemporary and future wireless communications systems should better understand the electro-space in order to improve their communications. However, introducing new dimensions into electro-space is not solely enough to establish the entire framework of signal intelligence. In each dimension of electrospace, there are numerous characteristics and issues to be considered as well. Radio propagation channel characteristics, interference and noise temperature, radio's operating environment, user requirements and applications, other available networks (infrastructures) and nodes, local policies and other operating

11
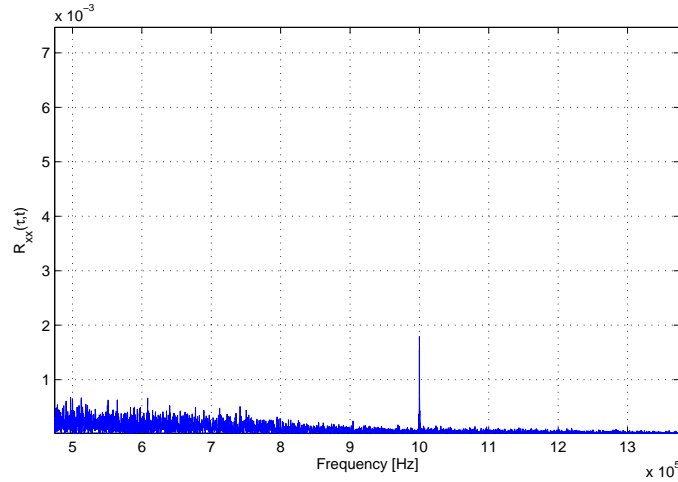
Figure 1.7: Cyclostationary feature detection after filtering

restrictions are just few to name. Moreover, based on these dimensions and items, future wireless communications systems need to adapt their transmission parameters intelligently to achieve better performance. Hence, signal intelligence also requires the evaluation of the items within the dimensions to provide better adaptation for future generation wireless systems. The general research domains of multidimensional signal analysis and the specific areas where the contributions are achieved can be seen in Fig. 1.8.

1.3 Challenges of Multidimensional Signal Analysis

Beside the signal processing constraints of wideband sensing, rapid changing communications environment requires the multidimensional signal analysis to be conducted as quick as possible. Gaining extra knowledge about the communication traffic and extending spectrum sensing to the dimensions of the electro hyperspace also bring the extension to the set of detection, classification, and sensing algorithm along with additional signal processing requirements such as bandpass filtering. Sequential application of signal identification procedures to the monitored wideband spectrum also leads extended identification process and time. Implementation of parallel filtering architectures such as filter banks can alleviate the identification latency, however, the introduced complexity to the identification system should be quantified carefully. On the other hand, signal identification processes can also benefit from a cooperative communication architecture by distributing the work load between the nodes in communication. Collaboration scenarios similar to the spectrum sensing can be discussed for the signal identification as well.

12
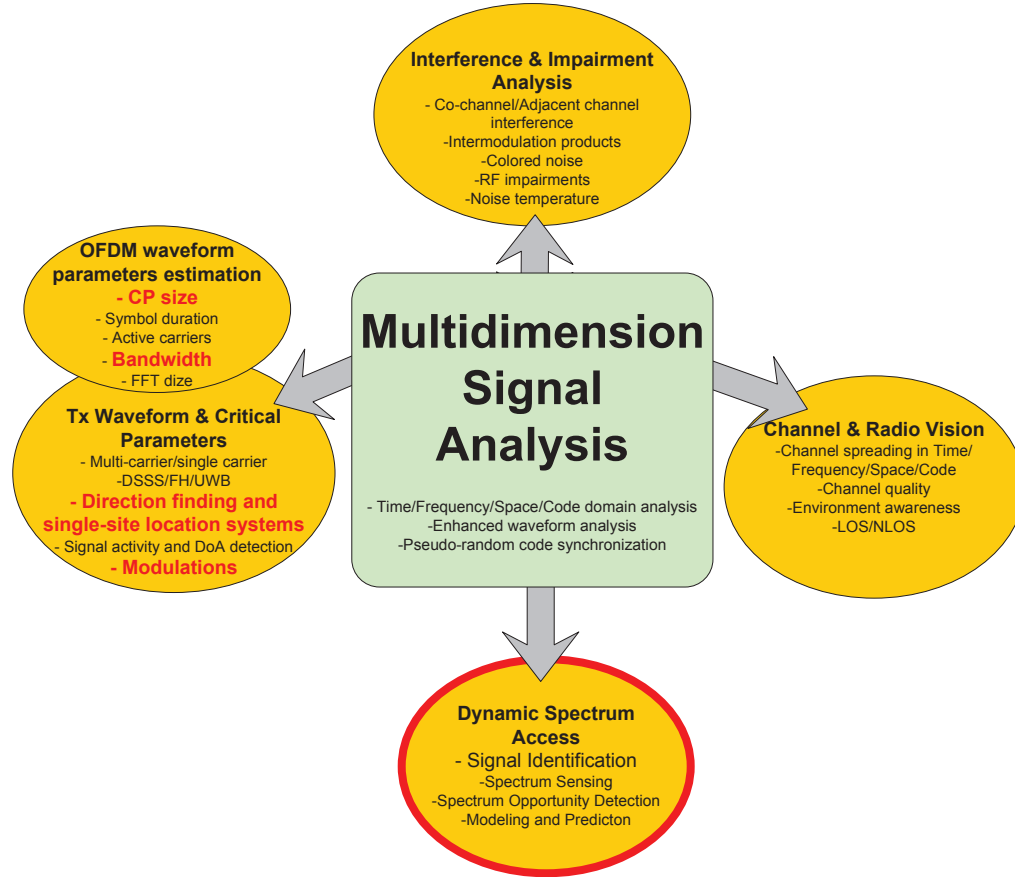
Figure 1.8: Research domains of multidimensional signal analysis

1.4 Application Areas for Multidimensional Signal Analysis

One of the application areas for the proposed system is the detection, identification and estimating the location of illegal emitters. In this context, when the illegal transmissions are encountered, multidimensional signal analysis can provide information such as the signal type, signal arrival of direction which can lead the regulatory officials and field engineers to the source of abusive usage. Beside that, there can be some unintentional emissions in the communications environment caused by uncalibrated or broken access point or base station circuitry such as power amplifiers and oscillators. It can be problematic to find the source of such transmissions due to the number and distribution of the transceivers over the operation area. However, signal identification algorithms can directly find or quickly reduce the number of candidate transmitters to a few. An illustration of the potential application areas can be seen in Fig. 1.9.

Multidimensional signal analysis can also lead to information regarding to the co-channel, adjacent channel, narrowband, and wideband interference sources. Interference monitoring applications can benefit

13
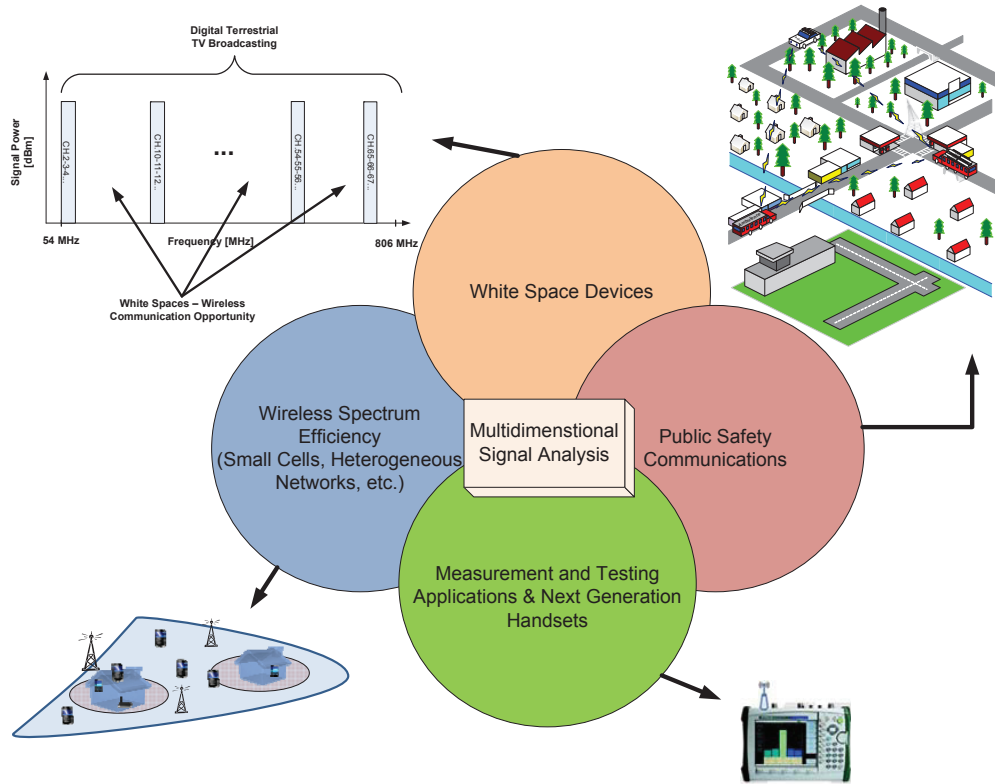
Figure 1.9: Multidimensional signal analysis applications

from methods such as filter bank based sensing, signal autocorrelation variance estimation, polarization correlation estimators of magnitude variance of the received signals and sweep tuned sensing. IEEE 802.16 Broadband Wireless Access Working Group working on the interference detection and measurement indicates that "Based on the above conditions, an accurate detection and measurement of the intranet interference requires specific interference patterns to be evaluated across a given cluster of cells subject to the interference detection and measurement". Even though this document is standard specific, it defines the "interference pattern" concept which binds the modeling and prediction efforts to the interference detection problem. Thus, interference analysis methods can benefit from the outputs of the multidimensional signal analysis procedures as the spectrum modeling efforts.

The proposed procedure can be used for numerous governmental, commercial, and military applications. The potential applications are frequency management, security and surveillance, interference management, geolocation of target emitters. Therefore, multidimensional signal analysis can be beneficial to frequency regulation agencies, public safety agencies, cellular operators, broadcasters, transportation agen-

14

cies for navigation and communication, and law enforcement. One very important field that multidimensional signal analysis methodology can contribute is the public safety communications. For instance, emergency call services such as enhanced 911 (E911) are designed to provide improved service including instant delivery of the victims location information to the local Public Safety Answering Point (PSAP). Taking the requirements of the 911 services into consideration, wireless service providers took incentive to employ precise location estimation techniques based on their network capacities and structures. Even though these systems are very helpful for limited number of calls and specific events, it is not possible to maintain such services under extreme cases affecting an important section of the population living in an area. The disasters such as Pakistan and Australia vast area floods, California wild forest fires and earthquakes in China and Japan showed that the first hours and days are very crucial to save the lives of the victims. In this important period of time, the victims who are scattered around the disaster area would be looking for a way to communicate to get help. However, the wireless network infrastructure can be damaged during the extreme situation. Beside that, if the victims are calling to reach the 911 services at the same time, congestion due to the capacity limit of either network or PSAP can result latency or it may not even be possible to provide most of the victim location information to the public safety officers in a timely manner. The signals transmitted by the devices of the victims can be detected, tracked and the direction of the signals can be estimated by the deployed ad-hoc signal identification hardware located around the disaster area. Moreover, the signal detection, location estimation and direction finding algorithms can be developed in a flexible manner and these technologies can be employed by the first responders to detect and locate victims even for cases in which the original core wireless communications network is down. The first responder teams and their equipments can be used to detect the victim transmission which can lead to locate the victim transmitter via direction finding and location estimation algorithms.

1.5 Dissertation Outline

1.5.1 Chapter 2: OFDM Signal Identification and Blind Cyclic Prefix Size Estimation Under Multi-path Fading Channels

Modulation identification is an important part of wireless communications systems *e.g.*, blind receivers can benefit from the methods that can identify the modulation of the received signals without a priori information. Moreover, distinction of orthogonal frequency-division multiplexing (OFDM) systems from single carrier systems is highly important for adaptive receiver design algorithms for CR systems. OFDM signals exhibit Gaussian characteristics in time domain in contrast with the single carrier signals. However,

15

when the wireless communications considered, Gaussianity of the received samples is affected from the channel impairments along with the frequency, phase offsets and sampling mismatch. In this chapter, we analyzed how the time-domain Gaussianity of fourth order cumulants of OFDM signals is affected under these conditions. A general chi-square constant false alarm rate Gaussianity test which employs estimates of cumulants and their covariances is adapted to the specific case of OFDM signals. A parametric simulation analysis which investigates the performance of the proposed method by the changes in the parameters such as signal to noise ratio, number of symbols, and modulation order is provided. The performance of proposed method is compared with moment based tests as well.

Cyclic prefix (cp) is a useful feature of OFDM systems which helps to mitigate the effects of inter symbol interference and provide simple synchronization. Estimation of cp size can help adaptive communications systems and especially to the blind receivers. Therefore, in this chapter we propose a blind cp size estimation algorithm which depends on an initial estimate of the cp and calculates the estimation error iteratively symbol by symbol.

1.5.2 Chapter 3: A Two-Antenna Single RF Front-End DOA Estimation System for Wireless Communications Signals

Beside the efforts to improve the wireless systems throughput by the DSA methodology, both adaptive beamforming methods and interference management systems have important potential to improve the performance of wireless communications systems in terms of bit error rate, interference rejection, throughput, and multipath mitigation. The initial requirement of the these systems is the direction of arrival information of the wireless signals or interference sources. When this information is available, beamforming methods can be implemented accurately and interfering signal direction information not only leads to the optimization of adaptive interference mitigation and rejection techniques but also helps to the wireless network managers to find and isolate the interference sources. Direction of arrival (DOA) estimation methods can provide these information, however, these systems suffer from high complexity, computational and production cost, bulky size preventing mobility, and inflexibility which prevents prevalence of these systems over the whole wireless spectrum. In this chapter, a solution to these problems which benefits from the advantages of switched antenna systems along with the time-variant sequential sampling process is proposed: a two-antenna, single radio frequency (RF) front-end measurement system which adjusts the antenna spacing adaptively and achieves multiple measurements at different locations by shifting the antenna tuple together as a single entity. Proposed system introduces an extension to the total measurement time, however, when compared to

16

the DOA estimation systems which have separate RF front-end for each antenna, the system has moderate complexity and size. A measurement setup is developed and performance analysis of the proposed system for extensive set of wireless standards and measurement parameters including line of sight and non-line of sight conditions is given. The angle estimation performance of the proposed system is compared with that of pseudo-Doppler DOA estimation system as well. The measurement results indicate the feasibility of the proposed system for wireless communications.

1.5.3 Chapter 4: An Autoregressive Approach for Spectrum Occupancy Modeling and Prediction Based on Synchronous Measurements

As a part of DSA efforts to improve wireless access efficiency, spectrum monitoring methods bring a statistical approach to the problem of efficient spectrum allocation. The utilization of spectrum is related to the dynamic usage which is dependent on the parameters like transmitter power, antenna types, location information of the transmitters and local environment effects. Therefore, spectrum monitoring methodologies provides statistical models of the utilization of the frequency spectrum as a function of time, space, frequency, and angle dimensions of the spectrum hyperspace. Monitoring activities are conducted either by classical measurement methodologies including the equipments such as spectrum analyzers, antennas, data recorders and computers or by using the data collection equipments like wireless sniffers [23]. The spectrum monitoring methodology aims to:

- Collect data to build a statistical model for the frequency band usage,

- Investigate the usage variation of signals in different environments, times etc.,

- Investigate the possibilities of congestion of signals,

- Collect the information necessary for effective regulations of new bands like 5 GHz band.

Spectrum monitoring approach requires robust and efficient spectrum detection, estimation, and sensing methods to conduct the tasks listed above. Moreover, these methods can benefit from the modeling and prediction of the wireless spectrum usage. Markovian, regressive and other approaches are introduced for time or frequency domain channel modeling however, the research on the spectrum allocation methods indicates that location information has also an important influence on the spectrum occupancy characterization. In this chapter, a linear autoregressive prediction approach for binary time series is employed to investigate channel occupancy prediction performance based on spectrum measurements conducted in four different locations synchronously. Through the modeling procedure, dependency in frequency domain is also taken into

17

consideration by modeling the adjacent frequency bands together. The model order is selected based on mean residual magnitudes and Akaike information criterion, mode order parameters are tabulated, and comparative prediction analysis considering the observation time is given for each location. The performance of the proposed linear modeling method is also compared with continuous-time Markov chain modeling in one of the locations.

1.5.4 Chapter 5: Template Matching for Signal Identification in Cognitive Radio Systems

The unique signatures or specific features of wireless signals can be utilized to improve the performance of spectrum sensing by identifying the signals. Moreover, spectral efficiency can be improved by achieving signal orthogonality in different domains such as code, polarization and location beside the frequency and time. However, such methods assume the types of the signals of interest to be known. In this chapter, template matching method is proposed as a new spectrum sensing technique to identify the wireless signals based on the spectral signatures in the spectrum. In contrary to the original template matching approach, the number of templates to be kept in the database is limited to one abstract signal for each signal type. The templates are constructed from the abstracts and scaled based on the template matching parameters. Two new metrics are introduced for signal identification method proposed. The performance of proposed metrics are also compared with that of energy detection for wireless fading channels. Identification of the signals with the similar signatures are discussed as well.

1.5.5 Chapter 6: A Recursive Signal Detection and Parameter Estimation Method for Wideband Sensing

Opportunistic spectrum access feature of cognitive radio systems introduces techniques to improve frequency underutilization of wireless spectrum. One of the techniques for detecting the unused bands in multi-channel scenarios is the energy detection for which selection of the threshold defines detection performance. Assumption of stationary noise over wide bands becomes problematic from the aspect of detection reliability and selection of the threshold procedure is also affected. On the other and, when the multiple channel monitoring is considered, a good estimation of signal bandwidth and center frequency can lead to robust initial classification and signal identification. Therefore, a signal detection and parameter estimation approach which recursively estimates the noise floor and classifies the signals is proposed as a solution to the threshold selection and signal detection problem.

CHAPTER 2

OFDM SIGNAL IDENTIFICATION AND BLIND CYCLIC PREFIX SIZE ESTIMATION UNDER MULTIPATH FADING CHANNELS

Modulation identification has always been a part of communications surveillance systems and electronic warfare, however gained more importance with the adaptive communication systems[1]. Seamless and efficient communications should be achieved between a wide variety of communications systems which may employ different modulation techniques. Therefore, simple, robust, and fast modulation recognition methods are required at the implementation of adaptive and intelligent receivers. Blind receiver design algorithms and the signal transmission procedures at the transmitter can also benefit from the modulation information [47].

Orthogonal frequency-division multiplexing (OFDM) is a multi-carrier (MC) multiplexing scheme which maintains adaptive communications features by employing sub-carriers in a flexible way. Deployments of OFDM based systems are increasing rapidly and distinction of OFDM signals from the single carrier (SC) signals is an important issue for contemporary communications systems. Modulation identification or recognition methods for OFDM systems can be classified into two of groups; non-coherent statistical methods which do not require any a priori information in general, and coherent techniques which include maximum likelihood (ML) modulation classifiers along with other methods that depend on the characteristics of the OFDM signals which are assumed to be known to the receiver. Statistical methods mostly depend on high order statistics (HOS) of cumulant or moment estimates of the received signals. The background of cumulant based modulation classification laid down by [48] for fourth and sixth order cumulants. Later, fourth order cumulants are adapted for OFDM modulation identification [49–51]. Moreover, fourth order moments of OFDM signals are combined with the amplitude estimation to improve signal detection in [52]. On the other hand, support vector machines in combination with specific fourth-order cumulants are used for the same purpose in [53]. Tabular values of high order moments which were implemented for SC modulation identification in [54] are adapted to a minimum mean-square error (MMSE) estimator for OFDM signals in [55].

---

[1]The content of this section is publishes in [65]. Copyright for these publications can be found in appendix B.

When the coherent techniques considered, the ML modulation classification algorithms are known with better estimation results when compared to statistical methods however they suffer from computational complexity and require channel estimation [56]. Bootstrap technique is also introduced as a pattern recognition based method in [57]. A wavelet transform algorithm is proposed to extract the transient characteristics of OFDM signals in [58]. On the other hand, time-frequency representation of the signals is employed to distinguish OFDM signals from SC frequency-shift keying (FSK) and phase-shift keying (PSK) signals in [59]. OFDM signals have unique second order cyclostationary features and a feature extraction algorithm based on the magnitude of the cyclic cumulants of OFDM signals is implemented in [60]. An analysis and comparison of second order cyclostationary, matched filter, MMSE, and normalized kurtosis methods can also be found in [61].

OFDM signals also exhibit time-domain Gaussianity. This is due to fact that the assignment of random data over orthogonal sub-carriers in a simultaneous way can be assumed as a composition of large number of independent, identically distributed (i.i.d.) random variables and central limit theorem implies Gaussian distribution for large enough sets of data. A Gaussianity test based on empirical distribution function is introduced for OFDM systems in [62]. On the other hand, a general chi-square constant false alarm rate (CFAR) Gaussianity test based on the estimates of the third and fourth order cumulants [63] is implemented for OFDM signals without considering the channel effects in [64].

In this chapter, a comprehensive analysis of the fourth order cumulants for wireless OFDM systems is conducted by taking the wireless channel and other impairments into consideration [65]. Our analysis shows that channel coefficients have significant influence on the test statistics along with the other impairments such as frequency offset, phase offset due to sampling mismatch and other factors. Secondly, considering all combinations of possible lags for cumulant estimations is a computationally consuming process. For the peculiar case of OFDM signals, inclusion of certain lags in the analysis will be sufficient to retain the Gaussianity. Therefore, we provided the fourth order cumulant equations for OFDM signals. Moreover, the proposed method requires the computation of the estimate of the covariance matrix of fourth order cumulants and this is a complex and detailed operation. However, this process is reduced down to three particular equations in case of OFDM signals. The only parameter required is the symbol duration which determine the degree of freedom of the test. The numerical values that satisfy the confidence levels for correct detection can be found iteratively thus the test can become fully blind.

The proposed OFDM signal model is defined in Section 2.1. The fourth order cumulant expressions for OFDM signals under wireless fading channels, the Gaussianity test, and the decision mechanism are

20

discussed in Section 2.2. The estimates of the covariances of the cumulants are derived in the Appendix. The parametric performance analysis of the proposed Gaussianity test is given in Section 2.3 by taking the parameters such as modulation order, SNR, and number of symbols into consideration for FSK, PSK, and quadrature amplitude modulation (QAM) SC signals sequentially.

2.1   Signal Model

Inverse discrete Fourier transform (IDFT) is employed by OFDM systems for transmission. The baseband continuous-time OFDM signal is given by

$$x_m(t) = \sum_{k=1}^{K} S_m(k) e^{j \frac{2\pi \eta(k)t}{T_D}} \qquad -T_G \leq t < T_D, \tag{2.1}$$

where j at the exponential term is the imaginary unit, η is the set of K subcarriers in total, $S_m(k)$ is the mth OFDM data symbol which is transmitted at the kth sub-carrier from the set of $\eta(k)$, T_D is the useful data duration, T_G is the cyclic prefix (CP) duration, and the total OFDM symbol duration is $T_S = T_D + T_G$. The transmitted total signal can be written as

$$x(t) = \sum_{m=-\infty}^{\infty} x_m(t - mT_S). \tag{2.2}$$

The signal is modulated after digital analog (D/A) conversion and passed through mobile radio channel. The channel can be modeled as a time-variant linear filter

$$h(t) = \sum_{i=1}^{L} h_i(t)\delta(t - \tau_i), \tag{2.3}$$

where L is the number of taps and τ_i is delay for each tap. It is assumed that the taps are sample spaced and the channel is constant for a symbol but time-varying across multiple OFDM symbols. Therefore, baseband model of the received signal after down conversion also considering the channel model given in (2.3) becomes

$$y(t) = e^{j\theta} e^{j2\pi\xi t} \sum_{i=1}^{L} x(t - \tau_i) h_i(t) + n(t), \tag{2.4}$$

where ξ is frequency offset due to inaccurate frequency synchronization, θ is the carrier phase, and $n(t)$ corresponds to additive white Gaussian noise (AWGN) sample with zero mean and variance of σ_n^2. The received signal is sampled with sampling time of Δt at the analog to digital converter (ADC) and discrete-

21

time received signal can be represented in vector notation by

$$y(i) = [y(1), y(2), \ldots, y(N)].\tag{2.5}$$

where $i = 1, \ldots, N$. Models of FSK, PSK, and QAM modulated SC signals are not listed due to the space limitations and can be found in [49] and references therein.

2.2 Proposed Method

The cumulants of a process are defined as the generalization of the autocorrelation function $E\{y(i)y(i+i_1)\}$. Thus, the general formulation of third and fourth order cumulants for the stationary random processes with zero mean are given by

$$c_{3y}(i_1, i_2) \triangleq E\{y(i)y(i + i_1)y(i + i_2)\}\tag{2.6}$$

and

$$
\begin{aligned}
c_{4y}(i_1, i_2, i_3) \triangleq {} & E\{y(i)y(i + i_1)y(i + i_2)y(i + i_3)\} \\
& - c_{2y}(i_1)c_{2y}(i_2 - i_3) - c_{2y}(i_2)c_{2y}(i_3 - i_1) \\
& - c_{2y}(i_3)c_{2y}(i_2 - i_1),
\end{aligned}\tag{2.7}
$$

where $c_{2y}(i_1) \triangleq E\{y(i)y(i + i_1)\}$. Note that, the distributional characteristics of the complex signals are also retained by the real and the imaginary parts. Therefore, the analysis for wireless OFDM signals can be given over either of these parts and the analysis can be extended to complex domain [64]. When the real part of the received wireless signals given by

$$y(i) = \sum_{j=-\infty}^{\infty} x_r(i - j)h(j) + n(t), \qquad \sum_{i=-\infty}^{\infty} |h(i)| < \infty\tag{2.8}$$

where $x_r(i)$ is the real part of the signal, k-th-order cumulants becomes [66]

$$c_{ky}(i_1, i_2, i_3, \ldots, i_{k-1}) = \gamma_{kx} \sum_{i=-\infty}^{\infty} h(i)h(i + i_1) \ldots h(i + i_{k-1}).\tag{2.9}$$

Assuming that the $x_r(i)$ is i.i.d., in case of non-Gaussian signals, zero lag cumulants will converge to the finite moments of $\gamma_{3x} \triangleq c_{3x}(0, 0) \neq 0$ or, $\gamma_{4x} \triangleq c_{4x}(0, 0, 0) \neq 0$ and for Gaussian signals $\gamma_{3x} = 0$ and $\gamma_{4x} = 0$, therefore $c_{3y}(0, 0)$ and $c_{4y}(0, 0, 0)$ will converge to zero. However, when the signal model given in

22

Section 2.1 is considered the real part of the signal can be written as

$$x_r(i) = Re\left\{ \sum_{m=1}^{N} \sum_{k=1}^{K} S_m(k) e^{j\frac{2\pi(\eta(k)(i-mT_S)+\xi_i)}{T_D}+\theta_i} \right\}, \tag{2.10}$$

and the i.i.d. property will not perfectly hold. Thus γ_{3x} and γ_{4x} will not converge perfectly to zero and the value of the $c_{3y}(0,0)$ and $c_{4y}(0,0,0)$ will be determined by the channel coefficients along with the γ_{3x} and γ_{4x} as indicated in eqn. (2.9).

When the selection between third and fourth order cumulants is considered, the kth-order cumulants will vanish for $k > 3$ if $x(i)$ is Gaussian [67]. However, third order cumulants can converge to zero although $x_r(i)$ is non-Gaussian but symmetrically distributed [63]. Therefore, 3rd-order cumulants will be ignored and 4th-order cumulants will be analyzed for OFDM signal identification. Note that noise component $n(t)$ is independent from the rest of the components of the signal and will also vanish due to its Gaussianity.

The region of all combinations of all lags defined in (2.9) is given by $I_k^\infty \triangleq \{0 \le i_{k-1} \le \cdots \le i_1 \le \infty\}$. However, it is shown in [68] that cumulant lags that comprise distribution characterization of the series are finite and it is not required to estimate the cumulant values for the majority of the possible lag combinations. Therefore, the region of the lags that should be taken into consideration for the analysis is given by

$$I_4^N = \{0 \le i_3 \le i_2 \le i_1 \le N\}. \tag{2.11}$$

When the calculation of the estimates of the cumulants is considered, for the probabilistic convergence of estimated cumulants $\hat{c}_{ky}$ to the c_{ky}, $y(i)$ samples should be independent and well separated in time. This is called mixing conditions. However, the autocorrelation $c_{2y}(i_1)$ is estimated using sample averaging because instead of the series $y(t)$, the samples of the original series $y(i)$ are employed in the process. Moreover, there is no synchronization process involved in the sampling stage. Therefore an irreducible error is introduced to the estimation of the cumulants. On the other hand, $\hat{c}_{ky}$ should be absolutely summable [66] and the linear process which is defined for wireless OFDM signals in (2.8) satisfy this condition. Under these conditions, the estimate autocorrelation becomes $\hat{c}_{2y}(i_1) = \frac{1}{N} \sum_{i=0}^{N-1-i_1} y(i)y(i+i_1)$, and 4th-order cumulant

23

estimate is given by

$$\hat{c}_{4y}(i_1, i_2, i_3) \triangleq \frac{1}{N} \sum_{i=0}^{N-1-i_1} y(i)y(i + i_1)y(i + i_2)y(i + i_3)$$

$$- \hat{c}_{2y}(i_1)\hat{c}_{2y}(i_2 - i_3) - \hat{c}_{2y}(i_2)\hat{c}_{2y}(i_3 - i_1)$$

$$(2.12)$$

$$- \hat{c}_{2y}(i_3)\hat{c}_{2y}(i_2 - i_1), \quad (i_1, i_2, i_3) \in I_4^N.$$

The sample estimates in (2.12) should only be calculated over I_4^N which is defined in (2.11). The Gaussianity test will use lags of $\hat{c}_{4y}$ that can be collected into an $N_c \times 1$ vector. This vector constitutes a 3 dimensional triangular region and its length is given by $N_c = N(N + 1)(N + 2)/6$. If the vector is simply called as $\hat{c}_{4y}$, the asymptotic Gaussianity of these summable cumulants of leads to [63]

$$\sqrt{N}(\hat{c}_{4y} - c_{4y}) \overset{dist.}{\underset{N \to \infty}{\sim}} D^r(0, \Sigma_c) \tag{2.13}$$

where D^r denotes real Gaussian distribution, c_{4y} is the 4th-order cumulant vector which holds the theoretical cumulant values $c_{4y} \triangleq \lim_{N \to \infty} E\{\hat{c}_{4y}\}$, and Σ_c is the asymptotic covariance matrix of c_{4y} which has the close form of

$$\Sigma_c \triangleq \lim_{N \to \infty} NE\{(\hat{c}_{4y} - c_{4y})(\hat{c}_{4y} - c_{4y})'\}. \tag{2.14}$$

where $'$ denotes the transpose operation.

2.2.1 Fourth Order Cumulants for OFDM Signals

When the wireless signals are considered, the length of the data can be orders of thousands or tens of thousands of samples depending on the sampling rate and the recording time. Defining the I_4^N lag region and computing the components of vector $\hat{c}_{4y}$ can become impractical in many cases. Moreover, covariance matrix estimation for the 4th-order cumulants is a complex procedure which requires involvement of products of the cross moment terms [63].

The data set can be divided into smaller sections and processed in parallel or the data set can be shortened. However, even though the choice of N and consequently N_c is application dependent, in practice when a strong non-Gaussianity (*e.g.*, due to the multipath fading channel) present in short records *i.e*, $N < 200$, this will lead to power reduction in the Gaussianity test and make it unreliable. Therefore, even for the shortest data sets, the size of the $\hat{c}_{4y}$ vector can be quite large and the computation of the cumulants and the Σ_c can become impractical. However, [69] and [64] showed that shrinking the lag region into $I_4^M = \{i_3 =$

24

$0 \leq i_2 = i_1 \leq M\}$ does not lead to loss of significant distribution information for communications signals because the terms that are left over have very small influence on the features of the modulation type of the signal when compared to the set in the hand. Note that the lag distance is also limited with $M \approx 1.5 T_s$ where T_s is the symbol duration for the signal under test. Therefore the cumulants should be evaluated only for the set of lags of $(\lambda, \lambda, 0)$ where $i_1 = i_2 = \lambda \in [0, 1.5 T_s]$. Under these conditions (2.12) can be written as

$$
\begin{aligned}
\hat{c}_{4y}(\lambda, \lambda, 0) \triangleq \frac{1}{N} &\sum_{i=0}^{N-1-\lambda} y(i)y(i+\lambda)y(i+\lambda)y(i) \\
&- \hat{c}_{2y}(\lambda)\hat{c}_{2y}(\lambda) - \hat{c}_{2y}(\lambda)\hat{c}_{2y}(-\lambda) \\
&- \hat{c}_{2y}(0)\hat{c}_{2y}(0), \quad (i_1, i_2, i_3) \in I_4^M,
\end{aligned}
\tag{2.15}
$$

and the open form becomes

$$
\begin{aligned}
\hat{c}_{4y}(\lambda, \lambda, 0) = \frac{1}{N} &\sum_{i=0}^{N-1-\lambda} y^2(i)y^2(i+\lambda) - \left[\frac{1}{N} \sum_{i=0}^{N-1-\lambda} y(i)y(i+\lambda) \right]^2 \\
&- \left[\frac{1}{N} \sum_{i=0}^{N-1-\lambda} y(i)y(i+\lambda) \right]\left[\frac{1}{N} \sum_{i=\lambda}^{N-1} y(i)y(i-\lambda) \right] \\
&- \left[\frac{1}{N} \sum_{i=0}^{N-1} y^2(i) \right]^2.
\end{aligned}
\tag{2.16}
$$

Note that eqn.(2.16) differs from the derivations of [64] in the sense of squares of sums.

2.2.2 The Gaussianity Test and Decision Mechanism

Various cumulant based time-domain Gaussianity tests are proposed in the literature for OFDM signal identification *i.e.*, [50, 52, 55, 60]. These tests depend on the output of combination of several order of cumulant estimates which are fixed numerical values thus, it can be problematic to define a threshold selection procedure because the sample estimates of the cumulants show relative high variance especially under fading channels. In this chapter, the $d_{G,4}$ test that was proposed in [63] is adopted for OFDM signal identification. It is an asymptotic chi-square CFAR test in which the selection of the threshold is done by using the χ^2 test tables based on the degree of freedom of the distribution. Moreover, effects of fading channels which can lead to stronger non-Gaussian components are minimized by the involvement of covariances of the cumulants. Originally, the test is applied to real processes and in this chapter the same approach is maintained because the Gaussian features of the complex data set is also retained by the imaginary and real parts of the OFDM signals. Besides, operating in real domain reduces the computation time for the test output when compared to

25

complex domain, however the test can be easily extended to complex data sets. The time-domain Gaussianity test can be formulated as a binary hypothesis problem of

$$\mathcal{H}_0 : \hat{c}_{4y} \sim D^r(0, N^{-1}\Sigma_c) \quad vs. \quad \mathcal{H}_1 : \hat{c}_{4y} \sim D^r(c_{4y}, N^{-1}\Sigma_c), \sim c_{4y} \neq 0. \tag{2.17}$$

This problem can be addressed by a chi-square test which can be defined by $d_{G,4} \triangleq N\hat{c}_{4y}\hat{\Sigma}_c^{-1}\hat{c}_{4y}$. The theory of large samples can be employed to derive the test [70].

$$\sqrt{N}(\hat{\theta}_N - \theta) \underset{N \to \infty}{\overset{dist.}{\sim}} D^r(0, \Sigma_\theta) \tag{2.18}$$

where $\hat{\theta}_N$ is the asymptotic Gaussian estimator of the vector θ with the length of $N_\theta \times 1$. In case $\theta \neq 0$,

$$\sqrt{N}(\hat{\theta}_N' \hat{\theta}_N - \theta' \theta) \underset{N \to \infty}{\overset{dist.}{\sim}} D^r(0, 4\theta' \Sigma_\theta \theta). \tag{2.19}$$

If $\theta = 0$ and $\Sigma_\theta = I$, where I is the $N_\theta \times N_\theta$ identity matrix, the estimator converges to chi-squared distribution with the degree of freedom of N_θ and can be written as

$$N(\hat{\theta}_N' \hat{\theta}_N - \theta' \theta) \underset{N \to \infty}{\overset{dist.}{\sim}} \chi_{N_\theta}^2. \tag{2.20}$$

Therefore, under $\mathcal{H}_0$, $c_{4y} = 0$ and

$$\sqrt{N}(\hat{c}_{4y}) \underset{N \to \infty}{\overset{dist.}{\sim}} D^r(0, \Sigma_c). \tag{2.21}$$

The estimator for the cumulant covariance matrix which is $\hat{\Sigma}_c$, converges to Σ_c and (2.21) becomes

$$\sqrt{N}(\hat{\Sigma}_c^{-1/2}\hat{c}_{4y}) \underset{N \to \infty}{\overset{dist.}{\sim}} D^r(0, I). \tag{2.22}$$

If $\hat{\Sigma}_c^{-1/2}\hat{c}_{4y}$ is associated with $\hat{\theta}_N$, under H_0 and $c_{4y} = 0$, from (2.20) and (2.22) it can be inferred that

$$d_{G,4} = N\hat{c}_{4y}'\hat{\Sigma}_c^{-1}\hat{c}_{4y} \underset{N \to \infty}{\overset{dist.}{\sim}} \chi_{N_c}^2. \tag{2.23}$$

26

Note that the pseudo-inverse of $\hat{\Sigma}^{-1}$ should replace inverse in the equations below if $\hat{\Sigma}$ rank-deficient. There-fore, for an α level significance the test in (2.17) becomes a chi-square test which can be defined by

$$d_{G,4} \underset{\mathcal{H}_0}{\overset{\mathcal{H}_1}{\gtrless}} t_G = \chi^2_{N_c}(\alpha). \tag{2.24}$$

The probability of the false alarm is given by

$$P_F \triangleq \alpha \leq P[d_{G,4} \geq \chi^2_{N_c} | \mathcal{H}_0] \tag{2.25}$$

Under $\mathcal{H}_1$, the distribution of $d_{G,4}$ is estimated from (2.19) as

$$d_{G,4} \sim D^r[N\hat{c}'_{4y}\hat{\Sigma}^{-1}_c\hat{c}_{4y}, 4N\hat{c}'_{4y}\hat{\Sigma}^{-1}_c\hat{c}_{4y}] \tag{2.26}$$

and the probability of detection is given by

$$P_D \triangleq \alpha \leq P[d_{G,4} \geq t_G | \mathcal{H}_1]. \tag{2.27}$$

Mathematical evaluations of the probability of false alarm and probability of detection now can be made by substituting the estimates given in (2.16) instead of c_{4y} and computing the estimate of Σ^{-1}_c. Note that, fourth order cumulant covariance matrix estimate computation is a long and complex procedure as indicated in [63]. However, peculiar to the OFDM signals, under the conditions defined in Section 2.2.1, covariance matrix estimate calculation becomes a simpler process. Therefore, the general form of covariance estimates of the cumulants for OFDM signals is derived based on the computations in [66] (eqn. 2.3.8) and [63] and reduced to three equations which are consist of several moments of the received signal. The computation process can be found in the Appendix A.

2.3 Simulation Results

The performance of the proposed test is discussed taking various parameters into consideration. A simulation setup is developed to generate PSK, FSK, QAM and OFDM modulated signals based on the proposed signal model in Section 2.1. The OFDM signals employed 64 active carriers with 250kHz spacing. T_G is also selected as $1/4T_D$. The wireless channel is modeled as Rayleigh fading channel with $L = 4$. Doppler shift and delay spread are also included in the channel model depending on 802.11g communication
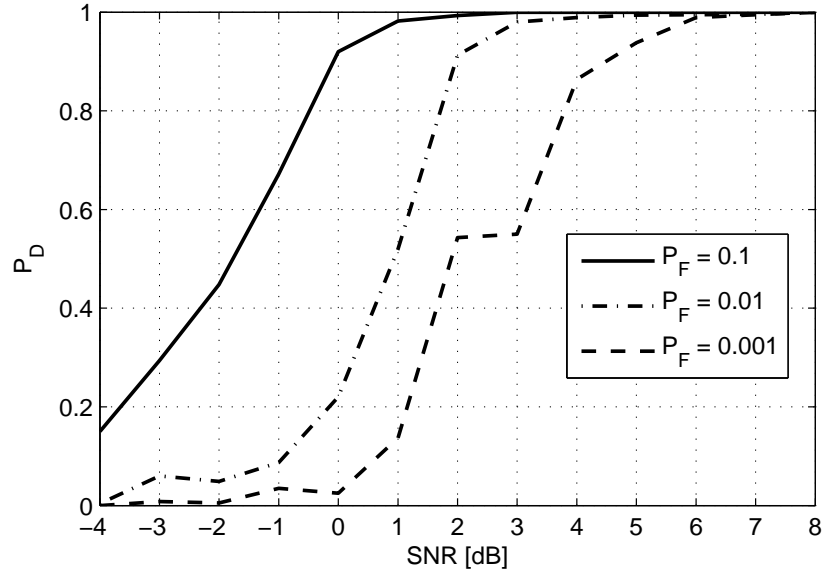
27

Figure 2.1: Probability of detection: FSK vs. OFDM

channel requirements. The simulations are repeated for 10000 times to be able to examine the impairments introduced by the random wireless channel.

Table 2.1: SNR vs. $\sigma^2_{d_{G,4}}$

SNR	PSK	QAM	FSK	OFDM
-6	15487	380752	88332	178266
-4	31759	2950	677687	13440
-2	27807	107989	53049	3125334
0	484857	18932209	29504333	1100245
2	081359	40929	8688517	1164
4	654790	51823	8553835	2123
6	514926	18568	18655826	181
8	145467	30571	41565932	2310
10	641	2824	166865946	214
12	635	655	85193125	235
14	680	874	67534593	84
16	696	996	831423678	3
18	696	1007	998653396	3
20	670	1168	2343610200	2

The variance of the output of the $d_{G,4}$ test introduce important information about the distribution characteristics and the test performance. The $\sigma^2_{d_{G,4}}$ for each modulation type is listed in Table 2.1. While the dispersion of the test results shows a random nature for the SNR values below 0, as the SNR increase PSK,

28

QAM, and OFDM tests start to become less disperse and more stable. On the other hand FSK signals exhibit more disperse behavior with the increasing SNR.
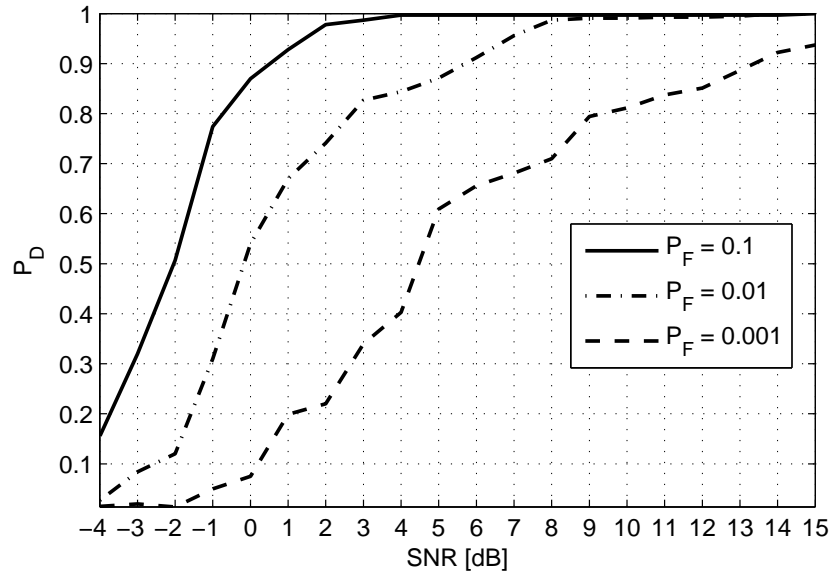

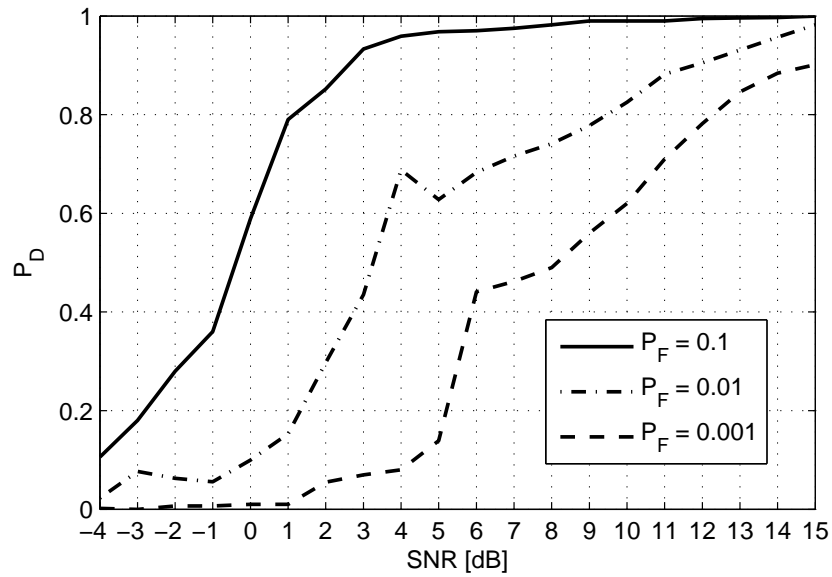Figure 2.2: Probability of detection: PSK vs. OFDM

Figure 2.3: Probability of detection: QAM vs. OFDM

29

A CFAR detector is implemented based on equations (2.22)-(2.27) in Section 2.2.2 for P_F of 0.001, 0.01, 0.1. In Fig. 2.1, 2.2, and 2.3 the P_D results for OFDM vs. SC signals are given for 1024 symbols, modulation order of 32 and various SNR levels. The results indicate that best separation is achieved against FSK, PSK and QAM follows consecutively. Especially for P_F of 0.1, and 0.01, a certain confidence level is achieved at 2 dB of SNR for FSK signals, 6 dB for PSK, and 11 dB for QAM.

The effect of the change of modulation order on the test statistics is investigated in Fig. 2.4 when the SNR is 7 dB and 1024 symbols are recorded. While FSK separation does not depend on modulation order, as the order increase to 4, the test performs better for PSK steadily. In case of QAM SC signals, the best performance is achieved at modulation order of 2 and it is followed by the order of 32.
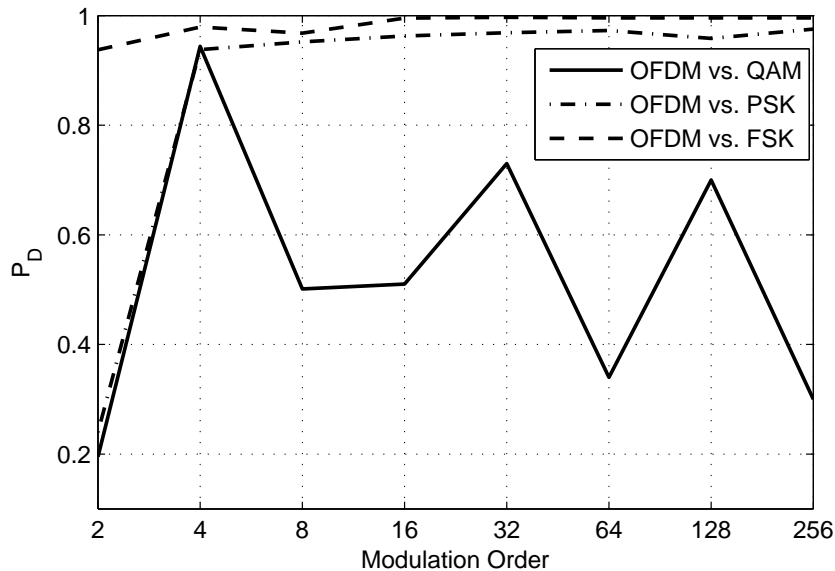

Figure 2.4: OFDM - SC separation: effect of modulation order

Data length or number of symbols used is also another important parameter which affects the performance of the statistical tests. Fig. 2.5 displays the performance of the proposed Gaussianity test with the changing number of symbols for 7 dB SNR and modulation order of 32 for each signal type. While the test performs well for FSK signals over 256 symbols, for all SC signals the test performance is optimized as the number of symbols reaches 1024. The degradation in the test performance below this level is due to the problems discussed in Section 2.2.

We finally compared the detection performance of the proposed method with two of the non-coherent methods that are available in the literature. One of these methods, which is introduced in [54] depends
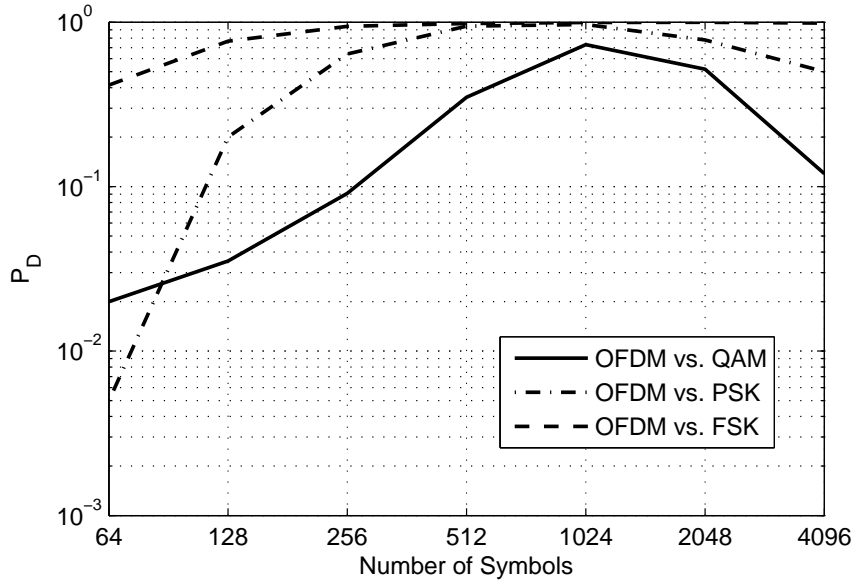
30

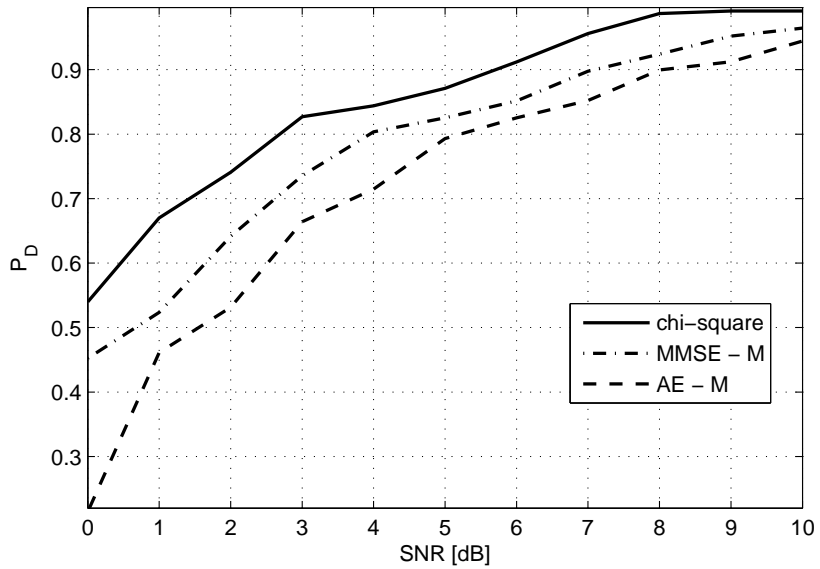Figure 2.5: OFDM - SC separation: effect of number of symbols

Figure 2.6: Performance comparison: OFDM vs. PSK ($P_F = 0.01$)

on fourth and sixth order moments and introduces an MMSE algorithm based on these moment function ($MMSE - M$). On the other hand, in [52] a method based on the combination of fourth order moments and amplitude estimation is introduced ($AE - M$). The performance comparison with these methods can be found in Fig. 2.6 for the PSK signals. Modulation order is 32, $P_F = 0.01$, and $N = 1204$. The chi-square

31

test over-performs both methods because, while these techniques (also as the other non-coherent methods introduced in [49–51]) depend on only the estimates of the cumulants, the chi-square test also includes the estimates of the covariances of the cumulants. Note that, performance comparison for FSK and QAM signals are not included because of space limitations. However, the comparison for these signals also yield similar results.

2.4   Blind Cyclic Prefix Size Estimation

Cyclic prefix (cp) size estimation algorithms depend on the fact that cp is the repetition of a part of an OFDM symbol. Therefore application of autocorrelation function in time domain should lead the estimation of the cyclic prefix size when the peak detection is applied to the autocorrelation spectrum. The optimum level of correlation is achieved when the correlated data length is exactly the same with the cp size. Hence, when the sample by sample correlation is conducted over the signal samples with the assumption that the useful symbol duration is known, the correlation peaks will have their maximums distanced exactly at the useful symbol duration away from each other on the spectrum. However, cp size itself is the parameter that is aimed to known, thus, one straightforward way of estimation would be optimizing the correlation peaks by applying the correlation operation with a set of previously decided cp sizes. Even though this approach can lead to estimation of the cp size in the end, the brute force nature of the algorithm makes it unattractive for time-sensitive wireless communications applications. Therefore, the proposed method modifies the brute force nature of the correlation algorithm and starts with an assumed value of cp size and conducts the correlation operation based on this assumption. The maximization is performed in two steps: First, the repetition caused by the cyclic prefix is used to estimate the symbol duration T_D. The discrete correlation of the received signal can be written as:

$$R_y(\Delta) = \frac{1}{D-\Delta} \sum_{n=1}^{D-\Delta} x(q)y[n]y^*[n+\Delta] \tag{2.28}$$

When enough statistics are acquired:

$$R_y(\Delta) = \begin{cases} \sigma_s^2 + \sigma_m^2 & \text{if } \Delta = 0 \\ \frac{N_G}{N_D+N_G}\sigma_s^2 e^{-j2\pi\xi\Delta t N_D} & \text{if } \Delta = N_D \\ 0 & \text{if elsewhere} \end{cases} \tag{2.29}$$

32

Therefore, auto-correlation based estimation of N_D can be formulated as:

$$\hat{N}_D = \arg_\Delta \max\{|R_y(\Delta)|\}, \Delta > 0. \tag{2.30}$$
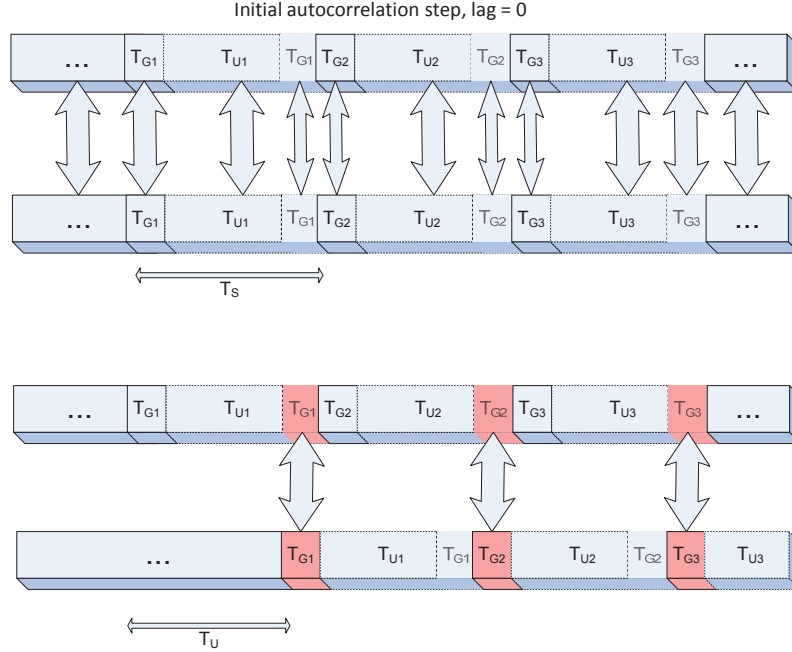
This process can be visualized in Fig. 2.7.

Figure 2.7: Useful symbol duration estimation via autocorrelation

Then we applied the proposed ML estimator to WLAN signal. Figure 2.8 illustrates the result for lab. recorded data. The sampling rate is 33.28 MSPS and the distance between the peaks is 106 samples. The duration therefore becomes $106/33280000 = 3.1851\mu$ seconds. Symbol duration T_D for WLAN is 3.2μ seconds.

As the second step, if the OFDM symbol duration N_D is known, the cyclic prefix (CP) duration can be estimated by testing for different N_G values as:

$$\hat{N}_G, \hat{\theta} = \arg_{N_G,\theta} \max\{\hat{\Lambda}(\mathbf{y}; \hat{N}_D, N_G, \theta)\} \tag{2.31}$$

This approach is helpful simply because the CP length is selected as a multiple of OFDM symbol duration *e.g.*,$1/4, 1/8, 1/16$ of symbol duration. For further reduction in the complexity, these ratios can be tested in the first place as indicated before. The total symbol duration can be defined as $T_S = T_U + T_G$. Taking
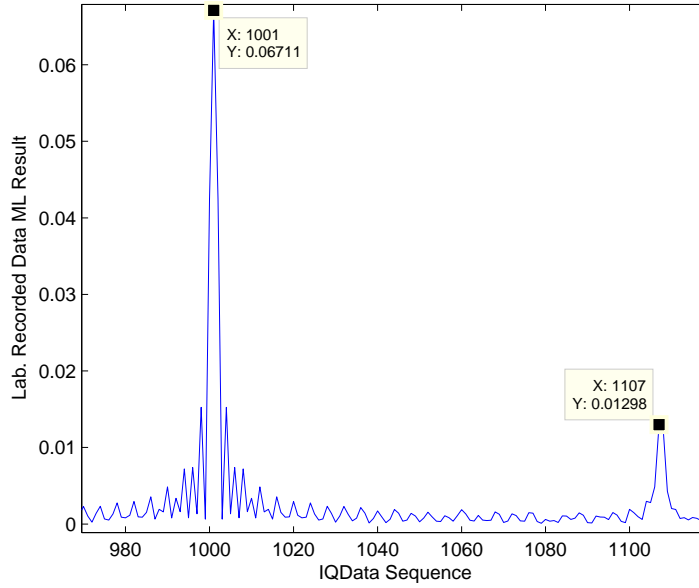
33

Figure 2.8: ML estimator output for WLAN

the fact that T_U is known into consideration an algorithm that will give the information of CP duration can be developed which starts with an assumption of CP duration *i.e.,* $1/4, 1/8$ or $1/16$ of T_U. Then, starting from the initial sample of the selected data, each sample is correlated with T_U shifted ones for the length of assumed CP size. This process is illustrated in Fig. 2.9 and can be defined as:

$$R(j) = \frac{1}{N_G} \sum_{i=1}^{k*N_S-N_U} \sum_{i}^{N_G} y(j)y^*(j+N_U) \qquad (2.32)$$

where k is number expected symbols in selected part of the burst; N_S, N_U and N_G are number of samples corresponding to symbol, useful symbol and cyclic prefix durations.

If the selected number of symbol increases the correlation and detection properties of (2.32) becomes better. In practice, it is better to have $k \geq 5$. The R(j) values are expected to exhibit high correlation properties when sample $y(j)$ is a part of CP. Therefore, the maximum correlation values are obtained with the repetition of T_S. Taking the fact that T_U is already estimated, T_G can be calculated simply by $T_G = T_S - T_U$. Figure 2.10 shows R(j) values for correct cp size selection (1/4) for WLAN signal. The sampling rate is 33.28 MSPS therefore estimated T_S and T_G becomes $3.9663e - 006$ and $0.76630e - 006$ respectively for the distance between 3rd and 4th peaks. Detection performance can be increased by including more symbols to the process. For instance, starting from the first detected peak, for CP size of 1/4 useful symbol duration expected and
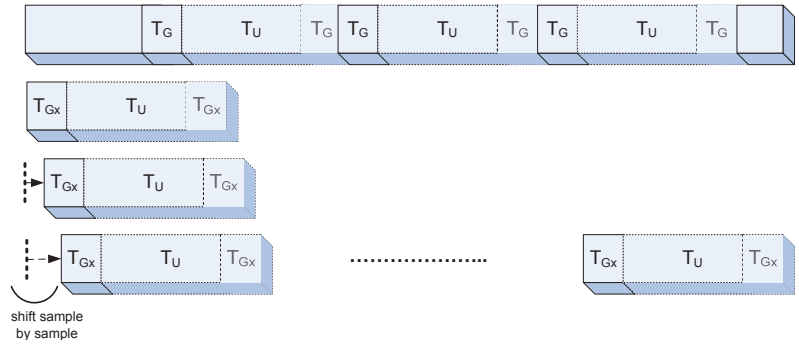
34

Figure 2.9: Sample by sample correlation

estimated peak locations are given in Fig. 2.11. The mean of the estimation error will be minimized when all 5 estimations are taken into consideration for this case. Figure 2.12 illustrates the estimation results when CP is considered to be 1/3. The figure indicates increasing drift for the expected value starting from the initial peak because actual CP size is 1/4. The minimization of the cumulative error for both cases (1/4 and 1/3) indicates that the MSE approach can estimate correct CP size considering the amount of drift when the expected CP size is selected wrong or a simple cumulative error comparison operation between different selected CP durations *i.e.,* $1/4, 1/8$ or $1/16$ will yield to the correct CP size duration. Both approaches are implemented for the sake of application integrity.
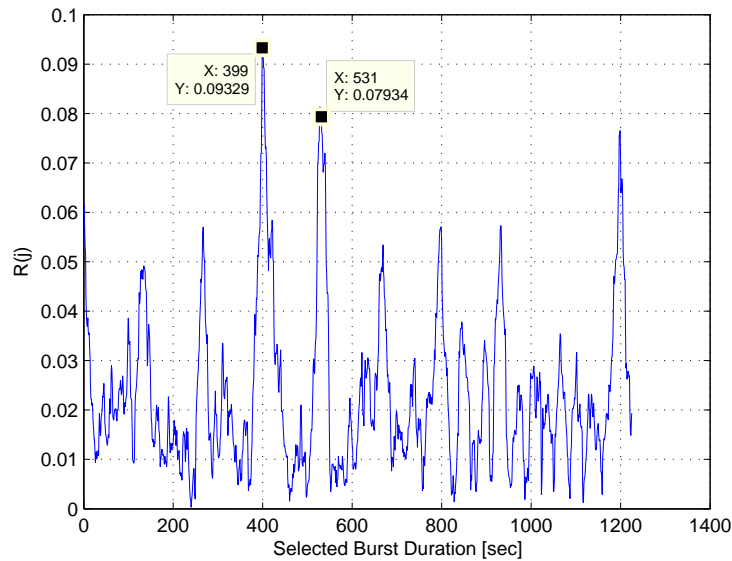

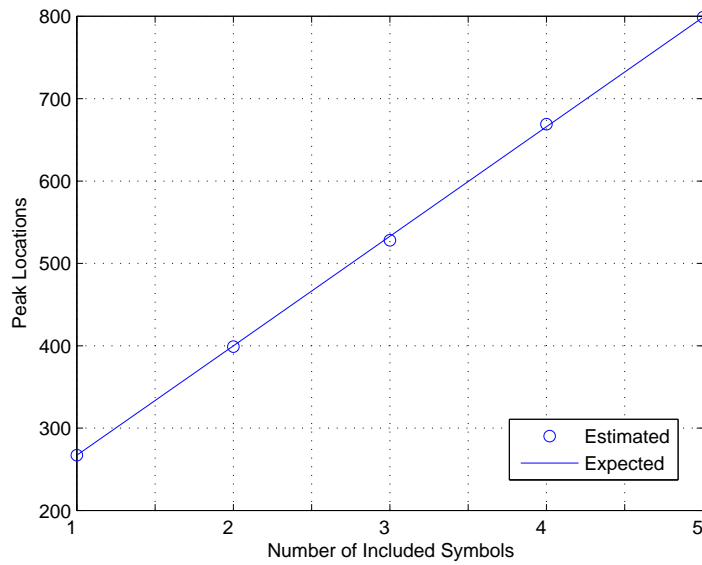Figure 2.10: R(j) operation output

35

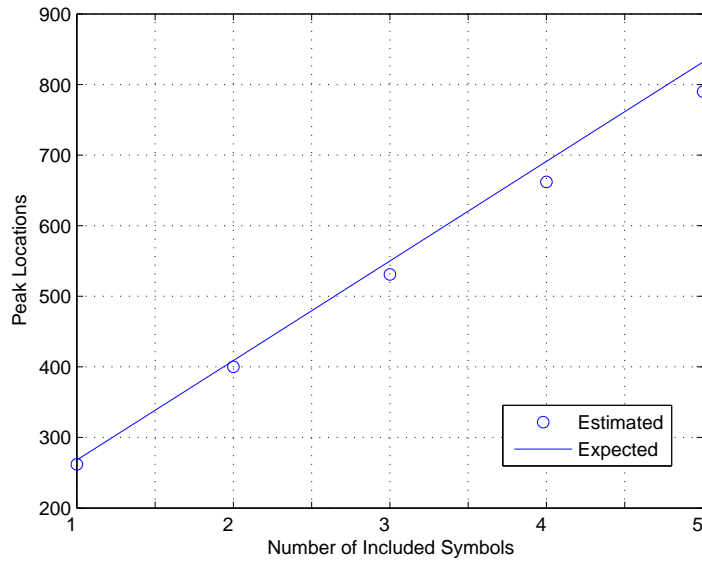Figure 2.11: Peak locations, expected v.s. estimated

Figure 2.12: Peak locations, expected v.s. estimated T_G of 1/3

In conclusion, adaptive receiver algorithms require estimation of received signal parameters with the least possible information and complexity. In this context, the proposed method can provide modulation identification information based on real or imaginary part of the received signal. Note that the only parameter in hand should be the symbol duration which determine the degree of freedom of the test. In practice, degree

36

of freedom which is $M > 10$ satisfies the confidence levels for correct detection thus the need for symbol duration can also be ignored. The test is robust against the changes in the modulation order or data length however performance is affected under low SNR because it depends on the Gaussianity of the data set. The derivations of covariance matrix of cumulant estimates leaded to three straightforward equations for OFDM systems which simplify the whole procedure for the implementation and execution of the test.

A novel algorithm which achieves blind estimation of the cyclic prefix size of OFDM signals is also introduced. The algorithm depends on the fact that cyclic prefix is the repetition of a part of a symbol. Therefore, initially an expected value is assigned to the cp size and sample by sample autocorrelation operation is conducted. The increasing symbol by symbol shift between the observed peaks and the expected peak locations on the correlation spectrum directly led to the correct cp size in case the pre-set cp size is shorter or longer than the real one.

CHAPTER 3

A TWO-ANTENNA SINGLE RF FRONT-END DOA ESTIMATION SYSTEM FOR WIRELESS COMMUNICATIONS SIGNALS

3.1   Introduction

Improving the efficiency of the wireless communications systems has substantial importance because of increasing demand for more communications capacity. Wireless signal direction of arrival (DOA) estimation methods are required to estimate the incoming signal direction so that adaptive beamforming techniques can be applied to improve the bit error rate (BER) performance [72], to achieve better throughput by mitigating the effects of multipath fading [73]- [75], to enhance capacity due to reuse increase [76], and to reduce the interference and delay spread [13, 75]. Moreover, the increasing number of users, networks, and deployment of wide variety of communications systems are leading the wireless communications towards the heterogeneous networks in which interference source direction estimation and allocation are crucial components of the interference management systems. Besides, public safety communications systems can benefit from direction of arrival (DOA) estimation methods for search and rescue operations based on estimated DOAs from victim mobile devices [74].

The DOA methods are considered as a part of position location systems along with time of arrival (TOA) and time difference of arrival (TDOA) techniques [13], however, they differ from these systems when it is aimed to estimate only the direction of arrival of the signals instead of locating the source of transmission. TOA and TDOA systems require multiple receivers with a certain distance *e.g.*, adjacent base-stations, and precise synchronization at the level of microseconds between the receivers. These systems provide the location of the emitter with certain accuracy under these conditions. On the other hand, when also deployed in multiple locations, DOA systems can provide emitter location information, however, a DOA system, in a single location, can also provide the angle of arrival (AOA) of the incident signals. DOA methods are applied over antenna arrays of various geometries [77], and one of the techniques is the phase interferometer that measure the phase differences over the antennas and provide an angular estimate [78, 79]. Another approach is the beamforming method which steers the antenna array beam over an angular field and provide the

38

power distribution over the field [80]. On the other hand, subspace methods such as multiple signal classification (MUSIC) [81] and estimation of signal parameters via rotational invariant techniques (ESPRIT), and minimum-norm (min norm) define signal and noise subspaces over the signal covariance matrix and searches for signals orthogonal to noise subspace. Deterministic and stochastic maximum likelihood (ML) algorithms, Capon's or minimum variance method which can be assumed as an extension to beamforming constitute the rest of the methods.

The DOA estimation methods have some advantages and disadvantages when they are compared with each other. Beamforming method is simpler than other techniques because, the AOA estimate is directly acquired from the data however, it has low resolution therefore, in case of closely located sources or when coherent multipath exists it provides poor performance [82]. On the other hand, ML is asymptotically optimal, however, it is computationally complex due to multidimensional search over the multipath components of each signal [83]. On the other hand, in [81] and [84], it is shown that MUSIC performs better than conventional beamforming and maximum entropy methods in general. [85] indicates that subspace rotation (SR) methods of Toeplitz approximation and an ESPRIT variant are statistically less efficient than MUSIC. Simulation results in [86] and measurements in [87] indicate that MUSIC provides better performance in the context of angular estimation accuracy and error variance when compared to Capon's method and min norm algorithm especially when the array element number is low *i.e.*, below 10 antennas. Moreover, Capon's method requires matrix inverse computation which can be computationally expensive for large arrays. Note that, under the condition that the interference source of interest is isolated from other signals by a signal identification process, MUSIC is asymptomatically efficient [83] and it can be implemented to arrays of arbitrary geometry while methods such as ESPRIT are applicable over some special arrays [88]. Therefore, MUSIC provides a good trade off in terms of estimation accuracy, stability, a priori requirements, computational cost which also makes MUSIC and its variants one of the most implemented method [77].

When the hardware and digital signal processing (DSP) perspectives of the implementation of DOA systems, especially when the subspace methods are considered, direction estimation of multiple signals becomes possible under the condition that the number of sensors are more than the impinging signals. Moreover, simultaneous sampling via separate RF front ends and designated DSP hardware blocks for each sensor indicate the ideal system configuration for high performance DOA estimation. Therefore, majority of the applications assume large number of sensors and accompanying circuitry [77]. On the other hand, adaptive DSP techniques applied to process the data received from the antenna array increase the system complexity, and hardware components such as analog to digital converters and DSP chips consume a considerable amount

39

of DC power when there is a separate DSP circuitry for each channel. Moreover, as number of channels connected to the array elements is also a cost increasing factor, thus these systems become more complex and expensive [13]. When the array sensitivity is also considered, as the number of antennas increase, the effect of mutual coupling gets worse [89, 90]. Besides, estimation performance degrades as the receiver circuitry gets larger, because it becomes harder to keep the calibration settings same through the measurement for each receiver block even if they are identical [91] and in general, additional sensitivity mitigation techniques are introduced to the system to overcome these problems [92]. Thus, even though DOA estimation systems introduce important advantages for wireless communications systems, their high complexity, power consumption, size, cost, and mobility problems can prevent their feasibility.

3.1.1 Related Work

The relationship between the sensor number and the incident signals is one of the areas that some progress can be made towards the solution of implementation issues of DOA estimation systems for wireless communications. Initially, three beamforming algorithms are implemented over a single-port, electronically steerable, four-element monopole switched parasitic antenna (SPA) array for base-station tracking in mobile communications [93]. Direction estimation resolution improvements for SPA are achieved by employing MUSIC instead of beamforming and extending the system to five and seven element monopoles [94]. Later, [95] developed a handheld direction finding device based on electronically SPA radiators for the fixed frequency channel of 2.484 GHz. Moreover, a significant reduction in the number of receivers is achieved by a passive sensor array that utilizes time-varying preprocessing of the sensor outputs [96] and it is proved in [97] that when sequential sampling is applied, only two receivers are sufficient to localize multiple sources with the MUSIC method. Later, a switch antenna array system is introduced as a substitute to the multi-channel array in which sequential sampling with a single receiver using a time-varying steering vector model is utilized to localize multiple narrowband targets [98]. On the other hand, a direction finding system based on received signal interpolation over a single receiving channel is proposed and simulated in [99]. Another single channel direction finding system for sonar and radar applications that employs phase shifting and specific DSP hardware is proposed in [100]. A two-antenna DOA estimation system inspired by the human ear from the perspective of antenna isolation can be found in [101] and an application of MUSIC algorithm to the detection of life signs via a two antenna setup is introduced in [102].

40

3.1.2 Proposed Method

Some progress is achieved towards compatible DOA systems to satisfy the requirements of commercial wireless communications systems. However, aforementioned problems along with the inflexibility of the antenna arrays prevent DOA applications to become a general and feasible solution. On the other hand, the developments on DSP techniques led to advanced portable measurement systems that are capable of capturing and recording wideband complex signals over the wireless spectrum. These systems, along with the wideband antennas that emerged concurrently, can constitute the basis for a wireless signal DOA estimation system which covers the frequency bands of interest with a single receiver deployed at one location. Therefore, in this chapter, a two-antenna single RF front-end DOA estimation system which adjusts antenna spacings adaptively based on the frequency of interest is proposed. Moreover, instead of introducing a fixed number of sensors or antennas, the proposed system extends the sensor locations by shifting the antenna system from initial measurement position to new measurement points and benefit from the sequential sampling process. Thus, by trading off a justifiable extension to the total measurement time with significant reduction in system complexity, a certain level of DOA estimation performance is achieved. We chose MUSIC method as the DOA estimation technique in our system due to its applicability to the arbitrary arrays and sensor direction characteristics, along with the aforementioned advantages. Also note that the effect of mutual coupling is significantly low when compared to the multi-channel arrays and single channel systems are also easier to calibrate [100].

A measurement setup is developed depending on the system model provided in Section 3.2 and extensive measurements are conducted by changing various setup parameters. Note that, majority of the applications in the related literature are based on simulations that could not include the factors such as calibration errors [103] which can introduce significant impact in the system performance. Moreover, the research on the field also lack of detailed parametric analysis depending on real measurements which should provide insight about the performance of the DOA methods with changing parameters such as antenna spacing, antenna number, measurement duration, wireless technology deployed to access the spectrum, line of sight (LOS) and non-line of sight (NLOS) conditions. In this study, the DOA estimation performance of the proposed system is provided in detail based on measurement results for major communications systems such as cellular technologies and wireless local area network, Bluetooth, cordless phone, and digital video broadcasting (DVB) signals. A measurement setup for a four antenna pseudo-Doppler system is also developed for performance comparison purposes. The applications areas of the proposed system include deployment at base-stations for mobile user direction estimation, as compact carry on systems for wireless network field engineers to

41

estimate high-resolution direction of arrival of interference signals or transient signals such as intermodulation products, and as a part of public safety communications systems for mobile device tracking in extreme situations.

3.2   Proposed System

The proposed system consists of two identical, omni-directional wideband antennas mounted on a scaled platform, an electronic switch, a controller board, a commercially available handheld super-heterodyne spectrum analyzer with complex signal (I/Q data) recording capability, and the DOA estimation component as depicted in Fig. 3.2. The system components prior to the DOA estimation block provide data acquisition via sequential sampling over the single channel. This step of the process is achieved as follows: First, the distance between two antennas are set to a fixed value (Δd). Second, after the initial measurements are taken from both antennas, they are shifted to the next measurement point together as a single entity. The distance of each antenna, from the initial measurement point is a pre-measurement set, user defined, fixed value *i.e.*, Δx. Third, again, as the measurements are taken from each antenna, the Δd distanced antennas are shifted to the next data measurement point which is again Δx away form the previous location. This process is repeated until the user defined number of shifting points are covered as illustrated in Fig. 3.2.

The initial antenna placement and the following shifting operations can be accomplished automatically via an electronically tuned mechanical steering mechanism which can be mounted to the scaled platform or manually by mounting the antennas to the predefined points on the scaled platform and by shifting the pair as the measurements are completed at each measurement point. In [13] it is indicated that independent wireless channel paths at each antenna can be achieved when the antenna spacing is half-wavelength or more. Therefore, antenna spacings can be adjusted with reference to the fractions of the wavelength, λ. In the proposed system, λ can be simply computed at the receiver using the wavelength equation, $\lambda = c/f_c$, where, f_c is the center frequency that the receiver is set, and c is the speed of light. Then, this information is used to calculate the exact values of Δd and Δx as these parameters are selected as fractions of λ by the user. Secondly, Δd and Δx are transferred to the controller board along with the switching time (which defines the duration of measurement at each antenna) and the total number of shifting operations to be conducted. Finally, the controller commands the mechanical system to set the antennas to their initial positions and the data acquisition procedure will be started. Note that if the total number of shifting operations and the total number of measurements taken are defined by L and M consecutively, the maximum number of measurements will be $M = 2(L+1)$ under the condition of $\Delta d/\Delta x \notin \mathbb{Z}^+$. The number of total measurements will be $M = 2(L+1)-K$

42

in case of $\Delta d/\Delta x \in \mathbb{Z}^+$, where K is the total number of shifting operations where antenna 1 in Fig. 3.2 is shifted exactly to the position which was held by antenna 2 before the shifting operation. These special cases can be easily computed in advance at the receiver as the user choses Δd, Δx, and L before the measurement procedure is started and measurement duplications can be avoided by only taking measurements from the antenna 2 when antenna 1 is allocated to the previous antenna 2 position after a shifting operation.

The super-heterodyne receiver is set to data recording mode during the data acquisition stage and it is tuned to the user defined f_c and frequency span. Received signal is combined with a signal from the local oscillator by a mixer and down converted to an intermediate frequency (IF) at the antenna input as depicted in Fig. 3.2. Note that, mixer is a device with non-linear characteristics, therefore, the RF attenuator and the low-pass filter at the input circuitry aim to prevent mixer gain compression, distortion and block high-frequency signals from mixer input. Next, the IF gain is introduced to compensate for the input attenuator losses. Then, the input signal is digitized and transferred to the DOA estimation block through the central processing unit (CPU) of the receiver. On the other hand, the input signal is also sent to the IF filter which is a bandpass filter that operates as a window to detect signals. IF filters bandwidth is defined as the resolution bandwidth (RBW). The following envelope detector rectifies the signal further and its output is converted to the video signal by the video filter which operates at the selected video bandwidth (VBW). Finally, the received signal is displayed on the device screen.

DOA estimation accuracy therefore the system performance is dependent on the quality of receiver hardware and accurate estimation necessitates that the received signals are processed in an identical manner. Therefore, the receiver must be highly linear and coherent in terms of frequency response, mixing and sampling operations [13]. One of the main factors that affect the coherency is the instruments internal timebase which determines frequency reference and time domain recording fidelity. The ovenized, high-performance crystal oscillator of the spectrum analyzer provides necessary performance in these terms. Moreover, the digital filters of the spectrum analyzer have identical transfer characteristics. Therefore, the synchronization errors due to hardware components are minimized. Other factors that affect the measurement performance are impedance mismatch between the system components and the voltage standing wave ratio. These are out of the scope of this work, however the catalog information that will be referenced in the next section will provide the information required regarding to these characteristics of the utilized hardware components.

When the DOA estimation process is considered, assuming that there are D plane waves from the directions of $\{\theta_1, \ldots \theta_D\}$ impinging on the antenna at the mth measurement point, the received signal can be

43

expressed as

$$x_m(t) = \sum_{n=1}^{D} s_n(t) e^{jk(x_m \sin \theta_n + y_m \cos \theta_n)} + n_m(t) \tag{3.1}$$

where $k = 2\pi/\lambda$ is the wave number, $s_n(t)$ is the complex envelope of the varying signal, x_m and y_m are the coordinates of the mth measurement point with respect to a reference point such as the origin of the utilized coordinate system, and $n_m(t)$ is the additive noise introduced to the system. The data recorded at each measurement point constitutes each row of data matrix formed at the data construction module of the DOA estimation block based on the signal model which can be given as

$$
\begin{bmatrix} x_1(t) \\ x_2(t) \\ \vdots \\ x_M(t) \end{bmatrix} =
\begin{bmatrix}
e^{jk\beta(x_1,y_1,\theta_1)} & e^{jk\beta(x_1,y_1,\theta_2)} & \dots & e^{jk\beta(x_1,y_1,\theta_D)} \\
e^{jk\beta(x_2,y_2,\theta_1)} & e^{jk\beta(x_2,y_2,\theta_2)} & \dots & e^{jk\beta(x_2,y_2,\theta_D)} \\
\vdots & \vdots & \dots & \vdots \\
e^{jk\beta(x_M,y_M,\theta_1)} & e^{jk\beta(x_M,y_M,\theta_2))} & \dots & e^{jk\beta(x_M,y_M,\theta_D)}
\end{bmatrix}
$$

$$
\times \begin{bmatrix} s_1(t) \\ s_2(t) \\ \vdots \\ s_D(t) \end{bmatrix} + \begin{bmatrix} n_1(t) \\ n_2(t) \\ \vdots \\ n_M(t) \end{bmatrix}
$$

where $\forall m, n : \beta(x_m, y_m, \theta_n) = x_m \sin \theta_n + y_m \cos \theta_n$, $m = 1, \dots, M$ and $n = 1, \dots, D$. This expression can be represented in a simpler notation of

$$x(t) = As(t) + n(t), \tag{3.2}$$

where $A = [a(\theta_1), \dots, a(\theta_D)]$ is the $M \times D$ array response or steering matrix and $a(\theta_n)$ is the steering vector for the signal impinging from the direction of θ_n. The real valued covariance matrix of the received signal becomes

$$R_x = \mathbb{E}\{x(t)x^H(t)\} = APA^H + \mathbb{E}\{n(t)n^H(t)\}, \tag{3.3}$$

where H represents Hermitian transpose and $P = \mathbb{E}\{s(t)s^H(t)\}$. Assuming that the noise and the incident signals are uncorrelated, $\mathbb{E}\{n(t)n^H(t)\}$ can be written as $\lambda_m R_0$ where λ_m is one of the eigenvalues of Rx, and R_0 is the normalized noise covariance matrix. Under the assumption that $M > D$, APA^H becomes singular, thus the determinants can be written as $|APA^H| = |R_x - \lambda_m R_0| = 0$. On the other hand, the impinging signals can be uncorrelated or some of them can have correlation of a certain degree. Therefore, P can be assumed to be positive definite, *i.e.*, $\forall z$, $\mathbb{R}(z^H P z) > 0$, where z is an arbitrary non-zero complex column vector. Also

44

considering that A is full rank, APA^H should be nonnegative which can only be satisfied when $\lambda_m = \lambda_{min}$, where λ_{min} is the minimum eigenvalue in R_x and it can be written as

$$R_x = APA^H + \lambda_{min}R_0, \qquad \lambda_{min} \geq 0. \tag{3.4}$$

When the wireless signals are considered, noise can be assumed as additive white Gaussian noise with zero mean and variance σ_n^2, therefore $\lambda_{min}R_0 = \sigma_n^2 I$, where I is the M × M identity matrix. On the other hand, APA^H has a rank of D, therefore its positive valued $\lambda_1, \ldots, \lambda_D$ eigenvalues will be followed by M − D zero eigenvalues. Since $APA^H = R_x - \lambda_{min}R_0$, eigenvalues of R_x are constituted from the eigenvalues of APA^H but shifted by λ_{min}. Thus, the minimum eigenvalue λ_{min} in the R_x is repeated N = M − D times. If e_m are the eigenvectors of R_x, $\forall e_m : R_x e_m = \lambda_m R_0 e_m$ and $APA^H = R_x - \lambda_{min}R_0$ leads to $APA^H e_m = (\lambda_m - \lambda_{min})R_0 e_m$. When λ_m is λ_{min}, $APA^H e_m = 0$, and $A^H e_m = 0$, indicating that the eigenvectors associated with λ_{min} are orthogonal to the space spanned by the steering vectors of A. Therefore, N-dimensional noise subspace spanned by N eigenvectors $E_n = [e_{D+1} \ldots e_M]$, and D-dimensional signal subspace spanned by the steering vectors are disjoint. Considering that $a(\theta)$ is the continuum of all possible steering vectors, the squared Euclidean distance $|E_n a(\theta)|^2$ should converge to zero, thus the DOA spectrum can be obtained from

$$P_{MU}(\theta) = \frac{1}{a^H(\theta)E_n E_n^H a(\theta)} \tag{3.5}$$

and the detected peaks at the spectrum will correspond to the DOA of the incident signals. Note that, for the wireless signals, multipath effect due to reflection of the waves through the communications medium leads to angular spread and causes performance degradation for DOA estimation [104]. This problem can be partially mitigated by spatial smoothing [105] which provides optimal performance when the array elements are identical and uniformly spaced [106]. Therefore, spatially smoothed covariance matrix is given by

$$R_s = \frac{1}{X} \sum_{x=1}^{X} R_x, \tag{3.6}$$

and in this work, the recording is divide into $X = 10$ subarrays. The eigenvalue decomposition and the rest of the DAO estimation process is applied over R_s as indicated in Fig. 3.2 and [107] can be consulted for the details of this process.

The total measurement time is an important parameter that should be considered for the proposed system because complexity, size, and cost reduction along with the frequency band coverage flexibility is

achieved by extending the measurement time and procedure by including the switching and shifting operations via sequential sampling. When the time taken by the DOA estimation process is excluded from the calculations, total measurement time, T_M, for a classical antenna array system which has separate RF front-end and signal processing block for each antenna will be equal to the data recording duration of the system which is defined by the switching time, T_S, in the context of the proposed system. However, when the sequential sampling is applied the total measurement time becomes

$$T_M = \mathrm{M}T_S + \mathrm{L}T_L, \tag{3.7}$$

where T_L is the time that each shifting operation takes. Therefore, while it takes $T_M = T_S = 50$ milliseconds (ms) for a $\lambda/2$ spaced 8-antenna array system to complete the measurement, when Δd is set to 2λ, Δx $= \lambda/2$, and $T_L = 5$ seconds, T_M becomes 15.4 seconds for the proposed system. Increased total measurement time for the sake of reduced cost and complexity dictates that the signal channel occupancy statistics is an important criterion for the feasibility of the introduced system. When the wireless communications signals are considered, the channel occupancy durations vary depending on the type of the transmission. For instance, some transient signal components and intermodulation products may occupy the channel for a couple of hundreds of milliseconds while the average channel holding time is around three minutes especially for cellular systems [108]. Therefore, the proposed system can achieve DOA estimation objectives set, when the system parameters such as Δd, Δx, and T_S are selected accordingly. Note that, if the system was based on solely single antenna, there would be a tremendous increase in the total measurement time. Moreover, it is possible to have a DOA estimate with measurements only from two antennas thus, the system can provide direction information for signals that occupy the spectrum for very short time depending on initial measurements conducted before the shifting operation is initiated. Moreover, the allocation errors would be more than 2-antenna system when the single antenna shifted because, Δx is a function of Δd in the proposed system therefore positioning errors during the shifting is limited. If there were more than 2 antennas, the total system complexity including the switch and controller mechanisms, switching combinations would increase and coupling between the antennas would become more of a problem. Therefore, 2-antenna approach balances the trade off between complexity and the measurement duration.

46

3.2.1 Simulation Analysis

The proposed system is first simulated in MATLAB. A set of random binary phase shift keying (BPSK) sequences are generated and transmitted them over a synthetically constructed wireless channel based on ITU-R M.1225 outdoor to indoor model. The Δd is set to λ and Δx = $\lambda/2$, T_S is selected as 25 ms. Shifting operation is assumed to be conducted twice, therefore for M = 5, L = 2 and for T_L = 3 seconds, the T_M = 6.125 seconds. The angular spectrum for various signal to noise ratio SNR values and arrival angle of 40° are shown in Fig. 3.1. The simulation results not only indicate the feasibility of the proposed system but also shows that as the SNR increases, the angular spectrum sharpens and the estimation error reduces significantly.
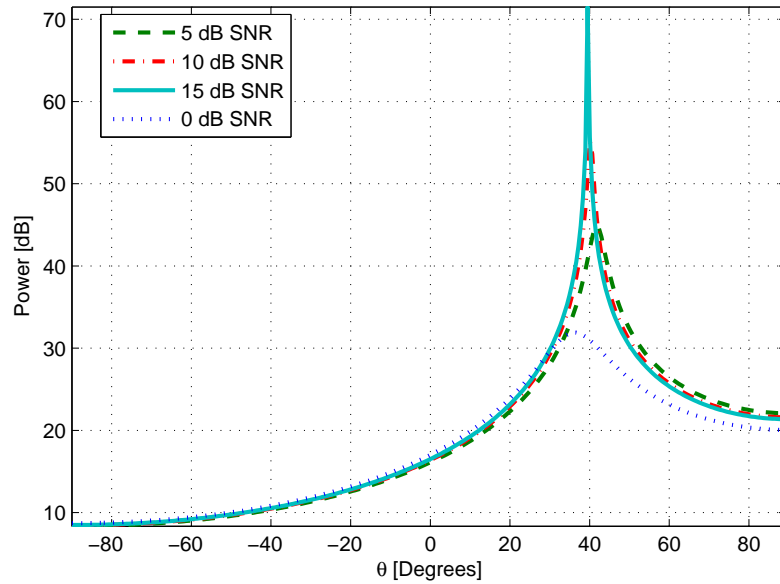
Figure 3.1: MUSIC simulations: effect of the SNR

3.3 Measurement Setup

A measurement setup is developed to investigate the DOA estimation performance of the proposed system by a parametric analysis, considering measurement parameters such as SNR, signal bandwidth, signal center frequency (consequently λ), Δd, Δx, LOS and NLOS cases.

47
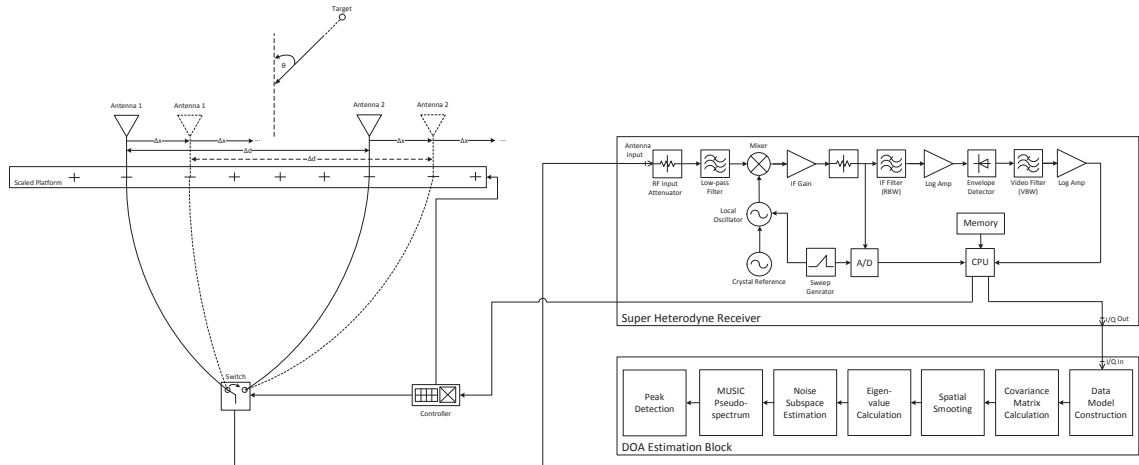
Figure 3.2: DOA estimation system model

3.3.1   The Measurement System

The measurement system consists of Anritsu MT8222A BTS Master handheld spectrum analyzer with complex signal (I/Q data) recording capability [109], a Mini Circuits ZSWA-4-30DR 4 input - 1 output switch, one Parallax controller card with BS2-IC micro-controller [110], a tuple of Anritsu 2000 series omni-directional antenna set to cover the wireless communications bands of interest, a Dell Vostro 1520 laptop computer, one ±5 Volts power supply, cables, and connectors.
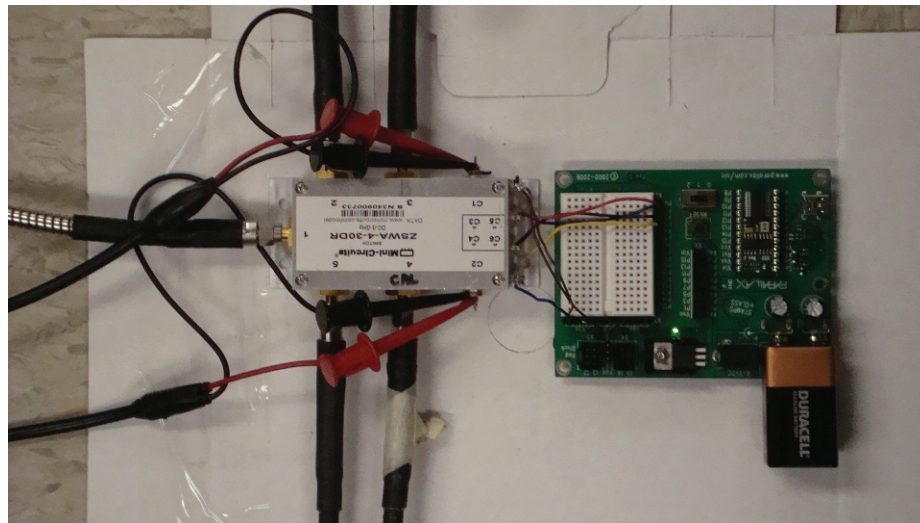
Figure 3.3: Switch and the controller

First, two Δd distanced antennas are connected to the 2 inputs of the $ZSWA - 4 - 30DR$ switch which is fed by the ±5 source. The control ports of the switch is connected to the Parallax controller card

which triggers the switching operation between the antennas. The switching operation and the its speed is controlled by the preprogrammed micro-controller which is mounted to the card after the controlling program is loaded to the chip on a computer. The data sheet in [111] can be consulted for further information on the switch characteristics and control port configuration. The chip is programmed with the BASIC programming language. Close up view of the controller, switch, and the cables can be seen in Fig. 3.3. Then, the output of the switch is connected to the MT8222A BTS Master spectrum analyzer which is set to the complex signal recording mode during the measurements. The amplification, filtering, downconversion and baseband digitization is achieved by the super heterodyne receiver architecture of the spectrum analyzer. The calibration of the system depends on the initial antenna array response however, it should be noted that an additional estimation error due to differences between array manifold used by the DOA estimation algorithm and the true manifold is inherently introduced to the system [91, 103].
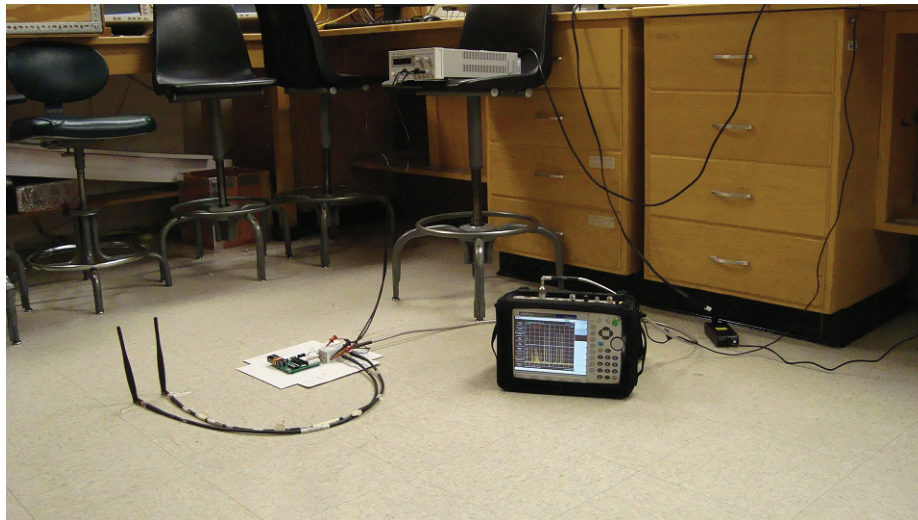
Figure 3.4: 2-Antenna DOA estimation system: 2.4 GHz measurements ($\lambda/2$, LOS)

The DOA estimation algorithms are not embedded to the spectrum analyzer currently. Therefore, the rest of the processes that follow the measurement procedure is completed off-line. Collected data is dumped to the laptop computer via the spectrum analyzer's universal serial bus interface for autocorrelation matrix calculations and signal DOA estimation processes based on the system model introduced in Section 3.2. The specifications of the spectrum analyzer during the measurements can be found in Table 3.1. The sampling rate and consequently the effective bandwidth of the recording is selected depending on the bandwidth of the signal aimed to be received. For instance, effective bandwidth of 25 MHz is selected for WLAN 802.11g signals which occupy 20 MHz bandwidth in the $2.4 - 24.8$ GHz range ISM band. As the measurement

system is set to theses initial conditions, shifting operation of the antennas are conducted manually and the linear array is formed. Plastic insulators are also deployed to fix the antenna positions and to minimize the electromagnetic scattering and diffraction. The general view of the setup during the WLAN 802.11g LOS ($\lambda/2$) measurements -except the laptop computer- can be seen in Fig. 3.4.

Table 3.1: Measurement setup: handheld spectrum analyzer features

Frequency Range	100 kHz to 7.1 GHz				
Tuning Resolution	1 kHz				
Frequency Span	10 Hz to 20 GHz including zero span				
Sweep Time	10 μs to 600 seconds in zero span autoset in non-zero span				
Resolution Bandwidth (RBW)	1 Hz to 3 MHz in 13 sequence 10%, (1 MHz max in zero-span) (3 dB bw) autoset in non-zero span				
Video Bandwidth (VBW)	1 Hz to 3 MHz in 13 sequence autoset in non-zero span				
Sampling Rates [MSPS]	9.25	11.1	12.95	14.8	50
Corresponding Effective Bandwidth [MHz]	5	6	7	8	25

On the other hand, an Agilent ESG signal generator is employed to generate and transmit the wireless signals[1] along with a laptop computer to transmit and receive Bluetooth signals, a microwave oven, and a DECT 5.0 Panasonic cordless phone as interference sources transmitting in the 910 MHz-2.4 GHz ISM bands.

3.3.2 Signal Parameters and Setup Allocations

In this section, the list of measurement parameters such as generated signal types (standards), receiver antenna distances (Δd), SNR, and the details of the geometrical setup are given. The list of the signals generated and the related measurement parameters are listed in Table 3.2. Note that, the generated signals and transmission parameters in the table are selected based on the uplink (UL) requirements of the relevant standards. The transmission frequencies are also selected from the UL transmission list approved by the Federal Communications Commission (FCC) in the United States (US) except the ATSC based DVB which is only downlink (DL). For instance, 849 MHz center frequency for GSM/EDGE signals is one of the GSM-850 UL frequencies which is frequently used in US rural regions.

The independence between the receiving paths of each antenna is related to the antenna distance (Δd) and theoretically, as the distance increases, better independence between the receiving paths therefore,

[1] [112] can be consulted for further technical information

50

Table 3.2: Measurement setup: wireless signal parameters

Signal Type	BW[MHz]	Cent. Fr.[MHz]	$\lambda/2[in]$	$\lambda[in]$	$2\lambda[in]$
GSM/EDGE	0.2	849	6.9510	13.9021	27.8041
WCDMA	5	1712	3.4471	6.8942	13.7884
cdma2000	1.25	1930	3.0577	6.1155	12.2309
LTE	4	1980	2.9805	5.9610	11.9221
WLAN (802.11g)	20	2440	2.4186	4.8372	9.6745
Bluetooth	1	2460	2.3990	4.7979	9.5958
DECT 5.0	1.728	1920	3.0737	6.1473	12.2946
ATSC b. DVB	6	800.31	7.3739	14.7479	29.4957

increased non-singularity at the correlation matrix and better performance is expected. To be able to evaluate the comparative effect of this factor, the measurements are conducted for $\Delta d = \lambda/2, \lambda, 2\lambda$.

When the channel conditions are considered, in LOS case, it is known that there is exactly a direct path between transmitter and *all* receiving antennas. There can also be some indirect paths, and in NLOS case, there is no direct path between transmitting antenna and *all* receiving antennas. However, there is at least one indirect path between transmitting antenna and all receiving antennas. Through the measurement process, four different allocations therefore, four different settings are created to test the performance of the proposed system. While two cases represented narrow angles (close to 10°) between the transmitter and the receiving system, the second tuple represented relatively larger angles. Another distinction between the allocations is whether there is a direct path between (LOS) or not (NLOS) between the transmitter and receiver which has vital effect on the performance of every DOA estimation systems. The geometrical parameters of each setting can be seen in Table 3.3.

Table 3.3: Measurement setup: transmitter & DOA estimator allocation

LOS/NLOS	Longitude[ft.]	Latitude[ft.]	Angle[Degrees]
LOS	25.4265	5.24934	11.66°
NLOS	19.357	5.24934	15.17°
LOS	49	80	58.51°
NLOS	128	468	74.7°

Measurement environment has also an important effect over the performance of the proposed system. The transmitters are fixed location in the laboratory environment which has scattering surfaces such as metal panels, other measurement and calibration equipments, tables, chairs etc. Therefore, the environment for the transmitter is a highly reflective indoor environment. On the other hand, receiving system can either be in a less reflective environment such as a corridor or in the same room with the transmitter. It should be noted that performance of any DOA system will be effected from the heavily reflective nature of the indoor

51

environments and the measurement settings in this case, can be assumed to be the bottom line performance circumstances for such systems. Therefore, it would be valid to assume that the angle estimation performance of the proposed system will increase as the system is deployed outdoors when the effects of reflected signal components will be lesser on the main component. The measurements with the listed Δds, for $\Delta x = \lambda/2$ and each signal type at the SNR values of -20 to 20 dB (with increment of 5 dB) seen at the receiver, for both of LOS/NLOS channel conditions (for Bluetooth and DECT 5.0 no NLOS measurements are included) in 4 listed settings at Table 3.3 are conducted for parametric analysis of the proposed system.

3.4 Measurement Results

Multiple measurements are conducted when the proposed system is allocated to each specific setting *i.e.*, signal type and corresponding spectrum analyzer configuration, SNR, Δd, and setup positioning. One of the important parameters is measurement duration at each antenna. This parameter is $T_S = 20$ *ms* unless the measurement duration itself is not the investigated parameter. Note that, total measurement time can be extended or shortened based on other system requirements such as expected transmission period peculiar to the observed wireless communications system as discussed in Section 3.2.
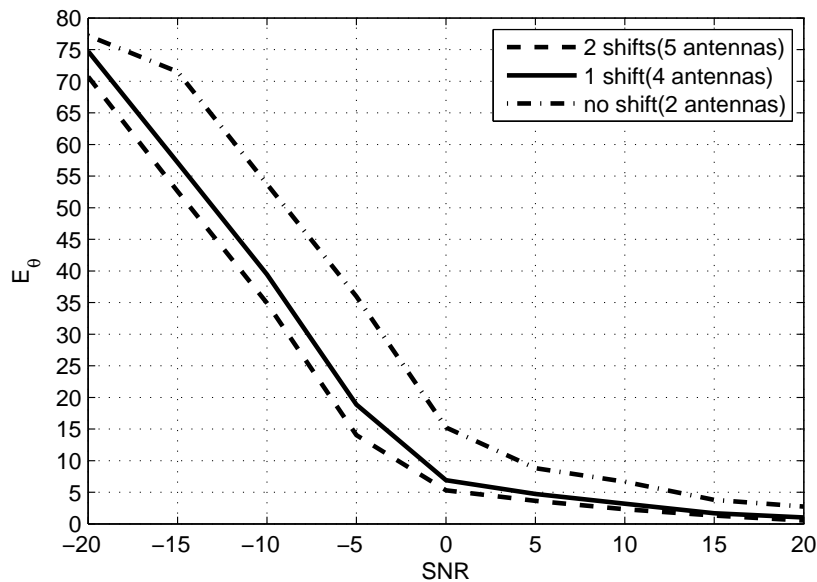
Figure 3.5: E_θ vs. shifting: GSM, $\lambda/2$

The measurements are repeated 10 times for each setting and the main performance evaluation metric for the proposed system is the absolute expected angular direction estimation error of the two-antenna

52
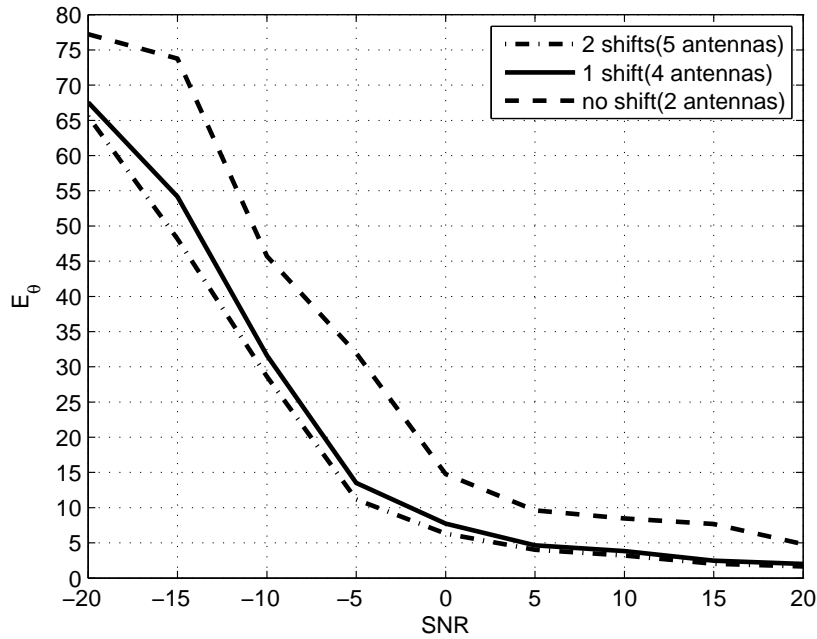
Figure 3.6: E_θ vs. shifting: LTE, $\lambda/2$

measurement system, $E_\theta = E\{|\theta - \hat{\theta}|\}$, where $\hat{\theta}$ is the estimate of the arriving angle of the signal to the two-antenna system while θ is the actual angle between the transmitter and the cross-section constituted by the two-antennas. E represents the expected value.

3.4.1 Effects of Shifting and Measurement Duration

The theoretical analysis [83] along with the supporting simulation and measurement results [77, 82] indicate that the resolution and the signal DOA estimation performance of the MUSIC method increases with the increasing SNR, sample number (measurement duration), array element number (M), and antenna spacing (Δd). The effect of shifting operation, therefore, array element number constituted by sequential measurements on the estimation performance is considered for one narrowband (GSM) and one wideband signal (LTE). Δd and Δx are selected as λ and $\lambda/2$ sequentially. Under the *LOS* conditions defined in Table 3.3, starting first with no shifting, antennas are shifted 2 times. The angular estimation error E_θ for each case and increasing SNR is shown in Fig. 3.5 and Fig. 3.6 respectively for both signals. In both cases, there is a significant reduction the estimation error between the no-shift case and first shifting operation and a slight performance improvement is achieved as M reaches from 4 to 5. Note that, the proposed system performs better for GSM signals than the LTE as the SNR increases because it is known that MUSIC performs bet-

53
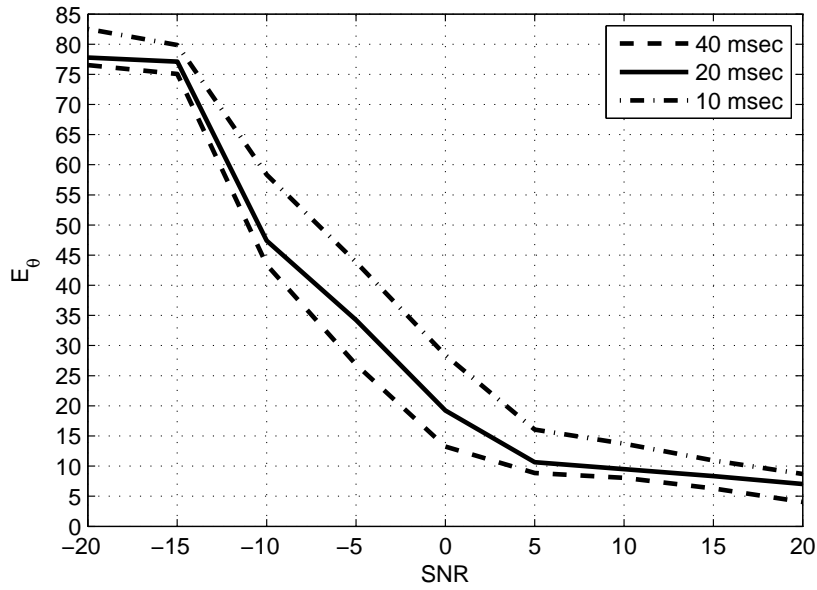
Figure 3.7: E_θ vs. data length: LTE, $\lambda/2$

ter under narrowband signal condition due to the fact that, in contrary to the wideband signals, waveform amplitude can be assumed to be constant over full aperture of the antenna array under narrowband conditions [113]. Therefore, for M = 4 and SNR = 15dB, in case of GSM E_θ = 1.68° and for LTE 2.48° which is also compatible with the indoor measurement results listed for a 4-antenna multi-channel system for BPSK signals in [114]. On the other hand, as the SNR reduces below 0 dB, a sharper reduction in the performance is observed for GSM signals when compared to LTE (M = 4 and SNR = −5dB, GSM E_θ = 18.87°, LTE E_θ = 13.51°), because narrowband signals are affected from the changes in the noise variance more than wideband signals.

A performance comparison should be done considering the increasing Δd vs. the effect of shifting, because E_θ also declines as the Δd increases. In this case, no shifting is made, and measurements are taken from 2 antennas only. Therefore, it should be investigated if the effect of shifting can be compensated by increasing Δd. The estimation error performance given in Fig. 3.12(a) which investigates the effect of changing Δd will provide the comparison information for the LTE *LOS* case. In Fig. 3.6, in case of no shifting, Δd = λ, which corresponds to the middle performance plot in Fig. 3.12(a). The next step in Fig. 3.6 is to conduct one shifting operation and increasing M to 4 while next step in Fig. 3.12(a) is Δd = 2λ. A close analysis of each case indicate no significant performance difference between two cases below −5dB, however, in between −5dB and 0dB, switched system performs nearly 4° better than Δd = 2λ case. After this point, as the SNR

54
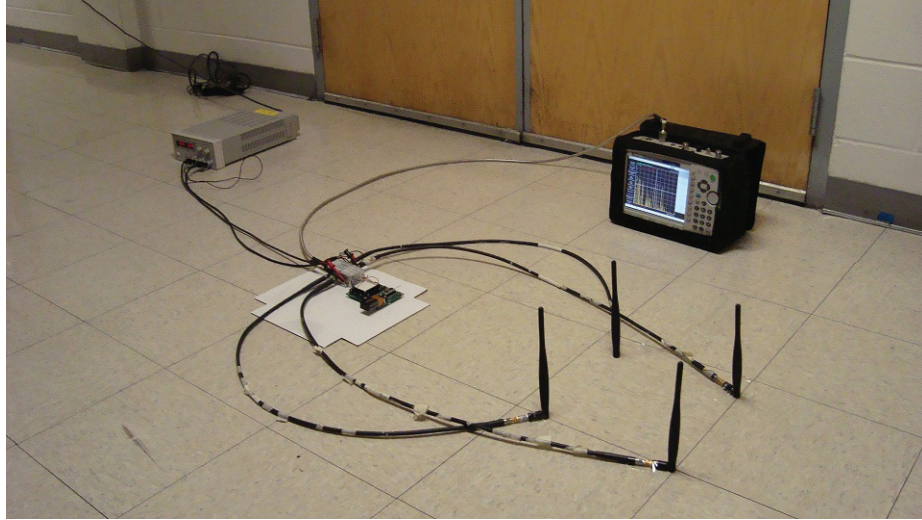
Figure 3.8: 4-Antenna pseudo-Doppler system setup (NLOS)
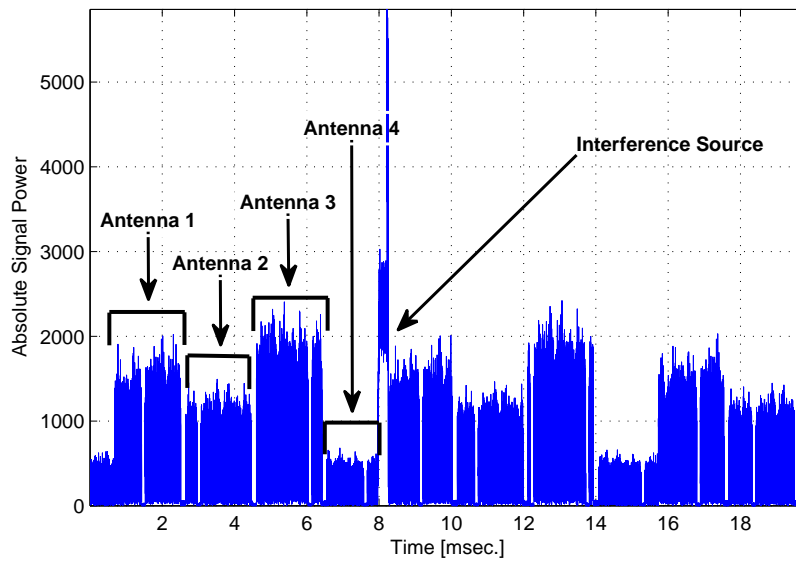
Figure 3.9: WLAN (802.11g) pseudo-Doppler system data (LOS)

increase, E_θ is halved in the switched system, *i.e.*, for 10dB SNR, shifting system $E_\theta = 3.82°$, while it is 7.5417° for $\Delta d = 2\lambda$ spaced 2-antenna case. Finally, it should be noted that more computational power will be consumed in shifted case because data recorded M = 4 will be processed instead of M = 2 for the latter one. However, the measurement results indicate the worth of the trade-off between computational power and error mitigation.
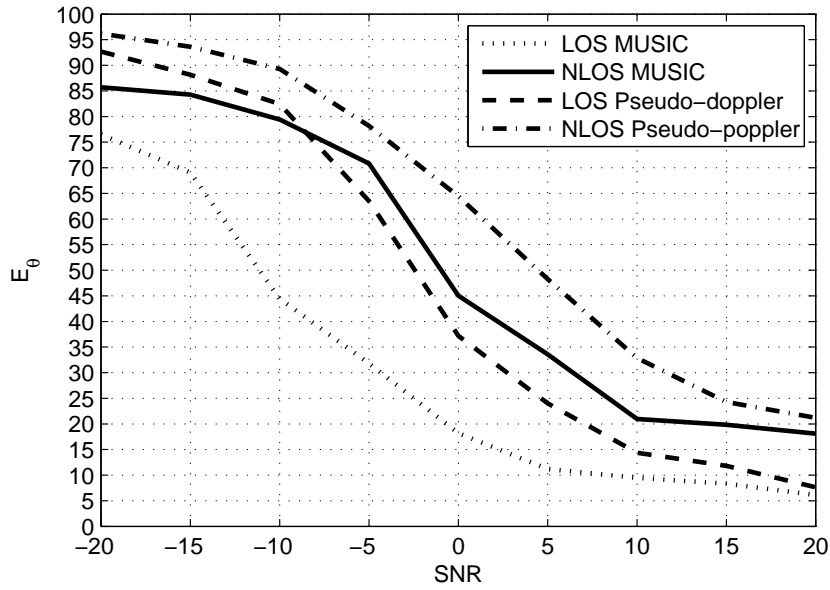
Figure 3.10: MUSIC & pseudo-Doppler comparison

The effect of measurement duration on E_θ is investigated again based on LTE signals, and M = 2(no shift), $\Delta d = \lambda/2$ in Fig. 3.7. The measurement durations at each antenna is selected as 10 ms, 20 ms, and 40 ms consecutively. A performance increase around 10° can be seen at the −10 dB - 5 dB interval when the measurement duration is increased from 10 ms to 20 ms. A couple of degrees of error are still recovered at the higher SNR values. This trend can also be seen between the 20 ms, and 40 ms measurements however, this time the error reduction is not as significant as the former case, for instance, *e.g.*, $E_\theta = 9.4968°$, $E_\theta = 8.036°$ consecutively when the SNR = 10 dB. A comparison between the effect of the measurement duration vs. increasing Δd would also give insight for the selection of the system parameter to be tuned or adjusted to improve the estimation performance of the system. 20 ms plot in Fig. 3.7 corresponds to the $\Delta d = \lambda/2$ in Fig. 3.12(a). Measurement results indicate that, when the data length is doubled to 40 ms for $\Delta d = \lambda/2$, a performance improvement around 3° is achieved when compared to the $\Delta d = \lambda$ in Fig. 3.12(a) for negative SNR values. As the SNR increases to the positive region, this margin reduces down to 1° indicating that no significant performance improvement is achieved when compared to increasing Δd.

3.4.2 Comparison with The Four-Antenna Pseudo-Doppler System

The performance of the proposed system is compared with another single RF front-end DOA estimation method which is called pseudo-Doppler DOA system [78]. This method is selected for comparison

56

considering its widespread deployment for direction finding in commercial systems and system level similarity to the proposed system. On the other hand, there is an extensive literature on the comparison of the eigenvalue decomposition based methods, therefore, replacing the MUSIC algorithm with an another eigenvalue method is excluded from the analysis.

Pseudo-Doppler system employs 4 or more omni-directional antennas which are switched consecutively to create a Doppler frequency shift which leads to the estimation of the direction of arrival of the wireless signal [79]. Four λ spaced 2.4 GHz ISM band antennas are connected to the 4 inputs of the ZSWA-4-30DR switch and the system is configured to the WLAN (802.11g) parameters listed in Table 3.2. Pseudo-Doppler system measurements are conducted for both first (LOS) and second (NLOS) allocations listed in Table 3.3 and the setup for NLOS case can be seen in Fig. 3.8. Note that, antennas are allocated in a square form because better performance is achieved when competed to the linear configuration in this topology. When the system parameters considered, minimum switching time that is available is 1 ms, however, it is selected as 2 ms considering the burst duration of the WLAN signals and each burst recorded from each of 4 antennas can be seen in Fig. 3.9 along with some interference introduce by other in-band transmissions. The peak change in the frequency (Doppler shift in Hertz) of the system is given by

$$\Delta Fc = \frac{2\pi r f_c f_r}{c}, \tag{3.8}$$

where f_r = 125 Hz (2 ms at each antenna) is the frequency of rotation, $r = \lambda/\sqrt{2}$ (3.4204 inches) is the radius of the antenna rotation, f_c = 2.44 GHz is carrier the frequency of the transmitted signal, and c is the speed of the light [115]. Under these conditions, the maximum shift becomes ΔFc = 555.3536 Hz. The estimation error of the pseudo-Doppler system is shown along with the proposed system results for WLAN signals, $\Delta d = \lambda$, M = 2 (no shift) case in Fig. 3.10. Even though at the high SNR (20 dB) region both methods perform relatively close, for 5 dB SNR and LOS, E_θ = 11.1986° for the proposed system and E_θ = 24.02° for the pseudo-Doppler method indicates significant performance difference. The E_θ of the 2-antenna system under $NLOS$ conditions are slightly above of the LOS performance of the pseudo-Doppler system. $e.g.$, for 5 dB SNR, E_θ = 33.5808° for the proposed system while $NLOS$ performance for the pseudo-Doppler method is E_θ = 48.27° .

As the effect if shifting operation and other parameters discussed, now the performance of the proposed 2-antenna system will be considered for various wireless communications systems under LOS and $NLOS$ conditions considering the changing Δd.

57

3.4.3 LOS Measurements

The E_θ of the proposed system for the signal types of WCDMA, cdma2000, ATSC based DVB, GSM/EDGE mixed signals, LTE, WLAN (802.11g), Bluetooth, and DECT 5.0 under *LOS* conditions are illustrated from Fig.3.11(a) through Fig.3.12(d). Each figure consists of three plots which shows the estimation error for the Δd of 2λ, λ, and $\lambda/2$. When all 8 plots are considered together, it can be seen that the estimation error reduces down as the distance between two antennas (Δd) increases. This result is consistent with the previous theoretical work [77, 83]. On the other hand, as the SNR reduces down below 0 dB, the error starts to incline with a more increasing slope. For WCDMA and cdma2000 signals, as of very low SNR = -20 dB, the proposed system can not provide any direction information. For other signals, this point is achieved a little bit earlier, i.e., GSM/EDGE, WLAN, and DECT 5.0 reach this point at -5 dB while ATSC based DVB, LTE and, Bluetooth reach at -10 dB.

If it is assumed that each figure is divided into two from 0dB SNR, for all the signals we can see that until 5 dB SNR the E_θ goes on reducing sharply (or increase of negative SNR values, this trend will be in the terms of increasing E_θ as indicated above) and then, as the SNR increase through the 20dB range, error reduces down with a lower but stable slope. In general, while the error was in the margin of $10°$ to $25°$ for 0 dB SNR, through 20 dB range, for all antenna distances and for each signal type the E_θ is around $5°$.

When the Δd is considered, for SNR values of 5 dB or higher, if the Δd = λ or 2λ, estimation error levels below $10°$ for all signals except for WLAN; in Δd = λ case, for 5 dB SNR, error is just above $10°$ and below $15°$. This characteristic of the WLAN signals stems from its wideband nature which leads to worse scattering characteristics especially under indoor measurement conditions when considered to the other signals transmitted. For particularly Δd = $\lambda/2$, as the SNR reaches to 20 dB, the angular estimation error settles down to the $5° - 10°$ margin, closer to $5°$ in general, which is also compatible with the experimental measurements listed in [72] under similar conditions.

3.4.4 NLOS Measurements

When there is no direct path between the transmitter and the receiving antennas, all the received signal components are comprised from reflected waves. Therefore, not only eigenstructure based methods e.g., MUSIC but also every other signal DOA estimation method experience serious angular estimation performance degradation. The E_{θ_k} of the proposed system for the same signal types under *NLOS* conditions are depicted trough Fig.3.13(a) to Fig.3.14(b). Bluetooth and DECT 5.0 are excluded from *NLOS* analysis due

58

(a) WCDMA

(b) cdma2000

(c) ATSC (DVB)
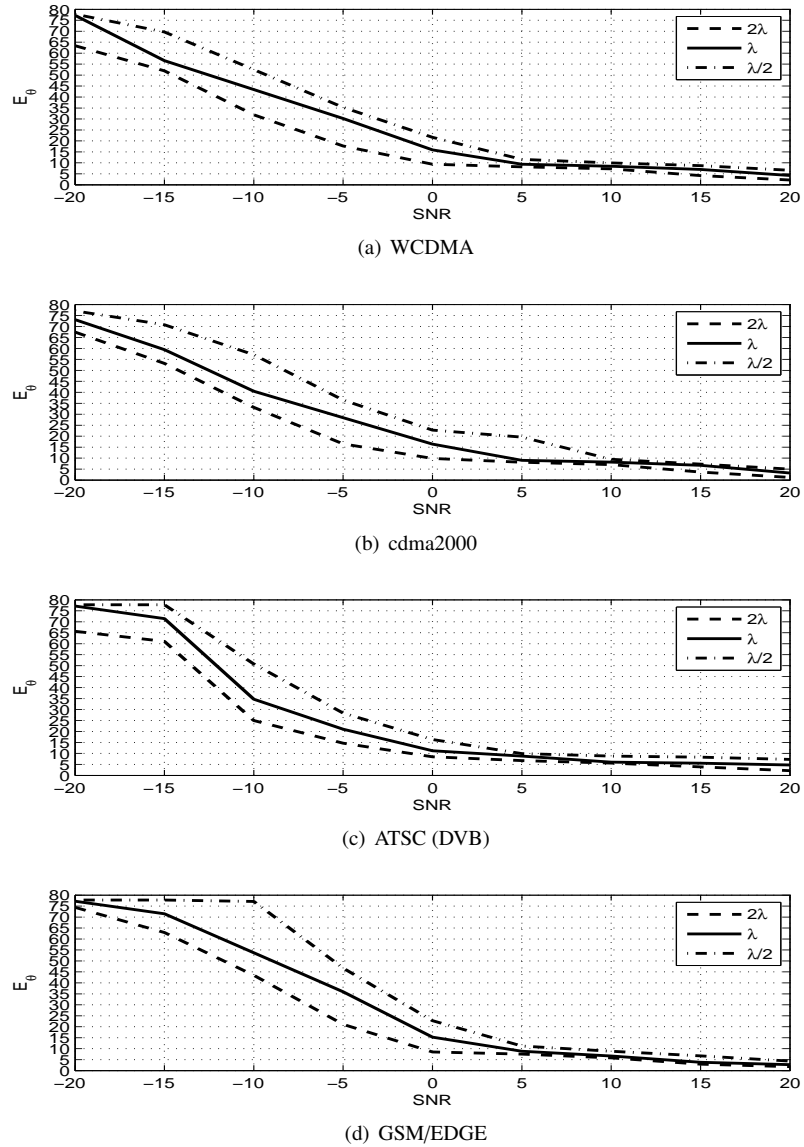
(d) GSM/EDGE

Figure 3.11: LOS measurements: pt.1

to their short range characteristics. Each figure consists of three plots which shows the estimation error for $\Delta d = 2\lambda$, λ, and $\lambda/2$.

When the $\Delta d = \lambda/2$ case excluded, ATSC, GSM/EDGE, and WLAN, the E_θ is less than $25°$ as the SNR reaches to 10 dB. For the rest of the signals, under same conditions the upper bound for angular estimation error becomes $35°$. However, the proposed system cannot provide any information regarding to signal DOA below 0 dB SNR when there is no direct path between transmitter and any of the receiver antennas for all signal types.

59

(a) LTE

(b) WLAN (802.11g)

(c) Bluetooth

(d) DECT 5.0
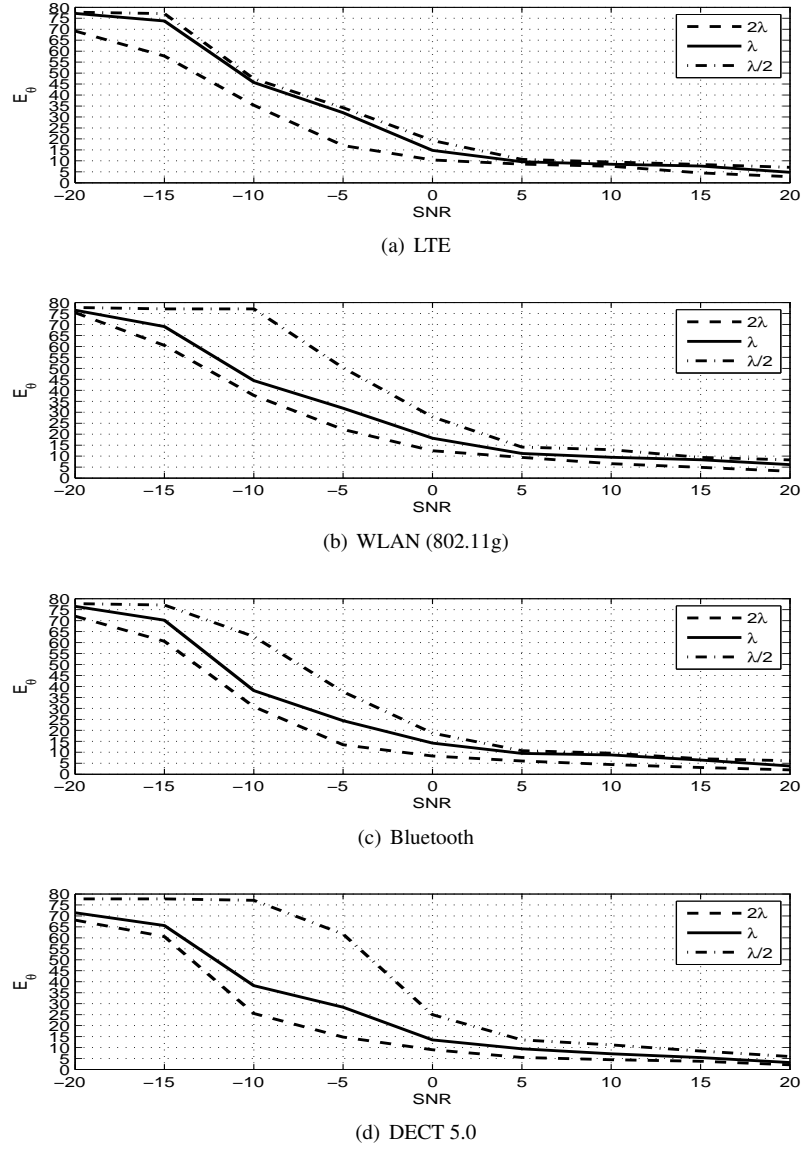
Figure 3.12: LOS measurements: pt.2

In case of $\Delta d = \lambda/2$, 15 dB of SNR is required to be able to reduce down the E_θ below 30° for cdma2000, WCDMA, and LTE signals. For the rest of the signals, under the same conditions, the error upper bound becomes 25°. As the SNR increases to the level of 20 dB, average estimation error reduces down below 25° for all signals and each antenna configuration.

In conclusion, a two-antenna, single receiver DOA estimation system based on switched antennas and sequential sampling is proposed for wireless communications signals. The proposed system performs better than the pseudo-Doppler system however, under LOS conditions, pseudo-Doppler system over-performs

60

(a) WCDMA

(b) cdma2000

(c) ATSC (DVB)

(d) GSM/EDGE
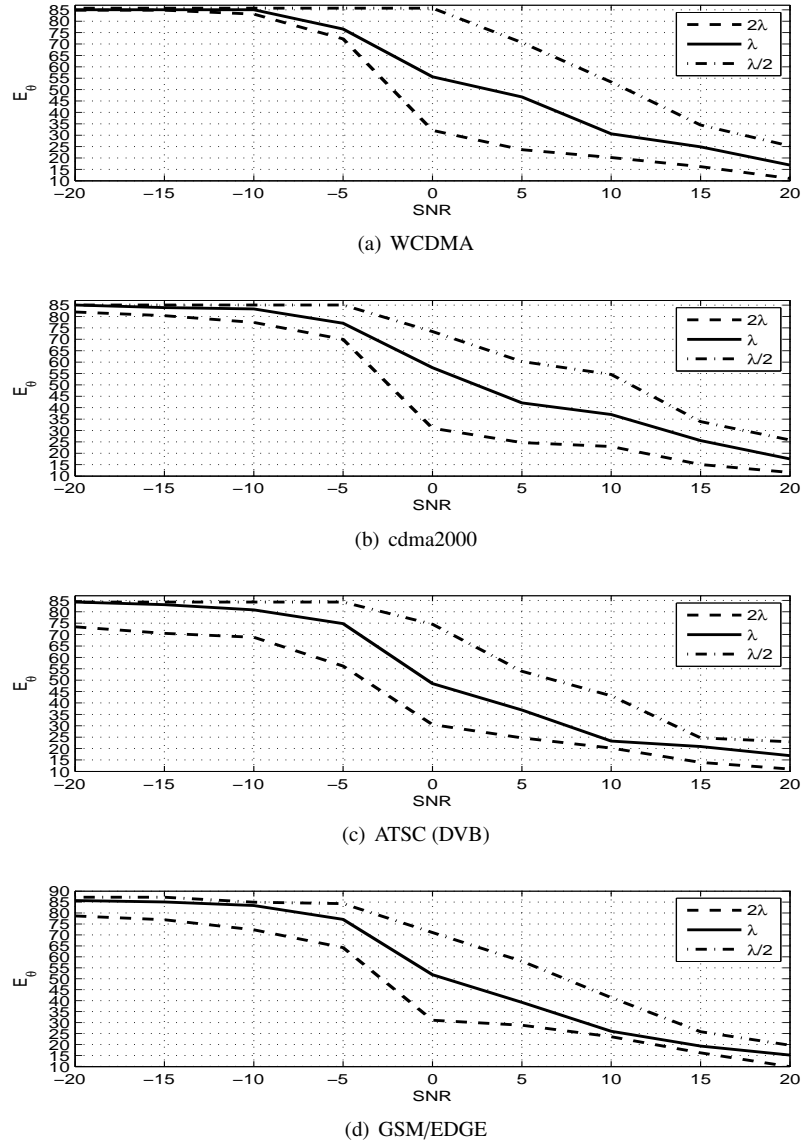
Figure 3.13: NLOS measurements: pt.1

the NLOS performance of the 2-antenna system. On the other hand, the 2-antenna system performs slightly better for narrowband signals when compared to the wideband signals and this is an expected results when the MUSIC method is considered. There is an important performance difference between LOS and NLOS cases in general which is due to the lack of direct path between signal source and the DOA estimation system. The 2-antenna system performs considerably well for positive SNR values for LOS conditions, however, a certain level of confidence is achieved for very high level of SNR in case of NLOS. Note that, improvements in the estimation performance can be achieved by increasing the total measurement time and shifting oper-

61
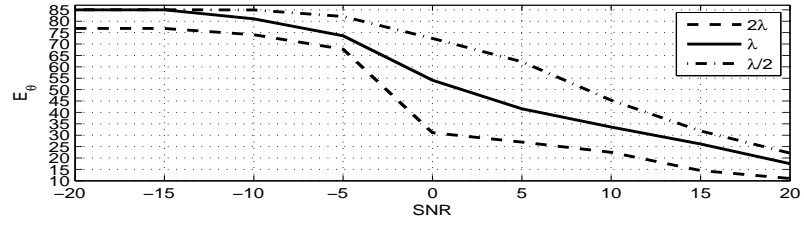
(a) LTE
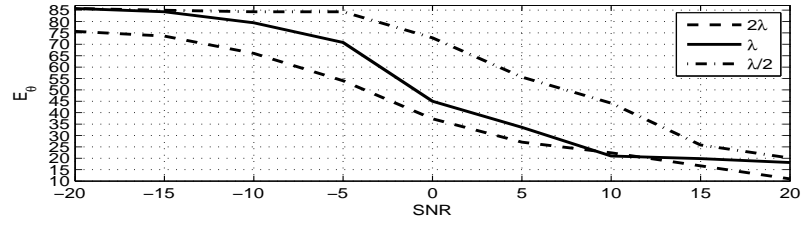
(b) WLAN (802.11g)

Figure 3.14: NLOS measurements: pt.2

ations also taking the channel holding durations into consideration. Tracking the DOA under the condition of mobility, multiple user scenarios including the coherent signals, and investigation of the effect of angular spread due to multipath fading channels are the open areas to be investigated in terms of system efficiency.

62

CHAPTER 4

AN AUTOREGRESSIVE APPROACH FOR SPECTRUM OCCUPANCY MODELING AND PREDICTION BASED ON SYNCHRONOUS MEASUREMENTS

4.1 Introduction

RF spectrum allocation inefficiency is an important problem when the increasing demand for more wireless bandwidth due to growing number of users and prevalence of the wideband applications are taken into consideration[1]. Cognitive radios (CR) introduce solutions to the problem via spectrum sensing methods which employ secondary users (SUs) in the spectrum when it is not occupied by the legacy or primary users (PUs). Even though the spectrum sensing procedures provide the information about the status of the wireless channels, modeling and prediction of the communications activity can contribute to the spectral efficiency improvement efforts. Channel status prediction information can be used by SUs to decide the sensing periods and channel occupation durations in single channel sensing scenarios [116]. Beside that, based on prediction information, SUs can select the channels with higher probability of vacancy in multi-channel wideband sensing scenarios [117] and PU occupancy models can be used as empty channel indicators replacing the spectrum sensing procedures [118].

The PU behavior modeling research followed the spectrum measurement campaigns and one of the main approaches is the continuous-time Markov chain modeling (CMCM). For example in [119], initially a 5-state CMCM is applied over simulated data considering the medium access control (MAC) layer requirements and assuming Poisson distributed traffic. Moreover, time-domain bursty transmissions of wireless local area network (WLAN) signals are also modeled via CMCM indicating generalized Pareto fit for idle (OFF) periods [120]. Later on, a constrained Markov chain process is proposed with throughput and collision analysis for unslotted traffic model [121]. On the other hand, the constrained partially observable Markov decision process (POMDP) is modified for unslotted systems assuming that the number of the channels monitored are fixed and PU activity is exponentially distributed [122]. In [123], duty cycle, first order Markov chains and periodicity detection methods are used to investigate the availability of a certain amount of bandwidth

---

[1]The content of this section is publishes in [108]. Copyright for these publications can be found in appendix C.

63

equal to the sensed frequency bands. A 2-state Markov model is also proposed indicating hyperexponential distribution for real measurements [124]. CMCM is also used for PU behavior modeling when active PU/SU numbers are known [125].

Beside the Markovian approaches, solutions of multi-armed bandit problem are also adapted via a regret function to the spectrum modeling assuming PU occupancy is Pareto distributed [126]. A proactive channel access method is also proposed based and ON/OFF processes which are exponentially distributed [127]. Duty cycle analysis in time domain is conducted by using the geometric and log-normal distributions [116] and a spectrum modeling and prediction framework is proposed in [128] assuming the PU activity is Poisson or exponential distributed. [129] proposed a neural network model over the multilayer perception predictor with two hidden layers which is simulated for spectrum prediction assuming that the PU traffic is Poisson distributed.

The Markovian modeling processes can be categorized as either restricted models that modeling parameters such as number of PUs are known [125] or models limited to the slotted/unslotted bursty trans-missions over a single channel [119–121]. In multi-channel scenarios, the channels are assumed to be in-dependent [122, 128]; however, this may not be the case especially for adjacent frequency channels [130]. Moreover, the general assumption of PU ON/OFF times are Poisson and exponential distributed is based on a MAC layer method proposed for spectrum agility over package transmission rates [131] and may not be valid for spectral occupancy at each section of the wireless spectrum. For instance, based on real-time mea-surements [132] indicates Beta distribution characteristics. Finally, beside the time and frequency, another orthogonal dimension of the electrospace is the location [133]. In the literature, several studies on modeling efforts conducted at different locations in different times indicate that location information can be used during the modeling procedures [130, 134]. Beside that, in [135] the authors investigated the distribution charac-teristics of the channel vacancy durations and proposed a pattern mining algorithm based on synchronous measurements at different locations.

In this chapter, we applied the binary time series prediction approach to a set of wideband spectral measurements conducted at four different locations in a synchronous manner [108]. The proposed autoregres-sive method enables us to compare the prediction of spectral occupation at four different locations through modeling parameters (*e.g.*, model order and observation duration) and prediction performance for each lo-cation are studied in a comparative manner. Note that, this study does not require having any knowledge of the characteristics of the signals captured in contrast to several studies in the literature [136, 137]. In addition, the proposed method does not assume any specific distribution about the wireless signals recorded.

64

It is shown that the proposed method performs reasonably even for low model orders. This stems from the fact that dependency of the frequency channels are also taken into consideration by including the channels in pairs here. The prediction analysis for each location is given comparatively with respect to observation time. The prediction performance is also compared with the CMCM.

4.2 Measurement Setup

4.2.1 Measurement Equipments, Setup, and Locations

The measurement setup and settings used are identical for each location and a Rohde & Schwarz FSH6 Portable Spectrum Analyzer (SA) is connected to a laptop via a USB-optical cable. The SA is also connected to a very high performance discone antenna (AOR DA5000) with a 700-3000 MHz frequency range and omni-directional horizontal receive capability. Data was collected concurrently in four different geographical locations starting at 6:00 PM local Qatar time (GMT+3) March 19, 2009 and ending 6:00PM March 22, 2009 [138]. The four locations are designated Location 1 to 4 and selected to represent different environments in the Doha, the capital city of Qatar. Location 1 is located in the west of Doha, and comprises a number of educational campuses surrounded by vast open and generally flat spaces with some construction work going on. There are no commercial/residential buildings or areas in the vicinity. Location 2 is in the south east of Doha and is a busy commercial area. Different radar (aviation) and communications systems are deployed and as such it is an electromagnetically rich environment. Location 3 is closer to what is considered the downtown of Doha and consists of high towers (average 30 floors +) and large commercial centers in addition to a hospital and a police station. Location 4 is in the south of Doha and consist of factories and workshops. For each location,(72 hours of continuous recording with one data set generated per minute) 4320 different readings of the $700 - 3000MHz$ spectrum are collected during the measurement campaign. The clock of each measurement setup is synchronized prior to placing them in their respective measurement locations.

4.2.2 Measurement Settings and Procedure

As stated earlier, one of the most prominent contributions of this study is the perfect synchronization for each measurement taken from four different physical locations simultaneously. In order to achieve such a synchronization between the measurements, the device capabilities such as sweeping time for the frequency band to be captured, resolution, capturing period, dumping time, and transferring the measurement to the computer all should be calculated and taken into account. Note that some of these parameters in recording

65

step can be different and some of them (such as frequency resolution) can be same for each measurement setup at every location. Therefore, a buffer period upon the completion of the transfer of the measurement to the computer is essential so that the synchronization between measurements is maintained. Given all these, it is found out that when sweeping time is set to 128msec and resolution bandwidth is set to 300kHz for a span of 2.3GHz of center frequency at 1.85GHz, perfect synchronization between different measurement campaigns can be established. In light of these, the time duration between each consecutive measurement start for each setup is set to one minute. It is also important to state that especially for cellular band over which the traffic carried is mainly voice oriented, one minute provides a very good resolution to capture the occupancy statistics since average channel holding time is around three minutes. Interested readers might refer to [138] for further information on the measurement setup and results.

4.3 Proposed Method

Spectrum occupancy and opportunities can be considered to be complementary notions. From this point of view, it is crucial to investigate what the main parameters of the spectrum are and how they are related to each other. Obviously, because power spectrum is of concern, frequency and received power are two prominent parameters. Received power is a function of transmitter receiver separation; therefore, space must be included into the model as well. Finally, because the occupancy pattern of spectrum changes in time, the model needs to take into account time as another parameter. It must be noted that for a specific frequency, received power and occupancy statistics evolve at different rates in time. For instance, generally speaking, user equipments need to know what the spectrum opportunities would be in the next time slot when they reside within the same physical region. Even though the user equipment is in motion in general and many statistics change due to mobility, the space parameter mentioned above can still be considered as constant for very small time slots so that the occupancy prediction can be established. Therefore, it is reasonable to think that some of the very slowly changing (or not changing at all) parameters can be represented with constants in order to fine-tune the model for different cases.

In parallel with the statements above, the model is desired to be as general as possible in such a way that it can handle multiple frequency bands simultaneously (and degenerate to one single band scenario as a special case). Moreover, the model should be independent of the transmission technologies while it can still support the history of the occupancy (if available). Therefore, the proposed model does not need to have a priori knowledge on the communication environment such as bursty transmissions in time, spread signals, or continuous control channel transmissions. It is important to state here that, absence of such a

66

priori information will reduce the model complexity. However, an irreducible error can still be observed in the performance since especially in downlink cellular bands control channels are active most of the times. Such measurements which do not actually contain any user activities will mislead the model and cause false alarm rate to increase in an irreducible manner.

In light of the aforementioned discussions, from the perspective of spectrum sensing, it is important to know if the wireless channels are occupied (busy) or unoccupied (idle). Therefore, the proposed method treats the previous available occupancy status as either busy or idle and this process can be represented with a binary time series which can be obtained by hard-clipping the underlying process, namely the power spectrum observed for a specific location in time [139]. The hard-clipping step is established by employing a threshold, where the underlying process F_t is transformed into binary series S_t given by

$$S_t = \begin{cases} 0 & \text{if } F_t < \lambda \\ 1 & \text{if } F_t \geq \lambda \end{cases} \tag{4.1}$$

where λ is the threshold and t is the time index. Note that the performance of the wireless signal detectors are out of the scope of this study however, selection of detection threshold is an important issue. Either analytical and empirical methods can be followed [140] but, especially for extensive measurement campaigns with wideband spectrum recording, empirical methods are preferred due to their simplicity. Besides, estimation of the parameters such as the noise variance and SNR are not required for empirical methods [128]. Therefore, in this study the empirical threshold which is 3dB above the noise floor of the recording equipment is selected similar to the threshold introduced for the extensive measurements at different locations in [130].

When the modeling procedures considered, if H is defined as the number of the past observations considered in modeling procedures, collecting H observations in its memory, the proposed method strives to obtain a binary time series model which accommodates the aforementioned properties in this section. Therefore, employing a linear regression would be natural choice, since it allows to consider multiple frequency bands simultaneously and in this study, the dependency in frequency is introduced by modeling the adjacent channels in pairs as indicated in Fig. 4.1. When the binary data in hand considered, direct implementation of the generalized linear models can become problematic because the expected value of the process may exceed the interval of [0, 1]. Therefore, in order to overcome this problem, linear regression of past observations can be evaluated by logit transformation [141] to search for probability of channel i to be occupied at the time

67
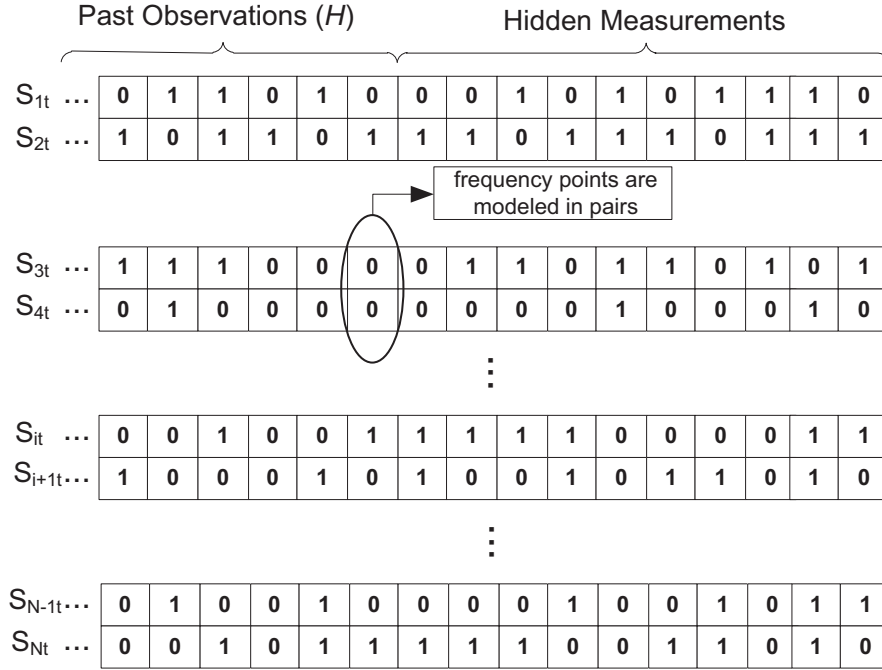
Figure 4.1: Binary time series representation and frequency pairs

instant t by:

$$P(S_{it} = 1 | \mathbf{S}_{t-1}, \mathbf{S}_{t-2}, \ldots, \mathbf{S}_{t-p}) = \frac{1}{1 + e^{-\mathbf{M}}}, \tag{4.2}$$

where $\mathbf{M}$ is the autoregression defined as in [142]:

$$\mathbf{M} = \mathbf{a}_0 + \sum_{j=1}^{d} \left(\mathbf{A}_j \mathbf{S}_{t-j} \right) + \mathbf{n}, \tag{4.3}$$

with the coefficient matrices $\mathbf{A}_j$, error vector $\mathbf{n}$, intercept (or offset) $\mathbf{a}_0$, model order d, and the past values observed $\mathbf{S}_{t-j}$. In fact, (4.3) can be written in a more compact form as $\mathbf{M} = \mathbf{A}\mathbf{s}_{\mathcal{F}} + \mathbf{n}$, where $\mathbf{A} = [\mathbf{a}_0 \ \mathbf{A}_1 \ \mathbf{A}_2 \ \ldots \ \mathbf{A}_d]$ and $\mathbf{s}_{\mathcal{F}} = [1 \ \mathbf{S}_{t-1}^T \ \mathbf{S}_{t-2}^T \ \ldots \ \mathbf{S}_{t-d}^T]^T$ [142]. Replacing $\mathbf{M}$ in (4.2), the problem can be presented in the following form:

$$\pi_t = \frac{1}{1 + e^{-(\mathbf{A}\mathbf{s}_{\mathcal{F}} + \mathbf{n})}}. \tag{4.4}$$

The nature of binary data in hand forces one to take the statistical characteristics of the noise (shock) term $\mathbf{n}$ into account. The stochastic variables which denote the noise can be assumed to be independent both

68

Table 4.1: Model order selection for spectrum occupancy data in four locations

Model (M)	Mean Residual Error				AIC			
	Loc.1	Loc.2	Loc.3	Loc.4	Loc.1	Loc.2	Loc.3	Loc.4
$a_0 + A_1 S_{t-1} + n$	0.0825	0.0766	0.0818	0.0831	595.7188	566.3450	563.3363	590.7037
$a_0 + A_1 S_{t-1} + A_2 S_{t-2} + n$	0.0775	0.0821	0.0523	0.0515	572.9014	560.5617	603.1760	587.4660
$a_0 + A_1 S_{t-1} + A_2 S_{t-2} + A_3 S_{t-3} + n$	0.0597	0.0625	0.0504	0.0125	551.6575	551.2957	568.0403	583.3040

of each other and of the data in hand. Moreover, the noise terms are assumed to be identically distributed and modeled via a logistically distributed probability density function accordingly, which is $f_n(x) = e^x/(1 + e^x)^2$ with $\mathcal{N}(0, (\pi^2/3))$ [141, 143].

4.4 Numerical Results

The monitored spectrum covers continuously occupied bands such as some of ultra high frequency (UHF) TV channels, barely occupied navigation channels, unlicensed bands, and cellular bands. The detailed analysis of the occupation statistics of these bands at each location can be found in [138]. The focus of this study is to predict the spectrum occupation under dynamic use. Therefore, the proposed modeling and prediction approach is implemented over the GSM-900, UMTS cellular bands and 2.4 GHz ISM band.

First step of applying the proposed autoregressive method to the recorded measurements is the selection of the model order that will be used throughout the modeling and prediction stages. The criteria such as Pearson residuals, mean response residual magnitudes, and Akaike information criterion (AIC) can be used for this purpose [141]. We employed mean of the response residual magnitudes and AIC which is given by $AIC(d) = K \ln(\det(\Sigma_e)) + 2N^2 d$ where Σ_e is the noise covariance vector, N is the number of the frequency channels recorded, K is the size of the system memory in which the bits of binary time series can be stored and selected as 5 megabits to be able to hold the information recorded in four locations. The determinant of Σ_e is defined by $\det(\cdot)$ and reliability condition of $N^2 d \ll KN$ is also satisfied [144]. Models, criteria and corresponding parametric values are listed in Table 4.1. As can be seen in Table 4.1 in general third-order model provides better results. Note that, due to space limitations, only the table attaining to GSM band results is shown. However, similar results are observed for other bands.

Secondly, after determination of the model order, we investigated the impact of observation time (which can also be considered to be history, H) on the prediction error in each location. The prediction error of the first hidden measurement with respect to observation time is shown in Fig. 4.2. Each point in Fig. 4.2 represents the mean of the prediction error which is calculated by $P_e = E\{|S_t - \hat{S}_t|\}$ at each location. Keeping in mind that the irreducible error mentioned earlier especially for GSM bands, it can be inferred

69
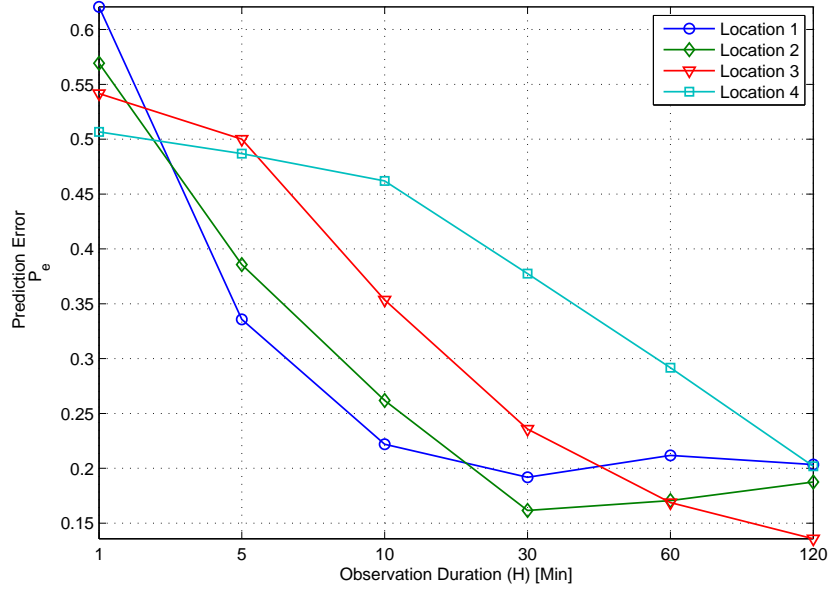
Figure 4.2: Prediction error vs. observation time

from the figure that while half an hour of training or observation time is sufficient for Location 1 and 2, up to two hours of observations are needed for the other locations. Next, the prediction performance of the proposed method is investigated. In order to evaluate the performance next ten minutes for two consecutive frequency points of uplink GSM channels are considered with the observation time of 30 min for Location 2. The results are illustrated in Fig. 4.3. Note that, the binary nature of the input data effects the prediction mechanism in two aspects: First, when there is no history information available, the threshold corresponds to the case of maximum uncertainty. However, since logistic transformation is required, the value of the threshold is calculated according to (4.4). Secondly, the modeling procedures may not immediately track the changes in the binary states and initial prediction of the state of the channels becomes prune to error. This issue can be addressed by optimizing the selection of parameters such as model order.

Finally, for comparison purposes, as the most common modeling tool, a Markov chain is implemented. Even though it is shown that there is no significant performance improvement achieved for higher order Markov chains [117], in order to have a fair comparison the Markov chain that is used is designed to store the last two bits of the occupancy status history. Hence, the Markov chain implemented consists of the following four states along with their inter and intra-state transition probabilities: {00},{01},{10}, and {11}. Prediction for Markov chain is established by evaluating the training data in hand. The prediction perfor-
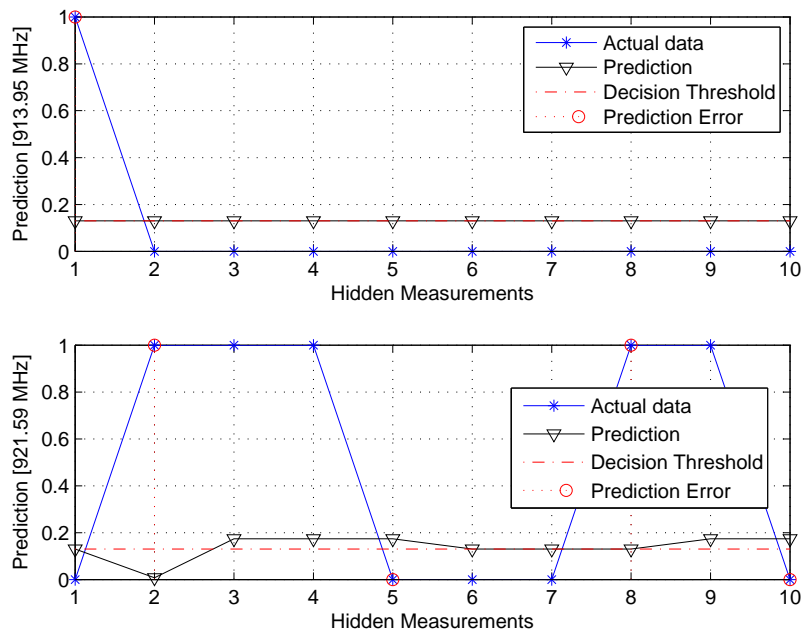
Figure 4.3: Prediction error vs. hidden measurements
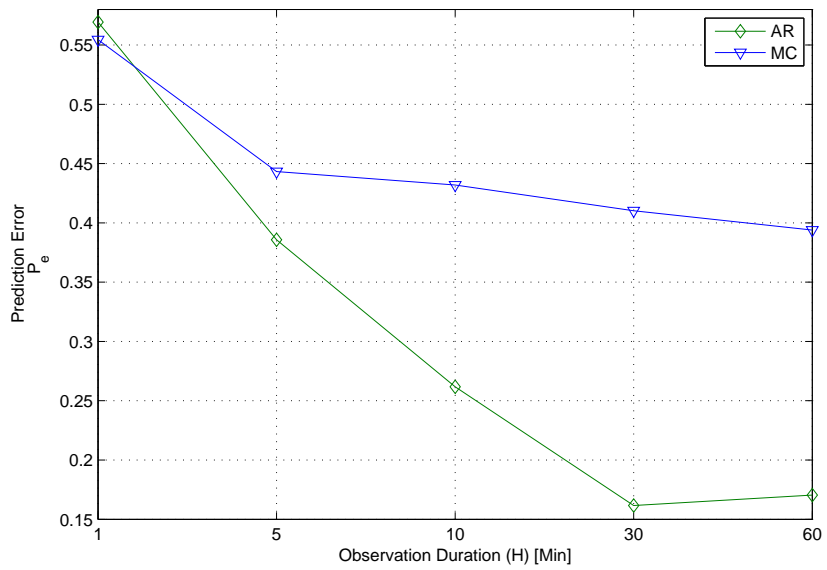
Figure 4.4: Autoregressive vs. Markov chain prediction in location 2

71

mance comparison is given in Fig. 4.4 only for Location 2 due to the space limitations, considering different observation intervals and the first hidden measurement. Note that, while the prediction error is close for the short observation durations, the autoregressive modeling approach outperforms the CMC as the observation duration is increased because while CMC updates its modeling parameters sequentially or step by step until the end of observation duration, autoregressive method uses the whole observation information at once considering the observations in two frequency channels together as pairs.

In conclusion, modeling and prediction efforts can contribute to the solve the spectral efficiency problem. Proposed autoregressive approach shows that beside time and frequency, location information should also be considered to optimize the prediction performance of modeling processes. This way, the occupancy statistics (observation time) can be taken advantage of along with the use of fine tuned parameters such as space. As the future work, the linear autoregressive method used will be extended into a new model including the location as an independent parameter, which will also lead to the direct comparison of the occupation differences in each location.

72

TEMPLATE MATCHING FOR SIGNAL IDENTIFICATION IN COGNITIVE RADIO SYSTEMS

Frequency spectrum inefficiency is an important problem for wireless communications systems[1]. Federal Communications Commission's (FCC) Spectrum Policy Task Force (SPTF) report [5] remarked this problem and following the SPTF report, FCC issued Notice of Proposed Rule Making that recommends the employment of communications techniques such as cognitive radios (CRs) to improve the efficiency of spectrum access [145]. The spectrum sensing feature of CRs focuses on detection of licensed or primary users (PUs) via digital signal processing methods of non-coherent energy detection, coherent techniques of matched filtering and cyclostationary feature detection [146]. The performance of the spectrum sensing techniques can be affected from the lack of a priori information and the wireless channel knowledge. Thus, sensing performance can be improved by the methods that can identify the wireless signals based on the signal signatures and characteristics.

On the other hand, SPTF report also recommends the improvement of wireless throughput by achieving signal orthogonality over a range of dimensions named grouped under a domain called as spectrum hyperspace [6]. Spectrum hyperspace includes but not limited to frequency, time, space, power, polarization and code and utilization of these dimensions to improve the throughput requires identification of wireless signals in the spectrum. Note that, signal identification solely based on energy detection is not possible and matched filtering and cyclostationary analysis only address some specific features in time and frequency dimensions. Therefore, beside these three techniques, new methods depending on specific features of wireless signals should be introduced for signal identification.

A time domain signature correlation based spectrum sensing method which leads to identification of ATSC digital television (DTV) signals is proposed in [147]. Spectral correlation sensing which depends on the spectral signatures of the ATSC and NTSC signals is introduced for the 802.22 standard in [148], but no performance analysis is given. On the other hand, scaling issues (especially vertical scaling representing the power) of the templates against the signals with unknown power level are addressed in [149] by the employing

---

[1]The content of this section is publishes in [155].Copyright for these publications can be found in appendix D.

the similarity functions based on Frobenius norm, geodesic distance, and Capon's method measures. These methods are applied to several scenarios including multiple antennas and frequency division multiple access based systems [150–152]. Periodogram correlation with a known spectral signature is investigated again for ATSC DTV signals in [153]. This method assumes that the templates are available to the receiver and performs well under low SNR however channel estimation is required to achieve optimum results. Radial basis function neuronal networks and cyclic autocorrelation method are implemented for blind wireless signal standard identification for software defined radio tools in [154].

In this chapter, template matching method which is widely used in the areas of feature tracking, face recognition, biomedical signal analysis is proposed for the identification of the wireless signals in the frequency spectrum [155]. Implementation of template matching methods for signal identification is advantageous from various aspects such as the single color dependency [156], total power computation [157], and the number of templates to be stored [158]. Template matching is applied to the wireless communications via template parameter calculation, template scaling and construction, and decision mechanisms. These are discussed and formulated along with the two new metrics, code block distance ($CBD(\alpha)$) and normalized area correlation ($NAC(\alpha)$) which are introduced to identify the wireless signals with the help of template signals that are held in CR itself. The performance of the proposed method is compared with the energy detection under fading wireless channels and the performance analysis of the metrics on distinguishing the signals with similar signatures is conducted considering the wideband code division multiple access (W-CDMA) and 3-carrier cdma2000-3x signals.

Through the rest of the chapter, first the system model is defined in Section 5.1. Secondly, the proposed method is introduced along with the template matching metrics, decision mechanism, and parameter calculation procedures in Section 5.2. The performance of the proposed metrics are discussed in Section 5.3.

5.1 System Model

It is assumed that multiple channels or a chunk of the frequency spectrum is monitored. Therefore transmit signal model can be given by

$$x(t) = As(t), \tag{5.1}$$

$s(t) = [s_1(t), ..., s_n(t)]^T$ represents n independent signals and T denotes transposition. $s_n(t) = \sum_{k=-\infty}^{\infty} b_k u(t - kT_s)e^{j2\pi f_{c,n}t}$, where $n = 1, 2, \ldots, N$, j is defined to be $\sqrt{-1}$, $u(t)$ is the pulse shaping filter for $f_n - f_{n-1}$ frequency range, b_k are the digitally modulated symbols, $f_{c,n}$ is the center frequency given by $(f_{n-1} + f_n)/2$,

74

and T_s is the symbol duration. A is $n \times n$ coefficient matrix with $a_{i,j}$ elements where $i, j = 1, ...n$. After digital conversion and modulation, each independent signal passes through a different channel which can be modeled as a time-variant linear filter

$$h(t) = \sum_{i=1}^{L} h_i(t)\delta(t - \tau_i), \tag{5.2}$$

where L is the number of taps for the channel h and τ_i is delay for each tap. It is assumed that the taps are sample spaced and the channel is constant for a symbol but time-varying across multiple symbols.The transmitted signal is received along with noise at the receiver. Therefore, baseband model of the received signal after down conversion also considering the channel model given in (5.2) can be given by

$$y(t) = e^{j2\pi\xi t} \sum_{i=1}^{L} x(t - \tau_i)h_i(t) + w(t), \tag{5.3}$$

where ξ is frequency offset caused by inaccurate frequency synchronization and $w(t)$ corresponds to additive white Gaussian noise (AWGN) sample with zero mean and variance of σ_w^2. The received signal is sampled with sampling time (Δt) at the analog to digital converter (ADC) and discrete-time received signal can be represented in vector notation by

$$y(n) = [y(1), y(2), \ldots, y(N)]. \tag{5.4}$$

The frequency domain representation of the received signal is given by a 2-tuple or pair $g(k, Y(k))$ where $Y(k) = \sum_{n=0}^{N-1} y(n)e^{-j2\pi k \frac{n}{N}}$ is the fast Fourier transform (FFT) over the discrete samples and $k = \{F_1, F_2, \ldots, F_N\}$ are the N frequency points of the wireless spectrum. On the other hand, the template signal is given by $y_t(t) = x(t) = a_1 s_1(t)$ and discrete-time template signal becomes $y_t = [y_t(1), y_t(2), ..., y_t(M)]$ and the frequency domain representation of the template is given by the pair $t(u, Y_t(u))$ where $Y_t(u) = \sum_{m=0}^{M-1} y_t(m)e^{-j2\pi u \frac{m}{M}}$ is the FFT of y_t on u, $u = \{1, 2 \ldots, M\}$ are the indexes of the template in frequency domain, and $N \geq M$.

5.2 Proposed Method

] Template matching is one of the fundamental operators in image analysis, computer vision and finds applications in the engineering field. When the wireless signals considered, it can be defined as solution to the problem of detecting an object in a two dimensional search space which is constituted by signal power and frequency [159]. Furthermore, power spectral density (PSD) of a complex signal can be interpreted as an image which is a single colored discrete plot over a white background. Under these conditions, template matching is applied most efficiently [156]. On the other hand, computation of total power of the image field

75
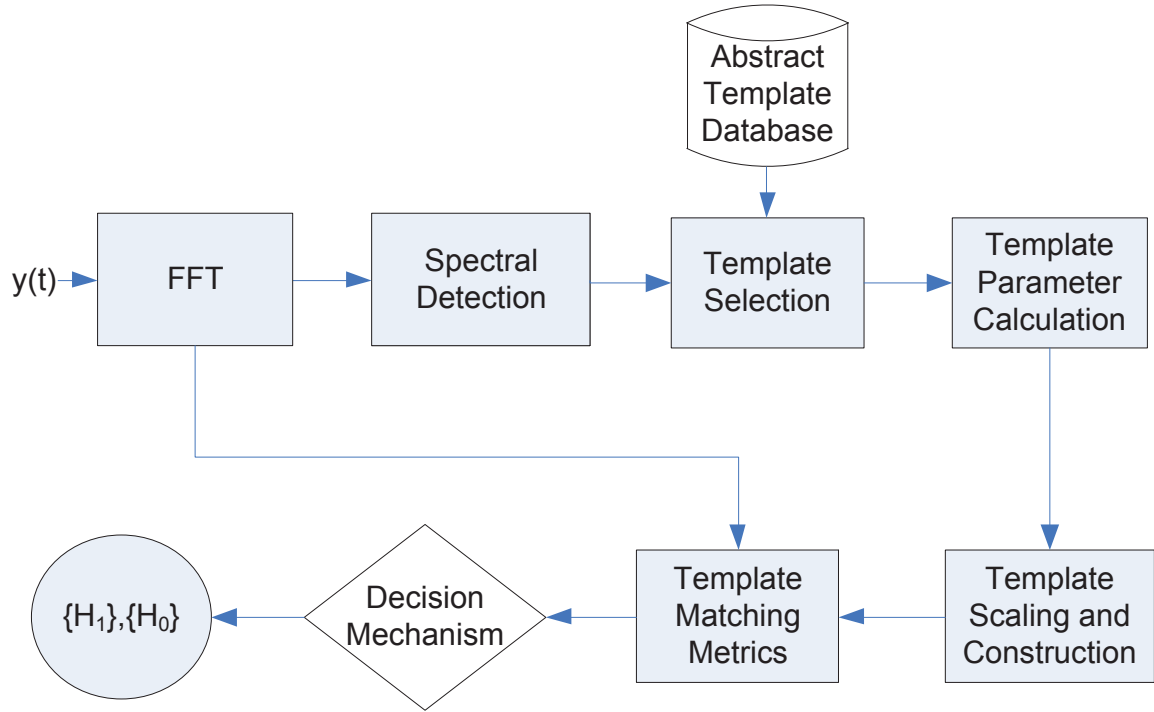
Figure 5.1: Flow diagram of the proposed template matching method

that is correlated with the template increases complexity of template matching procedures [157] therefore, fast template matching methods are proposed in the literature [163] and in the peculiar case of wireless signals, total power can easily be calculated. Another important aspect is the number of templates used. If the number of objects are not limited in some context, applying the template matching algorithms for many templates can be inefficient and time consuming [158]. Moreover, storing an excessive number of templates can be problematic. Again, in the literature, efficient template matching methods are proposed to overcome these problems [164]. However, in this peculiar case, number of templates are limited to the number of existing wireless standards. More importantly, template signals are stored in abstract, i.e, time-domain complex signal form and the abstract templates can be adjusted in power and frequency consequently. Therefore, there is no need to hold a different template for each signal to noise ratio (SNR) level and frequency span. Templates are resized or scaled by template scaling and construction methods

The flow digram of the proposed signal identification method is given in Fig. 5.1. It is assumed that complex baseband or intermediate frequency (IF) recording is acquired by CR. Number of PUs in the given spectrum are not known. Thus, a wideband spectral signal detection procedure is assumed to detect

www.manaraa.com

occupant signals and provide a priori information of signal power level and bandwidth. Next, in the template selection stage, the templates to be used are decided and the abstract templates are found in the database depending on the bandwidth information for each detected signal provided by the spectral detection stage. The number of selected templates can be more than one based on the estimated signal bandwidth. Then, in the template parameter calculation stage, the parameters that will be used for template scaling are computed by taking the recording parameters such as Δt, signal power levels, and recorded spectrum FFT size (N) into consideration. The calculated parameters are passed to the next stage for scaling and template construction along with the selected template abstract(s). After the template(s) are constructed in frequency domain, template matching metrics are applied as the templates are slided over the spectrum and the output is sent to the decision mechanism to decide the type of detected signals. Note that, in case the spectral detection stage can not detect any signal in the spectrum, the templates will be constructed with the minimum power level and slided over the spectrum for both signal detection and identification purposes. In this case, only the templates of the signals that are expected at the monitored part of the spectrum will be constructed. The scope of the study is limited to template matching metrics, decision mechanism, and template parameter calculation. Template selection is a straightforward comparison operation between the estimated signal and template bandwidths. Scaling and construction are also defined as the linear operations on the templates depending on the calculated parameters. Moreover, a simple empirical threshold can be used for coarse spectral detection and [140] can be consulted for further information.

5.2.1 Template Matching Metrics

Template matching is applied by shifting a constructed template signal through the spectrum and it is compared with the corresponding spectral region in order to detect similarities. If the match between an unknown signal and a template is close enough, the unknown signal can labeled as the template signal [157]. In general, there will not be an exact match because of the phase offset between samples, noise, spatial and amplitude quantization effects, and wireless channel impairments. Therefore, some metrics are needed to be defined in order to quantify how well the template signal matches to the signal to be identified on a section of the spectrum.

If the domain of definition of $g(k, Y(k))$, $\forall(k)$ is $[N, P_s]$, where P_s is the peak signal power detected in the spectrum and the domain of definition of $t(u, Y_t(u))$, $\forall(u)$ is $[M, P_t]$, where P_t is the peak power level

77

of the samples of the template, a metric called CBD is defined as [156]

$$D(\alpha,\beta) = \sum_p \sum_q |g(p,q) - t(p-\alpha, q-\beta)| \tag{5.5}$$

$\forall(p,q) : (p-\alpha, q-\beta) \in [M, P_t]$, where (α,β) are the displacement coordinates, $0 \le \alpha \le (N-M)$, and $0 \le \beta \le (P_s - P_t)$. Another general means of measuring similarity can be defined using expanded Euclidean distance of

$$E^2(\alpha,\beta) = \sum_p \sum_q [g(p,q) - t(p-\alpha, q-\beta)]^2 \qquad \forall(\alpha,\beta), \tag{5.6}$$

and when (5.6) is expanded

$$E^2(\alpha,\beta) = \sum_p \sum_q [g^2(p,q) - 2g(p,q)t(p-\alpha, q-\beta) + t^2(p-\alpha, q-\beta)]. \tag{5.7}$$

The term $t^2(p-\alpha, q-\beta)$ represents a summation of template signal energy which is constant and independent. The spectral energy over the window area represented by the first term $g^2(p,q)$ is generally accepted to be slowly varying. The second term is cross or area correlation $R_{gt}(\alpha,\beta) = \sum_p \sum_q g(p,q)t(p-\alpha, q-\beta) \forall(\alpha,\beta)$ between the spectrum and the template. When the best possible match occurs, the distance between the digital samples representing the template and the region of the spectrum will be minimum (theoretically zero) and the cross correlation becomes largest. However, because of the aforementioned effects e.g., the wireless channel impairments, variations of spectral energy can overshadow the accuracy of the difference and the cross correlation can still be large in spite of a template mismatch. This is can partially be avoided by NAC [156] which normalizes the cross correlation with the total spectral power. NAC is given by:

$$N_{gt}(\alpha,\beta) = \frac{R_{gt}(\alpha,\beta)}{\sum_p \sum_q [g(p,q)]^2}. \tag{5.8}$$

The corresponding region of the spectrum that the template matching metrics are implemented can also be represented in terms of the template by

$$g(p,q) \triangleq \delta t\left(\frac{p-\alpha}{\gamma_1}, \frac{q-\beta}{\gamma_2}; \theta\right) \tag{5.9}$$

where δ is an arbitrary constant which can be selected as $0 < \delta \le 1$, γ_1 and γ_2 are the scale factors, and θ is the rotation angle of the signals in the spectrum with respect to the template. In such cases, maxima of the

cross correlation function have to be searched in the quintuple parameter space $(\alpha, \beta, \gamma_1, \gamma_2, \theta)$ which can be impractical unless reasonable estimates of γ_1, γ_2, and θ are given [158]. However, peculiar to the wireless communications, vertical search is unnecessary because a single power value is assigned to each frequency point and vertical scaling defined by γ_2 leads to $(P_s = P_t) \Rightarrow \beta = 0$. Besides, wireless signals do not exhibit rotational behavior therefore $\theta \approx 0$. Taking the measures defined in (5.5), (5.8), and (5.9) into consideration with the assumptions above, expressions of proximity to a possible match become two metrics of

$$CBD(\alpha) = \Big| \sum_p \sum_q [\delta t\Big(\frac{p - \alpha}{\gamma_1}, \frac{q}{\gamma_2}\Big) - t(p - \alpha)]\Big| \tag{5.10}$$

and

$$NAC(\alpha) = \Big[\sum_p \sum_q [\delta t\Big(\frac{p - \alpha}{\gamma_1}, \frac{q}{\gamma_2}\Big)t(p - \alpha)]\Big]. \tag{5.11}$$

5.2.2 Decision Mechanism

The decision problem for the signal identification can be formulated by a binary hypothesis. If there is no a priori information provided by the signal detection stage, the null hypothesis, $\mathcal{H}_0$ indicates that there is no user in the band and alternate hypothesis, $\mathcal{H}_1$ states that the observed frequency spectrum is occupied by the PU signal same type with the template [160]. In case of a perfect match between the template and the region under the template, $\text{CBD}(\alpha)$ converges to zero. However, when the wireless signals are considered, if there is no PU, the average power over the spectrum becomes $\mathbb{E}[g(p,q)] = \sigma_w^2$. Assuming that the average power of the template can also be given by $P_T = \frac{1}{M} \sum_{u=1}^{M} Y_t(u)$, for sufficiently large number of samples, under $\mathcal{H}_0$ the binary hypothesis test statistics become $\mathbb{E}[CBD_0(\alpha)] = |\sigma_w^2 - P_T|$. Secondly, if there is a PU which occupies the spectrum implying $\mathcal{H}_1$, the test statistic becomes $\mathbb{E}[CBD_1(\alpha)] = |P_x + \sigma_w^2 - P_T|$, where $P_x = \frac{1}{M} \sum_{k=\alpha+1}^{\alpha+M} Y(k)$ is the average power of the detected signal. Note that, the perfect match between the signal and the template will imply $(P_T = P_x)$ and the test statistics will converge to $\mathbb{E}[CBD_1(\alpha)] = |\sigma_w^2|$. Assuming that $|\sigma_w^2 - P_T| > \sigma_w^2$, the test based on CBD metric is given by

$$CBD(\alpha) \underset{\mathcal{H}_1}{\overset{\mathcal{H}_0}{\gtrless}} \lambda_c \tag{5.12}$$

where λ_c is the decision threshold for CBD which should be selected based on the limit values provided. Note that, if the signal detection stage provides a priori information, if more there are more than one candidate template, the distinction between $\mathcal{H}_0$ and $\mathcal{H}_1$ will be determined by the difference of the spectral signatures of the wireless signals. Thus, the test statistics become $\mathbb{E}[CBD_0(\alpha)] = |P_x + \sigma_w^2 - P_T|$ and it can be inferred

79

that because $|\sigma_w^2 - P_T| > |P_x + \sigma_w^2 - P_T|$, the threshold will be selected from a narrower range of values. If the metric is greater than the selected threshold, it is decided that the signal to be identified is not occupied in the spectrum and if the it is smaller than λ_c, it is decided that the spectrum is occupied by the candidate signal which the template is constructed from. Thus, for both cases where the a priori information is available or not, the probability of detection and false alarm for $CBD(\alpha)$ can be defined as

$$P_D = P[CBD(\alpha) < \lambda_c | \mathcal{H}_1]. \tag{5.13}$$

and

$$P_F = P[CBD(\alpha) < \lambda_c | \mathcal{H}_0] \tag{5.14}$$

When an analysis similar to the CBD metric is conducted, it can be shown that under $\mathcal{H}_0$, $\mathbb{E}[NAC_0(\alpha)] = P_T \sigma_w^2$, and under $\mathcal{H}_1$, $\mathbb{E}[NAC_1(\alpha)] = ((P_X + \sigma_w^2)P_T)$. Again when the perfect match between the template and the signal is assumed, the test statistics will become $\mathbb{E}[NAC_1(\alpha)] = (P_T^2 + P_T \sigma_w^2)$. Taking that $(P_T^2 + P_T \sigma_w^2) > P_T \sigma_w^2$ into consideration, the binary decision test becomes

$$NAC(\alpha) \underset{\mathcal{H}_0}{\overset{\mathcal{H}_1}{\gtrless}} \lambda_n. \tag{5.15}$$

Therefore, the decision threshold λ_n can be selected accordingly to satisfy the detection requirements. On the other hand, if the a priori information is available, test statistics will be $\mathbb{E}[NAC_0(\alpha)] = P_x P_T + P_T \sigma_w^2$ and again $P_x P_T + P_T \sigma_w^2 > P_T \sigma_w^2$ will lead to narrower limits. If the metric is greater than the selected threshold, it is decided that the detected signal is the same signal with the constructed template and if the it is smaller than λ_n, it is decided that the spectrum is not occupied by the candidate signal. Probability of detection for $NAC(\alpha)$ can also be defined by

$$P_D = P[NAC(\alpha) \geq \lambda_n | \mathcal{H}_1] \tag{5.16}$$

and probability of false alarm will be given by

$$P_F = P[NAC(\alpha) \geq \lambda_n | \mathcal{H}_0] \tag{5.17}$$

Please also note that probability of missed detection can also be easily calculated by $P_M = 1 - P_D$ and in [153] it is shown that (5.8) therefore, (5.11) are asymptotically optimal according to the Neyman-Pearson criterion and approaches to the likelihood ratio decision statistics for large sensing durations.

5.2.3 Template Parameter Calculation

The analysis in the previous section showed that while constructing the templates, the two parameters that should be considered are γ_1 and γ_2, horizontal and vertical scaling factors which represent the frequency and power sequentially. Under these conditions, selecting the complex signal recordings as abstract templates becomes advantageous because of (i) the ability to normalize the template power in time domain depending on the power level of detected signal, and (ii) the flexibility of adjusting the FFT size while transforming to frequency domain. Power levels of templates can be selected as a fixed value e.g., 0 dBm during recording stage. Therefore, number of templates are limited to the number of wireless standards and there will be no need to hold a different template for each value of each scaling factor. Normally, such an approach requires a priori information about the size and/or the location of the signals over the spectrum. Methods such as two-stage [161] and coarse template matching [162] are proposed to solve this problem under the image processing research. However, here, γ_2 becomes the power normalization parameter and can be calculated by $\gamma_2 = P_s - P_t$. If z_t is the abstract complex signal of the selected template, then the template out of the scaling operation becomes

$$y_t = \sqrt{\gamma_2} z_t. \tag{5.18}$$

Scaling the spectral resolution of the template according to the recorded signal provides horizontal normalization. The distance between the spectral samples should be the same both for Y_k and Y_t. However, this should not be confused with the Δt or sampling rate F_s. These parameters define the effective bandwidth and are related to the sampling theorem. The requirement for optimum match is associated with spectral resolution and can be formulated by $N/B_k = M/B_t$, where B_k and B_t are effective bandwidths of recorded signal and template, respectively. Therefore, vertical scaling factor can be given by

$$\gamma_1 = \frac{B_t}{B_k}, \tag{5.19}$$

and M can be calculated automatically when the FFT size for the monitored spectrum, N is given.

5.3 Simulation Results

A simulation setup is developed to measure the performance of the proposed metrics. Simulated baseband signals employ 16 QAM modulation with the symbol rate of 5 kHz, 1024 symbols are oversampled 4 times and the FFT size (N) is selected as 256. Root raised cosine (RRC) filter with roll-off factor of 0.3 is

used for pulse shaping. Frequency selective fading channel compatible with the system model proposed in Section 5.1 is represented by $L = 6$ taps ITU-R 3G (ITU-R M.1225) outdoor to indoor channel model. Noise is assumed to be AWGN. Simulations are repeated for 10000 times for each SNR value to be able to examine the impairment introduced by the random wireless channel.
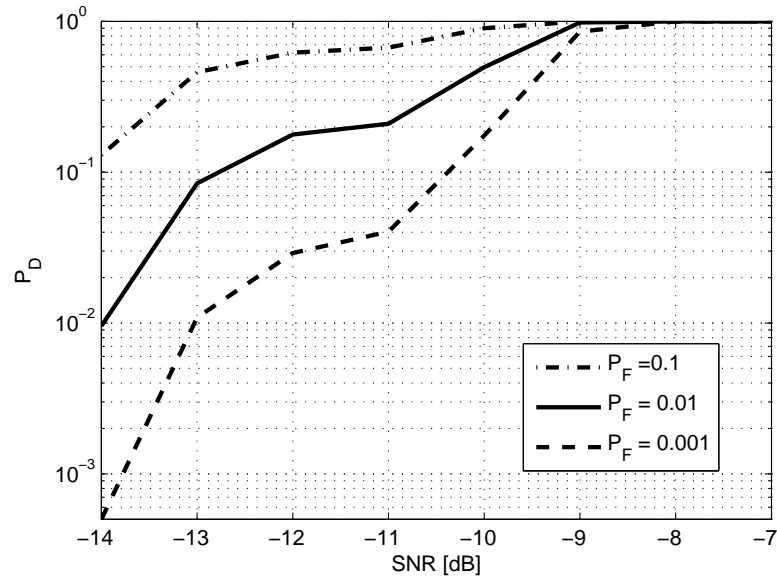
Figure 5.2: Probability of detection vs. SNR for CBD(α)
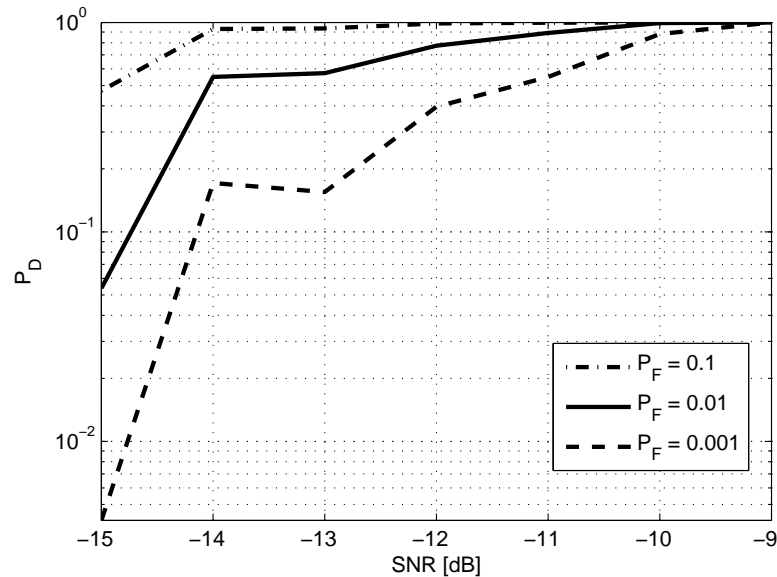
Figure 5.3: Probability of detection vs. SNR for NAC(α)

82

A constant false alarm rate (CFAR) detector is implemented based on equations (5.13)-(5.17) in Section 5.2 for false alarm rates (P_F) of 0.001, 0.01, and 0.1 consecutively. In Fig. 5.2 and Fig. 5.3, the probability of detection (P_D) results of the CBD(α) and NAC(α) are given for various SNR levels. It can be seen that NAC(α) performs better than CBD(α) due to asymptotic optimality. A certain detection performance is achieved by CBD(α) for all P_F values as the SNR reaches to -9 dB, and same applies to NAC(α) for the SNR of -10 dB. The detection performance of the template matching metrics are compared with the energy detector (ED) proposed in [146]. CFAR detector is applied again for the signals that are generated by the same simulation setup and P_D results are depicted for various SNR values when P_F is set to 0.01 in Fig. 5.4.
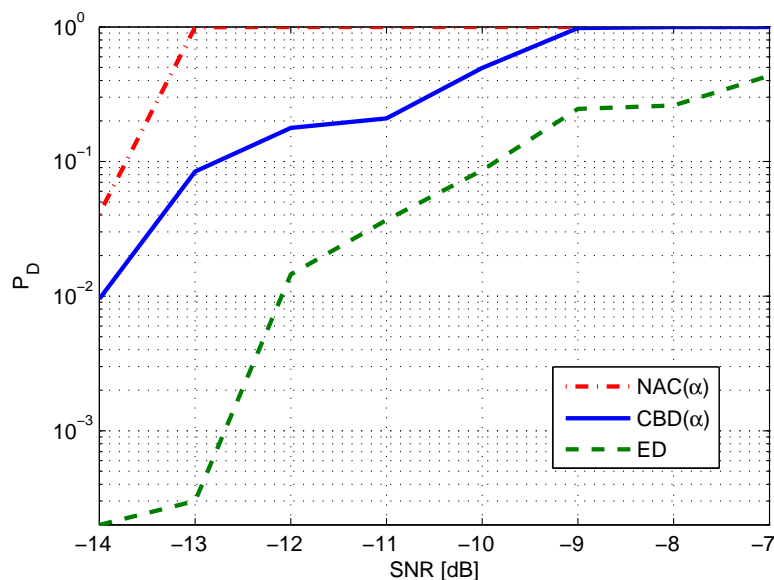
Figure 5.4: CBD(α) & NAC(α) vs. energy detection ($P_F = 0.01$)

Signals with similar signatures are also considered and signal distinction performance of the proposed metrics are analyzed by applying different templates to a candidate signal. The two direct sequence spread spectrum (DSSS) signals which are commonly confused in the frequency spectrum, especially in the reverse channel are W-CDMA and Cdma2000-3x signals. W-CDMA signals are spread with the chip rate of 3.84 mega chips per second (Mcps) employing RRC pulse shaping filter with roll-off factor of 0.22 [165] and Cdma2000-3x three carrier signals are spread with 3×1.2288 Mcps and shaped by the first order infinite impulse response (IIR) filter [166]. Peculiar to these signals, wireless channel is simulated by employing the 3GPP typical urban channel model (3GPP TR 25.943 V6.0.0 (2004-12)) to be able to achieve compatibility in the channel conditions.

83
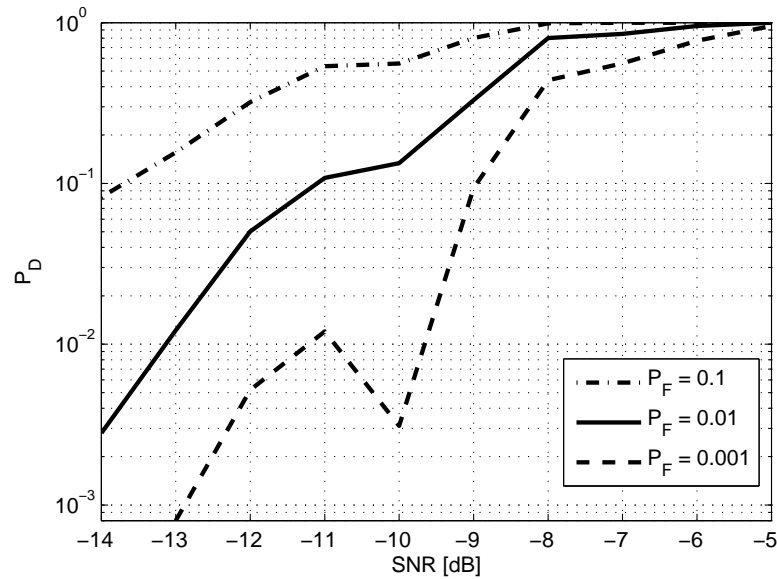
Figure 5.5: CBD(α): W-CDMA & cdma2000-3x
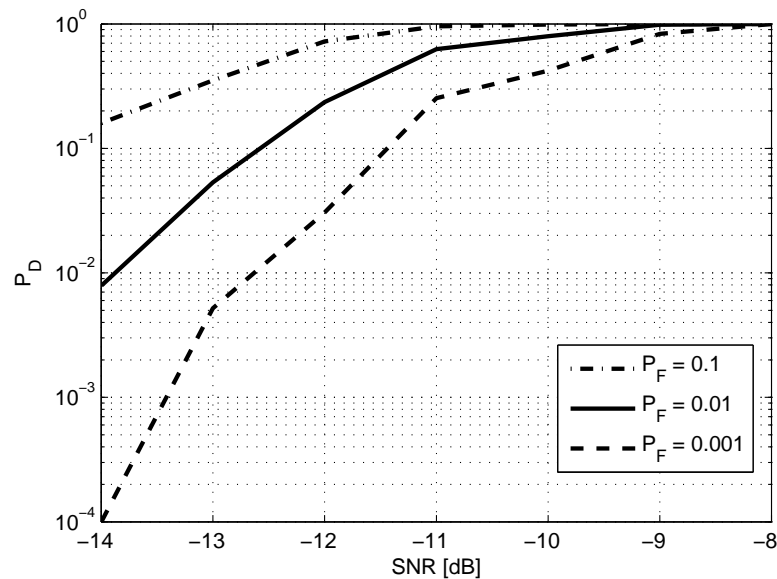
Figure 5.6: NAC(α): W-CDMA & cdma2000-3x

Fig. 5.5 and Fig. 5.6 illustrates the NAC(α) and CBD(α) performances when the primary signal is W-CDMA and the templates are cdma2000-3x and W-CDMA consecutively. Note that, NAC(α) again performs better than CBD(α) and due to the narrowing down statistics discussed in Section 5.2.2, a certain level of separation is achieved around −5 dB for CBD(α) and around −8 dB for NAC(α). The simulation results for

84

the cdma2000-3x primary signal is similar to the provided case, however these results are excluded due to the space limitations.

In conclusion, wireless spectrum scarcity is an important contemporary problem and cognitive radio systems propose solutions to this problem via the spectrum sensing methodology. Better sensing performance can be achieved by the identification of the wireless signals in the wireless spectrum and unique spectral signatures of the signals can be utilized for signal identification. In this study, template matching methods are adapted for the needs of spectrum sensing and the problem of template selection is solved by storing the abstract templates in complex signal format in the cognitive radio database. Therefore, the number of stored templates are minimized. Two new sensing metrics are proposed and the simulation results showed that even for low SNR values, the metrics can detect and identify wireless signals. The metrics can also distinguish the signals with the similar spectral signatures successfully.

CHAPTER 6

A RECURSIVE SIGNAL DETECTION AND PARAMETER ESTIMATION METHOD FOR WIDEBAND SENSING

Wireless spectrum became a more scarce and valuable resource due to requirement of more bandwidth for next generation networks and because of increasing number of users[1]. Even though the spectrum allocation charts indicate that there is not much space left in the frequency spectrum, in practice the spectrum is not efficiently allocated because the communications systems using the frequency spectrum dynamically such as cellular technologies, are assumed to be transmitting in a static fashion such as in the case of television transmitters. Federal Communications Commission's (FCC) Spectrum Policy Task Force report [5] investigates underutilization of the spectrum by precise definition of the spectral efficiency and makes specific recommendations for fostering uniform throughput. Moreover, FCC's Notice of Proposed Rule Making which is issued after the task force's report, recommends employment of flexible and reliable communications systems, such as cognitive radios for efficient spectrum use [145].

The spectrum sensing feature of cognitive radios (CRs) introduces techniques for detecting communications opportunities in wireless spectrum by the employment of secondary users with low-priority access to the spectrum. Three signal processing methods used for spectrum sensing are matched filter, cyclostationary feature extraction, and energy detection [146]. First two are coherent detection techniques with better detection probability than non-coherent energy detection [28]. However, the coherent detectors require a priori information. Matched filter provides optimal detection by maximizing signal to noise ratio (SNR) but requires demodulation parameters. Cyclostationary feature detection can detect random signals depending on their cyclic features even if the signal is in the background of noise but it requires information about the cyclic characteristics. Energy detection technique is applied by setting a threshold for detecting the existence of the signal in the spectrum. Even though it is simpler than the match filtering and cyclostationary feature detection, it requires at least $O(1/SNR^2)$ samples for detection [29] and it has fundamental problems: (i) susceptibility to changing noise levels, (ii) can not distinguish modulated signals, noise and interference.

---

[1]The content of this section is partially publishes in [24, 43, 44]. Copyright for these publications can be found in appendix E, F, and G.

86

Therefore it can not treat primary users, secondary users and noise in different ways, (iii) can not detect the direct sequence spread spectrum signals with very low SNR [21].

Initial spectrum sensing methods are mostly designed assuming that only a single channel is sensed. However, if a block or multiple channels of wireless spectrum is monitored instead of a single channel, more communications opportunities will become available. Therefore, wideband sensing approach is considered as an expansion of the spectrum sensing over the wireless spectrum and CR should focus on a wideband spectrum, if possible. However, introduced sensing methods mostly assumed that a single channel is monitored and the channel frequency response is flat. This assumption does not hold for wideband, multi-channel scenarios. Moreover, the binary decision mechanism of the sensing methods cannot discriminate multiple channels from a single one and can lead to the assumption of full occupancy even though the spectrum is not fully occupied. Thus, spectrum sensing methods cannot be directly applied to the wideband scenarios and consequently, wideband sensing techniques are proposed.

Despite the aforementioned drawbacks, energy detection can provide lower sensing period than other methods and it is applicable to multiple channels for wideband sensing. Hence energy detection is the most studied technique among all sensing methods. Research to improve performance of the energy detectors includes cooperative sensing with multiple CRs [30] and multi-band joint detection which evaluate each frequency band separately [31]. Various double threshold methods [25–27] are also proposed to improve the threshold selection process. Besides, an adaptive threshold setting algorithm is introduced for single channel duty cycle estimation [32]. On the other hand, [33] defined a system level threshold adaptation algorithm taking the detection performances of the thresholds selected for previous frequency sweeps into consideration.

Multiband joint, wavelet, sweep tune, filter bank detection methods are proposed in the literature [34] and they have several advantages and disadvantaged when compared to each other. Multiband joint detection and wavelet detection techniques require high sampling rate, high resolution analog to digital conversion (ADC) blocks which are computationally expensive and difficult to implement, however, rest of the sensing procedure is achieved simply either by dividing the time data into the bins and applying energy detection over the power spectral distribution (PSD) of each bin, or by applying wavelet transform over the PSD. On the other hand, sweep tune approach benefits from the superheterodyne receiver architecture and sweeps over the frequencies of interest by mixing the output of a tunable local oscillator (LO) with the input signal down converting it to intermediate frequency (IF) range. After a bandpass filter is applied to the channel of interest, spectrum sensing methods are applied. This method is slow and its sequential moni-

87

toring and sensing approach can lead to loss of significant spectrum occupancy information. In filter bank detection, a set of filters are designed to process the wideband signal and each filter down converts the corresponding part of the spectrum. Then, sensing methods can be applied over each part separately. The main drawback of this technique is the complexity of the parallel filter bank architecture implementation. The signal processing problems caused by the difficulty of providing a certain dynamic range *i.e.*, high resolution sampling while maintaining the Nyquist sampling rate let to a new set of sensing techniques which conduct ADC in sub-Nyquist rates and then apply spectral reconstruction on the sampled signal. These techniques provide a solution to the high speed ADC, however, the monitored spectrum should be sparsely occupied for these techniques to be successful. Maintaining this criteria can be difficult in many scenarios therefore, some improvements at the sensing performance should be expected in the Sub-Nyquist domain.

Even though the detection performance can be improved by the methods mentioned above, threshold selection is the most important process that defines the performance of the wideband spectrum sensing method because of noise uncertainty. Therefore, in this chapter, it is aimed to investigate how sensing process can be optimized with the knowledge of the minimum number of parameters. A recursive noise floor and signal parameter estimation algorithm is proposed. The aim is to define the application case as realistic as possible. Therefore, instead of focusing on a single communication channel under the assumption of having possible occupant user is known, it is assumed that the sensing mechanism has no prior information and is able to sweep a portion of the frequency spectrum which may dictated by regulators or selected randomly. We also assume that the spectrum can be swept any time of any sampling rate with a resolution bandwidth that will not lead to the loss of spectral information. The output can be either temporal (I/Q) or spectral data depending on the configuration the swept spectrum probably contains more than one signal during time of sweep. We believe that such a case will be realistic, considering the communication bands where the benefits of DSA techniques will be seen most due to the static allocation of frequencies for dynamic users, such as in cellular bands and 700 MHz band of public safety/private partnership.

It is assumed that complex baseband or intermediate frequency (IF) recording is acquired from either a simulated environment or a spectrum analyzer. Number of the wireless signal sources in the given spectrum are not known. Therefore, as the frequency spectrum of the recording is acquired in the initial stage, a noise floor estimation procedure applied to estimate the number of the signals. The developed algorithm works on spectral data and spectral characteristics of wireless signals are used for wireless signal identification; the decision tree simply constructed depending on signal bandwidth and center frequency and these parameters are estimated without any pre-requisite, expected bandwidth and center frequency (regulated by FCC) in-
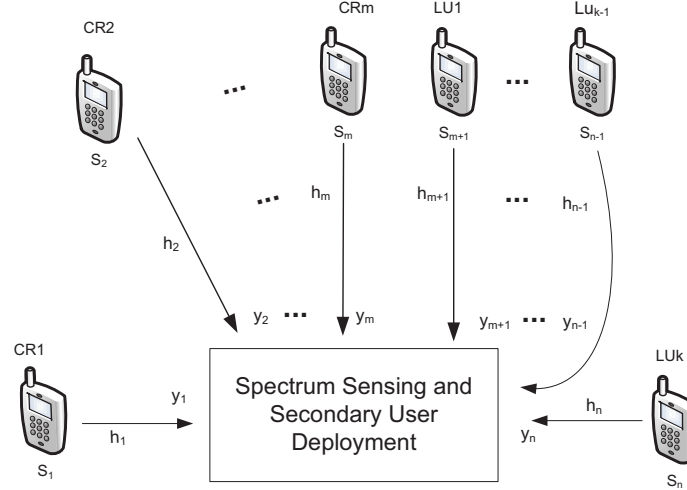
Figure 6.1: System model of the wideband communication environment

formation is used only for signal classification. Besides single signal identification, the signal identification application is also capable of identifying multiple signals occupying given frequency spectrum. Information about the carrier numbers of multiple carrier signals (e.g., multi-carrier CDMA) and information about adjacent channel interference are also provided. Developed application also informs the user if the signal has low SNR value or not.

6.1 System Model

It is assumed that cognitive radio is sensing multiple channels or a chunk of the frequency spectrum that may be occupied by multiple signals. Therefore, transmit signal model can be given by

$$x(t) = As(t),\qquad(6.1)$$

where $s(t) = [s_1(t), ..., s_n(t)]^T$ represents n independent signals and T denotes transposition. A is $n \times n$ coefficient matrix with $a_{i,j}$ elements where $i, j = 1, ...n$ and $x(t)$ represents n transmit signals where $x_j(t) = \sum_{i=1}^{n} a_{i,j} s_j(t)$. The proposed system model is illustrated in Fig. 6.1 and after digital conversion and modulation, each independent signal passes through a different channel as indicated in the figure. The channel for $x_j(t)$ can be modeled as a time-variant linear filter

$$h_j(t) = \sum_{i=1}^{L_j} h_i(t)\delta(t - \tau_i),\qquad(6.2)$$

89

where L_j is the number of taps for the channel h_j and τ_i is delay for each tap. It is assumed that the taps are sample spaced and the channel is constant for a symbol but time-varying across multiple symbols. Each of the emitters in the spectrum can be a legacy user (primary) or a secondary user.
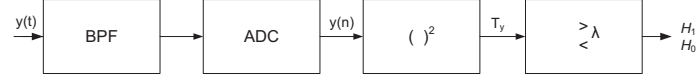
Figure 6.2: Block diagram of energy detector

Block diagram of proposed the energy detection scheme is given in Fig. 6.2. The transmitted signal is received along with noise at the receiver. Therefore, baseband model of a single received signal at the input of the energy detector, after down conversion can be given as

$$y_j(t) = e^{2\pi j \xi t}[x_j(t) \star h_j(t)] + w(t) \tag{6.3}$$

$$= e^{2\pi j \xi t} \int x_j(\tau) h_j(t - \tau) d\tau + w(t), \tag{6.4}$$

where $\star$ is the convolution operation and the j at the exponential term is the imaginary unit. When the channel model given in (6.2) is considered received signal becomes

$$y_j(t) = e^{2\pi j \xi t} \sum_{i=1}^{L_j} x_j(t - \tau_i) h_i(t) + w(t), \tag{6.5}$$

where ξ is frequency offset due to inaccurate frequency synchronization and $w(t)$ corresponds to additive white Gaussian noise (AWGN) sample with zero mean and variance of σ_w^2. The composite received signal then becomes

$$y(t) = \sum_{j=1}^{n} y_j(t). \tag{6.6}$$

The received signal is sampled with sampling time of Δt at the analog to digital converter (ADC) and discrete-time received signal can be represented in vector notation by

$$y(n) = [y(1), y(2), ..., y(N)]. \tag{6.7}$$

where $n = 1, ..., N$. After the received signal is digitized, discrete samples are squared and averaged to acquire received signal energy and the estimated energy is compared with the threshold λ and the decision is made

90

whether the signal is present or not as follows

$$T_y = \frac{1}{N} \sum_{i=1}^{N} (y(i))^2 \gtrless \lambda \tag{6.8}$$

6.2 Performance Analysis of Energy Detectors

The decision problem for the energy detection scheme can be formulated in a binary hypothesis form

$$
\begin{aligned}
H_0 : y(n) &= w(n) \quad \text{(no signal present)} \\
H_1 : y(n) &= h(n) \times s(n) + w(n) \quad \text{(signal present)}
\end{aligned} \tag{6.9}
$$

$s(n)$ represents a transmitted signal in the given frequency band and assumed to be independent and identically distributed (iid) with zero mean and σ_s^2 variance. $w(n)$ is the additive white Gaussian noise (AWGN) and assumed to be iid with variance of σ_n^2. $h(n)$ is the temporary amplitude gain of the channel. SNR can be defined in terms of the signal and noise variance as

$$SNR = \sigma_s^2 / \sigma_n^2. \tag{6.10}$$

Energy detection theory [35] indicate that T_y is a random variable with central and non-central chi-square distributed probability distribution function (PDF) under H_0 and H_1 respectively. When the observation interval N is large enough, the PDF of T_y can be approximated as Gaussian distribution

$$
\begin{aligned}
f(T_y) &\backsim \mathcal{N}(\sigma_n^2, 2\sigma_n^2/N) \quad \text{(under } H_0) \\
f(T_y) &\backsim \mathcal{N}(\sigma_y^2, 2\sigma_y^2/N) \quad \text{(under } H_1)
\end{aligned} \tag{6.11}
$$

where $\sigma_y^2 = \sigma_s^2 + \sigma_n^2$. When the derivations in [36] are taken into consideration probability of signal detection can be given by

$$P_{det} = Q\left(\sqrt{N/2}\left(\frac{\lambda}{\sigma_n^2(1 + SNR)} - 1 \right) \right) \tag{6.12}$$

and the probability of false alarm can be written as

$$P_{fa} = Q\left(\frac{\lambda - \sigma_n^2}{\sigma_n^2 / \sqrt{N/2}} \right) \tag{6.13}$$

91

Under H_1 hypothesis, for a fixed target of detection probability the threshold is derived as [36]

$$\lambda_d = \sigma_n^2(1 + SNR)\left(1 + \frac{Q^{-1}(p_d)}{\sqrt{N/2}}\right), \qquad (6.14)$$

and for a constant false alarm rate (P_{fa}) the threshold is given by

$$\lambda_{fa} = \sigma_n^2\left(1 + \frac{Q^{-1}(p_{fa})}{\sqrt{N/2}}\right). \qquad (6.15)$$

(6.14) and (6.15) indicate that the threshold estimation is dependent of noise variance, SNR, number of the samples, and required detection or false alarm probability. Therefore, in the literature, noise variance and SNR are either assumed to be known or methods to estimate these parameters are proposed. For instance, [37] proposes a combined approach which estimate the noise floor via histogram first, and then applies a constant false alarm rate (CFAR) detector. Performance of the thresholds are investigated when an estimate of noise variance from side or empty bands is used instead of exact values in [36]. Besides, in general it is also assumed that the noise floor is stationary. However, in practice, this assumption may become invalid due to the wireless channel and other impairments especially when the multi-band detection is considered. [26] and [33] introduce the channel impairments in the hypothesis model but these effects are assumed to be either deterministic or non-fading. On the other hand, in the literature, it is aimed to come up with a single threshold value. However, especially for the multi-band or wide-band detection single threshold value may reduce the detection performance.

6.3   Wideband Sensing

Three signal processing methods used for spectrum sensing are matched filter, cyclostationary feature extraction, and energy detection [29]. First two are coherent detection techniques which provide better detection probability than non-coherent energy detection however, the coherent detectors require a priori information. Matched filter provides optimal detection by maximizing signal to noise ratio (SNR) but requires demodulation parameters. Cyclostationary feature detection can detect random signals depending on their cyclic features even if the signal is in the background of noise but it requires information about the cyclic characteristics [39]. Moreover, computational complexities of coherent methods are higher than the energy detection which leads to sensing duration and sensing period degradation [29].

Sensing in multiple channels or over the whole uplink channel for FDD systems is necessary for the signal detection. Coherent detection techniques can not be applied to multiple channels at once. Therefore, beside the modulation parameters and cyclic features of the implemented technologies, the frequencies of the communications sub-channels that are assigned by the regulatory organizations over the operational area should be kept in a database and updated regularly. Under these conditions, applying matched filter and/or cyclostationary feature extraction to uplink sub-channels in a sequential way will lead to loss of sensing time and reduce the signal detection probability. Moreover, implementation of hardware and the software that will execute the coherent detection function and the database will increase the cost and complexity of the radio.

The problems related to the wideband sensing are addressed and solutions based on wavelet approach [40], compressed sensing [41], and optimization of a bank of multiple narrowband detectors [31] are proposed. However even though the sensing performance improved, implementations of these methods over the PSCRs are difficult due to the complexity issues and the hardware/software requirements. On the other hand, in [24], we adopted the adaptive threshold method from the literature of image processing. The adaptive threshold method is employed to determine the level of image intensity boundary for converting the color or the gray scale images to the binary images. The process is called image binarization [42] and it defines the threshold as linear function of the first and second order statistics of the data. This approach finds its validation in the fact that the standard deviation indicates the dispersion level of the spectral data around the mean value.

6.3.1 Recursive Signal Detection and Parameter Estimation

6.3.2 Noise Floor Estimation and Signal Separation

The frequency domain representation of the received signal is acquired by applying FFT over $y(n)$ as

$$Y(u) = \sum_{n=1}^{N} y(n)e^{-j2\pi u \frac{n}{N}} \tag{6.16}$$

where $u = 0, ..., N - 1$. The aim is to define the application case as realistic as possible. Therefore, instead of focusing on a single communication channel, it is assumed that the wireless equipment is able to sweep a portion of the frequency spectrum and there is no prior information about the occupant signal(s). It is also assumed that the spectrum can be swept any time of any sampling rate with a resolution bandwidth that will not lead to the loss of spectral information. When the focus is on the parameters in hand, it is known that there are N spectral samples out of fast Fourier transform (FFT) and because of the dynamic range of

93
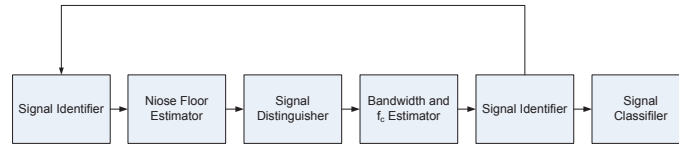
Figure 6.3: Recursive signal detection and parameter estimation block diagram

recording equipment, energy bearing samples lower than the minimum of the equipment's dynamic range will be represented at the minimum dynamic range level. These samples accumulated at the bottom of the spectrum will carry least of the information while the samples with highest power levels will carry most of the information about the wireless occupant signals. Therefore, it is plausible to divide the signal samples into two groups: One group starting from the bottom of the spectra until a level of power should constitute signal base or noise floor and the second group of samples should be evaluated as the information bearing samples for wireless signals. This approach is considerably different from applying a threshold for spectrum sensing where the threshold can be selected arbitrarily *e.g.*, mean value of the frequency spectrum.

Based on the provided information about the wireless spectrum and the requirements of the wideband sensing scenarios, we propose a modular signal detection and parameter estimation method. First, the proposed method estimates the noise floor and distinguishes the rest of the samples comparing them with the samples that are marked as noise. Then, the next module estimates the signal parameters such as bandwidth and center frequency. Next, these estimated parameters are compared with regulatory and wireless standard based information and detected signals are classified. However, it should be noted that noise cannot be assumed to be stationary over wideband. Therefore, noise uncertainty leads to estimation errors. The proposed method handles these cases by executing the procedures recursively over the frequency spectrum. The block diagram of the proposed system can be seen in Fig. 6.3.

Precise noise floor estimation is an extremely important requirement for accurate signal detection. Considering the two groups of samples, it can be stated that if the frequency spectrum is not fully occupied by a single signal (*i.e.*, if the captured spectrum is a part of wide band signal, it will be confused with empty spectrum) then for the empty parts of the spectrum, the samples accumulate at the bottom of the frequency spectrum will exhibit a denser distribution compared to the samples in the first group due to the facts mentioned earlier. The denser distribution means lower standard deviation, therefore starting from the minimum power level, detecting a significant increase in the standard deviation will mark the end of

94

noise floor for a given frequency spectrum. However, there are two issues that should be considered: (i) how to implement decision making process in general, (ii) requirement of a detecting the change of the number of samples which will determine the noise floor [43]. First problem can be handled by adopting quantization level approach from the analog signal digitization process: The frequency spectrum will be partitioned into horizontal segments and all the samples will be grouped depending on their corresponding segments. Therefore, if the power spectral representation of received signal is defined as $Y(n)$ where $n = 1, \cdots, N$, the spectrum can be divided into horizontal segments of:

$$L = \frac{\max(Y) - \min(Y)}{k\sigma_{Y(N)}} \tag{6.17}$$

where k is the standard deviation coefficient and can be selected as $0 < k \leq 1$, and $\sigma_{Y(N)}$ is the standard deviation of whole frequency spectrum which is defined by:

$$\sigma_{Y(N)} = \sqrt{\frac{1}{N} \sum_{p=1}^{N} (Y(p) - \bar{Y})^2}. \tag{6.18}$$

It should be noted that the segment length is adaptive and changes with the general standard deviation of the recorded spectrum. If the standard deviation is high there are more fluctuation in the frequency spectrum, then, the length of the segments L, become wider to catch the ripples in the spectrum. If the standard deviation is smaller, then, spectrum is relatively flat, segment length becomes narrower and detection can become more precise [44]. The second issue that should be addressed is the selection of quantization levels which will represent the noise. In this case, there is a need to detect the point where a significant change occurs in the number of samples falls into each quantization level. Assuming that the quantization levels are listed from bottom to up, in case of a significant reduction in the number of samples in a quantization level, when compared to the previous level, it can be assumed that the noise floor is limited with the previous level and the samples belonging to the level that the change occurs and the samples of other higher quantization levels belongs to occupant signals. To this end, when the change detection methods are investigated, cumulative sum (CUSUM) change detection method becomes a prominent alternative because, in contrary to the Bayes change detection, it does not require any information about the data distribution [45]. Moreover, CUSUM is not time sensitive, thus, in case of applications which are not time sensitive, CUSUM can be selected for implementation instead of on-line or off-line change detection methods. Therefore, if $m_1, m_2, \ldots, m_L$ are the number of samples at each quantization level, the average number of samples per level

95

can be given by

$$\bar{m} = \frac{1}{N} \sum_{i=1}^{L} m_i. \tag{6.19}$$

The cumulative sum can be started with $S_0 = 0$ and the rest of the cumulative sums can be given by

$$S_i = S_{i-1} + (m_i - \bar{m}) \tag{6.20}$$

where $i = 2, \ldots, L$. After each CUSUM value is calculated, the change point where the quantization levels above the noise floor starts is given by

$$S_{max} = \arg \max_{i=2,\ldots,L} S_i. \tag{6.21}$$

Table 6.1: RNFE confidence levels: SNR vs. k

SNR	k					
	0.05	0.1	0.15	0.2	0.25	0.3
-4	19.13	25.3	19.27	19.27	19.27	19.27
-2	31.61	43.6	30.54	30.54	30.54	30.54
0	53.04	69.2	71.41	71.41	71.41	71.41
2	85.78	92.85	96.52	96.52	96.52	96.52
4	92.48	98.75	98.75	99.10	99.70	99.96
6	94.84	99.64	99.96	99.96	99.96	99.96
8	95.97	99.82	99.96	99.96	99.96	99.96
10	97.99	99.83	99.96	99.96	99.96	99.96
12	98.98	99.96	99.96	99.96	99.96	99.96
14	98.99	99.96	99.96	99.96	99.96	99.96
16	98.99	99.96	99.96	99.96	99.96	99.96
18	98.99	99.96	99.96	99.96	99.96	99.96
20	98.99	99.96	99.96	99.96	99.96	99.96

The confidence levels of the change point detection method has vital importance from the aspect of signal detection performance. Therefore, we implemented the bootstrap analysis to quantify the confidence levels of the CUSUM method for wideband signal detection [46]. In this context, one of the main performance defining parameter is the standard deviation coefficient, k, which defines the resolution of $m_1, m_2, \ldots, m_L$. Therefore, for the average occupancy of 60%, the approximate confidence levels of the CUSUM method for various SNR levels and k values are given in Table 6.1. Note that, for $k > 0.3$, same confidence levels are maintained. Therefore, the table is limited with $k = 0.3$. The simulation results indicate that, when $SNR > 0$, a certain level of confidence above 90% is achieved for all k values.

Channel occupancy ratio has also important influence on the confidence levels. Therefore, the approximate confidence levels for changing SNR and wireless spectrum occupancy rates are given in Table 6.2

96

Table 6.2: RNFE confidence levels: *occupancy* vs. *SNR* pt.1

Occupancy Ratio	SNR					
	-4	-2	0	2	4	6
25%	36.7480	74.5660	94.0610	98.7510	99.6580	99.9070
60%	25.3440	43.6100	69.2080	92.8520	98.7490	99.6430
75%	22.5340	24.5370	47.7670	73.0890	93.5080	97.9930
90%	18.9990	20.4360	26.2010	40.6680	65.5230	86.0050

and 6.3 consequently. The simulation results indicate that as the occupancy ratio becomes lower, the confidence levels get slightly better. Actually, when the occupancy ratio reaches to 90%, the system model converges to the single channel systems in which the proposed method provides no further performance than the energy detection. Again, as the $SNR > 0$, a certain level of confidence is achieved for all occupancy rates.

Table 6.3: RNFE confidence levels: *occupancy* vs. *SNR* pt.2

Occupancy Ratio	SNR						
	8	10	12	14	16	18	20
25%	99.9500	99.9670	99.9699	99.9700	99.9730	99.9740	99.760
60%	99.8200	99.8300	99.9620	99.9650	99.9680	99.9690	99.9690
75%	99.1730	99.3970	99.7990	99.80	99.8680	99.8822	99.8990
90%	92.7060	92.9740	95.9640	96.9830	97.1910	97.7850	98.4310

Finally, signal distinguisher module groups spectral data depending on their neighborhood, relevant to the estimated noise floor. Each signal sample higher than the noise floor is assumed as a information bearing sample. Signal sample power levels and their sub-grouped series, frequency indexes and noise floor samples are the input to signal distinguisher. It would be a much more complex procedure if the frequency indexes were not stored separately, each time the application made a decision about a sample point, the application would have to search for its frequency index. This is because that the grouping process can not be handled in sequence. It is not possible to know at which point the algorithm will encounter with samples belonging to the same group. During the sample grouping frequency index trace has to be followed so that it should be possible to make bandwidth and center frequency estimation possible at the next stage. Finally noise power average calculation is also made in this section using the noise floor estimation information extracted from the initial module. This information is used at the next stage to decide if any detected signal is low-SNR or not.
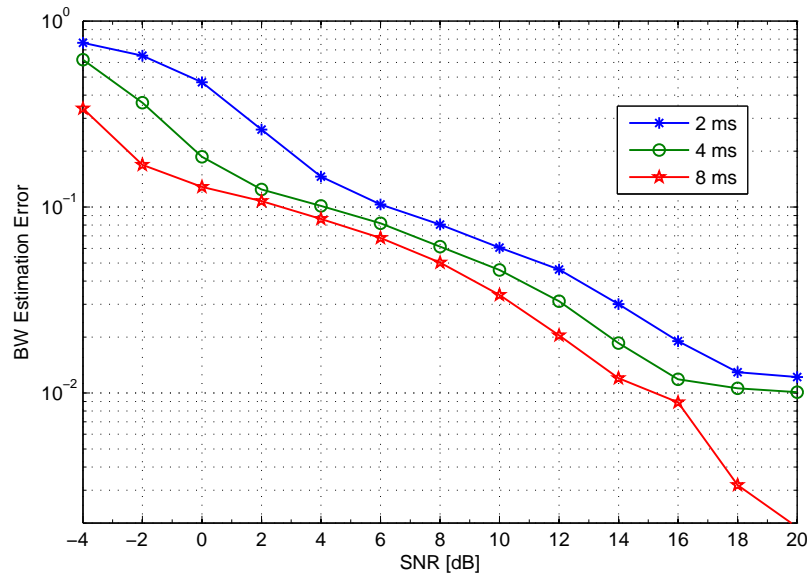
Figure 6.4: Bandwidth estimation performance

6.3.3   Bandwidth and Center Freq. Estimation Module

After the signal groups are constituted, these groups are sent to another module to make decision on their bandwidths and center frequencies. For each group this module also checks out if this signal is low-SNR or not. This procedure is handled so that if the signal average power is lower than 10 dBm added to the noise average calculated at previous module. Signal is accepted to be low power and bandwidth calculation is made depending on the minimum and maximum frequency indexes. The distance between these two values are accepted as the bandwidth.

If the signal is not low power, a flexible threshold is applied to the signal. This threshold located around the average power level of the signal depending on standard deviation of power levels. By this way it is possible to collect as much data sample as possible and a more accurate result is achieved. At this point it should be indicated that 3 dBm or 10 dBm thresholds were also applicable however, for low sampled signals these threshold sampling techniques could not deliver robust enough results. After the samples are collected again the distance between minimum sample and maximum sample is calculated as the bandwidth of the signal. For the case of choosing some point between the min. and max., it is possible to encounter a fluctuation point in power which results with an incorrect estimation for both bandwidth and center frequency. Again center frequency is estimated as the middle point of these two maximum and minimum points. The resultant center frequency and bandwidth values are returned to the calling routine in arrays for each data

98
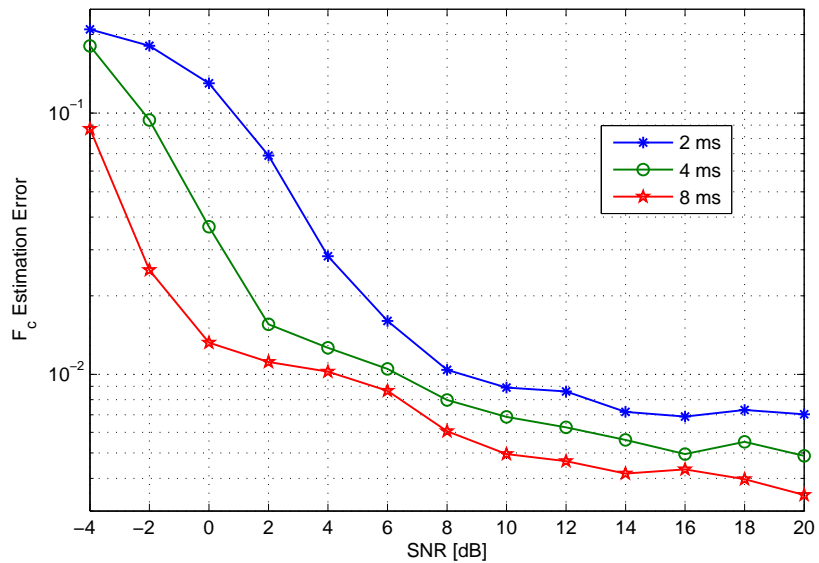
Figure 6.5: Center frequency estimation performance

group. Relative bandwidth and center frequency estimation errors in which the absolute estimation error are normalized with the real bandwidth and center frequencies are given in Fig. 6.4 and 6.5 for various sensing durations. The simulation results indicate performance improvement as the recording duration *i.e.*, the number of the samples introduced at the detection procedure increases. Bandwidth estimation error below 10% is achieved around 6 dB SNR and 1% center frequency estimation error becomes possible for 8 dB of SNR.

6.3.4 Signal Classifier

Estimated center frequencies and bandwidth information is sent as input to this routine. Signal classifier holds the regulations on the center frequencies and bandwidths of the signals in addition to some estimation routines developed for low power and interference signals. For each center frequency-bandwidth couple the comparison procedure is executed regarding to the regulations and standards with a flexible resolution and range. If the signal is possible to be classified then its information is stored to be passed back to the calling module. This module could be developed as a part of the bandwidth and center freq. estimation module, however, because of the fast changes in spectrum allocations and communications technologies, by making this module separately it will be easy to add new regulation and standard information depending on time, territory or region.

99
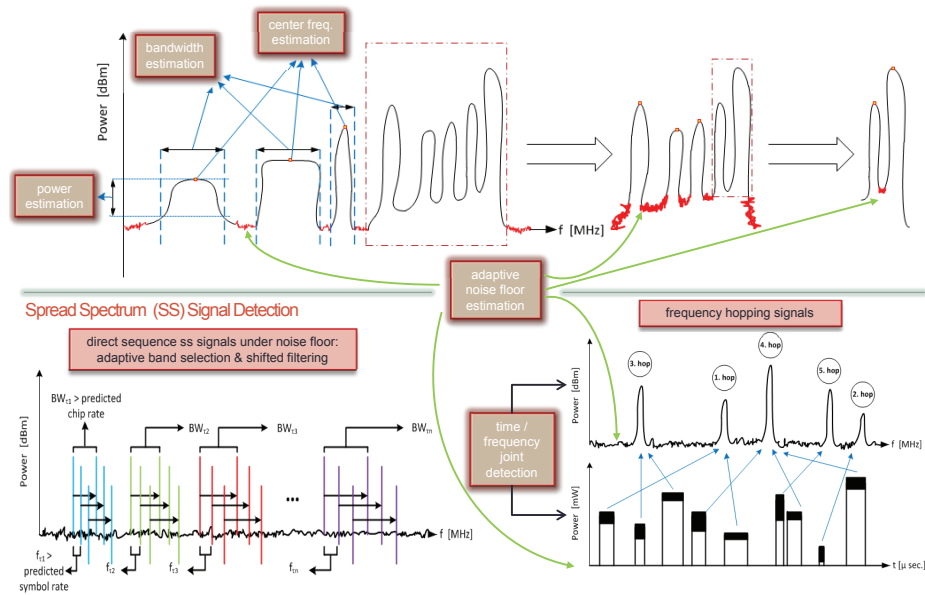
Figure 6.6: The general procedure and applications of recursive estimation

Table 6.4: RNFE vs. ED

SNR	RNFE		ED	
	P_D	F_A	P_D	F_A
-4	0.7390	0.2124	0.7505	0.2257
-2	0.8111	0.1951	0.8060	0.1816
0	0.8400	0.1718	0.8502	0.1737
2	0.8420	0.0555	0.8347	0.0594
4	0.8633	0.0452	0.8568	0.0489
6	0.8818	0.0360	0.8733	0.0351
8	0.8995	0.0308	0.8940	0.0339
10	0.9152	0.0264	0.9077	0.0251
12	0.9293	0.0234	0.9230	0.0236
14	0.9412	0.0208	0.9368	0.0231
16	0.9519	0.0191	0.9471	0.1920
18	0.9613	0.0175	0.9576	0.0191
20	0.9695	0.0168	0.9657	0.0158

6.3.5 Signal Identifier Module and Recursion

Signal identifier is the core module of the proposed method. After completing all identification processes, signal identifier returns back to the main application with the identified signal information, if exists. Mainly it calls the previous modules in the sequence of their introduction. However, for some cases, it has to take an action to make sure that all the signals occupying the sensed spectrum are identified. It calls

100

itself for the cases which the bandwidths of the data groups do not fit in any pattern defined by regulations and standards and if it is certain that these portions of spectrum are carrying some information. Recursive process of the signal identification module makes the application robust against noise uncertainty and measurement discrepancies.

Table 6.5: RNFE sensing time

Sensing Time	P_D	F_A
1 ms	0.8768	0.0469
2 ms	0.9007	0.0377
4 ms	0.9152	0.0264
8 ms	0.9250	0.0171

The general procedure of recursive algorithm is depicted in Fig. 6.6. Moreover, when all the procedures defined in the context of recursion are applied by the proposed method, the detection performance of the noise floor estimation module against the energy detection method can be seen in Table 6.4. The simulation results listed are under the assumption of 60% occupancy, P_D and F_A represent the corresponding probability of detection and false alarm rates. Total sensing time is also an important parameter which defines the detection performance. Therefore, in Table 6.5 the probability of detection and false alarm rates for increasing sensing duration is given.

REFERENCES

[1] G. P. Fettweis, K. Iversen, M. Bronzel ,H. Schubert, V. Aue,D. Maempel, J. Voigt, A. Wolisz, G. Walf, J. P. Ebert, "A Closed Solution for an Integrated Broadband Mobile System (IBMS)," *In Proc. of Intl. Conf. on Universal Personal Communications,* pp. 707-711, Cambridge, Massachusetts, USA, October 1996.

[2] Joseph Mitola III, Gerald Q. Maguire Jr."Cognitive Radio: Making Software Radios More Personal," *IEEE Personal Communications,* vol. 6, no. 4, pp. 13-18 1999.

[3] Erik Axell, Geert Leus, Erik G. Larsson, H. Vincent Poor, "Spectrum Sensing for Cognitive Radio: State-of-the-art and Recent Advances," In *IEEE Signal Processing Magazine,* vol. 29, no. 3, pp. 101-116, 2012.

[4] Qing Zhao, Brian M. Sadler., "A Survey of Dynamic Spectrum Access," In *IEEE Signal Processing Magazine,* vol. 24, no. 3, pp. 79-89, 2007.

[5] Spectrum Efficiency Working Group, "Report of the Spectrum Efficiency Working Group," Spectrum Policy Task Force, Washington, DC , Tech. Rep., November 2002

[6] W.D. Horne,"Adaptive Spectrum Access: Using the Full Spectrum Space," In *Proc. 31st Telecommunications Policy Research Conference (TPRC),* Arlington, Virginia, U.S.A., Sept. 2003

[7] Gorcin, A., B. Thiagarajan, "A Signal Identification Application for Cognitive Radio," In *SDR Forum Technical Conference 2007,* Denver, Colorado, USA, 2007.

[8] T. Yucek, H. Arslan, "A Survey of Spectrum Sensing Algorithms for Cognitive Radio Applications," In *IEEE Communications Surveys & Tutorials,* vol. 11, no. 1, pp. 116-130, 2009.

[9] ITU Radiocommunication Sector, "Definitions of Software Defined Radio (SDR)and Cognitive Radio System (CRS) Report," ITU-R SM.2152, 2009

[10] ITU Radiocommunication Sector, "Cognitive Radio Systems in the Land Mobile Services Report," ITU-R M.2225, 2011

[11] ITU Radiocommunication Sector, "CR Systems Specific for IMT Systems Report," ITU-R M.2242, 2011

[12] S. Geirhofer, L. Tong, and B. M. Sadler, "Dynamic Spectrum Access in Time Domain: Modeling and Exploiting White Space," In *IEEE Communications Magazine,* vol. 45, no. 5, pp. 66-72, May. 2007.

[13] Theodore S. Rappaport, Jeffrey H. Reed, and Brian D. Woerner, "Position Location Using Wireless Communications on Highways of the Future", In *IEEE Communications Magazine,* vol. 34, no.10, pp. 33-41, 1996.

[14] L. Gueguen, B. Sayrac, "Radio Access Technology Recognition by Classification of Low Temporal Resolution Power Spectrum Measurements", In *Wireless Communications and Mobile Computing,* vol. 10, no.8, pp. 1033-1044, 2010.

[15] T. Farnham, G. Clemo, R. Haines, E. Seidel, A. Benamar, S. Billington, N. Greco et al., "Ist-trust: A Perspective on the Reconfiguration of Future Mobile Terminals Using Software Download," In *Proc. IEEE 11th International Symposium on Personal, Indoor and Mobile Radio Communications (PIMRC 2000),* vol.2, London, Great Britain, 18-21 Sep 2000, pp. 1054-1059.

[16] Mehul Mehta, Nigel Drew, Georgios Vardoulias, Nicola Greco, and Christoph Niedermeier, "Reconfigurable Terminals: An Overview of Architectural Solutions," In *IEEE Communications Magazine,* vol. 39, no. 8, pp. 82-89, 2001.

[17] Jacques Palicot, and Christian Roland, "A New Concept for Wireless Reconfigurable Receivers," In *IEEE Communications Magazine,* vol. 41, no. 7, pp. 124-132, 2003.

[18] Matteo Gandetto, Carlo Regazzoni., "Spectrum Sensing: A Distributed Approach for Cognitive Terminals," In *IEEE Journal on Selected Areas in Communications,* vol. 25, no. 3, pp. 546-557, 2007.

[19] Menguc Oner, Friedrich Jondral, "Air Interface Identification for Software Radio Systems," In *AEU - International Journal of Electronics and Communications,* vol. 61, no. 2, pp. 104-117, 2007.

[20] Apurva N. Mody, Stephen R. Blatt, Diane G. Mills, Thomas P. McElwain, Ned B. Thammakhoune, Joshua D. Niedzwiecki, Matthew J. Sherman, Cory S. Myers, and P. D. Fiore, "Recent Advances in Cognitive Communications," In *IEEE Communications Magazine,* vol. 45, no. 10, pp. 54-61, 2007.

[21] H. Arslan and A. Gorcin, "Cognitive Radio and Software Defined Radio: Signal Processing Perspectives," In *Proc. IEEE 16th Signal Processing, Communication and Applications Conference (SIU 2008),* Didyma, Aydin, Turkey, April 20-22, 2008.

[22] Danijela Cabric, Robert W. Brodersen, "Physical Layer Design Issues Unique to Cognitive Radio Systems," In *Proc. IEEE 16th International Symposium on Personal, Indoor and Mobile Radio Communications (PIMRC 2005),* vol.2, Berlin, Germany, 11-14 Sept. 2005, pp. 759-763.

[23] F. Chinchilla, M. Lindsey, and M. Papadopouli, "Analysis of Wireless Information Locality and Association Patterns in a Campus", In*Proc. of IEEE Conference on Computer Communications (Infocom 2004),* Hong Kong, Mar. 2004.

[24] A. Gorcin, K.A. Qaraqe, H. Celebi, H. Arslan, "An Adaptive Threshold Method for Spectrum Sensing in Multi-channel Cognitive Radio Networks," In *Proc. IEEE 2010 17th International Conference on Telecommunications (ICT 2010),* pp. 425-429, Doha, Qatar, 4-7 April 2010.

[25] J. Vartiainen, J. J. Lethomäki and H. Saarnisaari, "Double-Threshold Based Narrowband Signal Extraction," In *IEEE 61st Vehicular Technology Conference, VTC 2005-Spring* vol. 2, Stockholm, Sweden, May 30 - June 1, 2005.

[26] J. Zhu, Z. Xu, F. Wang, B. Huang and B. Zhang, "Double Threshold Energy Detection of Cooperative Spectrum Sensing in Cognitive Radio," In *IEEE 3rd International Conference on Cognitive Radio Oriented Wireless Networks and Communications,CrownCom 2008* pp. 1-5, Singapore, 15-17 May 2008.

[27] W. Han, J. Li, Z. Li, J. Yao and D. Chen, "Double Thresholds for Judgment in Cognitive Spectrum Sensing," In *IEEE 19th International Symposium on Personal, Indoor and Mobile Radio Communications, PIMRC 2008*, pp. 1-5, Cannes, France, 15-18 September 2008.

[28] A. Sahai, N. Hoven, R. Tandra, "A Closed Solution for an Integrated Broadband Mobile System (IBMS)", In *Proc. of Intl. Conf. on Universal Personal Communications (ICUPC'96) pp. 707-711* Proc. of Allerton Conference, Monticello, Oct 2004.

[29] D. Cabric, A. Tkachenko, and R. W. Brodersen, "Spectrum Sensing Measurements of Pilot, Energy, and Collaborative Detection," In *Proc. IEEE Military Communications Conference* pp. 1-7, Washington D. C., U.S.A., 23-25 Oct. 2006.

103

[30] S. M. Mishra, A. Sahai, and R. W. Broderson, "Cooperative Sensing Among Cognitive Radios," In *Proc. of the IEEE International Conference on Communications, ICC 2006,* Istanbul, Turkey, June 11-15 2006.

[31] Z. Quan, S. Cui, A. H. Sayed and H. V. Poor, "Optimal Multiband Joint Detection for Spectrum Sensing in Cognitive Radio Networks," In *IEEE Transactions on Communications* vol. 57, number 3, pp. 1128-1140, 2009.

[32] D. Miao, F. Zhiyong, C. Huying and Y. Yanjun, "An Adaptive Threshold Method for Data Processing in Spectrum Occupancy Measurements," In *IEEE 69th Vehicular Technology Conference, VTC 2009-Fall* Anchorage, AL, U.S.A 20-23 September, 2009.

[33] J. W. Lee, J. H. Kim, H. J. Oh and S. H. Hwang, "Energy Detector Using Adaptive-Fixed Thresholds in Cognitive Radio Systems," In *14th Asia-Pacific Conference on Communications,APCC 2008* Akihabara, Tokyo, Japan, 14-16 October 2008.

[34] Hongjian Sun, A. Nallanathan, Cheng-Xiang Wang, Yunfei Chen, "Wideband Spectrum Sensing for Cognitive Radio Networks: A Survey," In *IEEE Wireless Communications,* vol. 20, no. 2, pp. 74-81, 2013.

[35] H. Urkowitz, "Energy detection of unknown deterministic signals," In *Proceedings of IEEE* vol. 55, pp. 523-531, April 1967.

[36] Z. Ye, G. Memik, J. Grosspietsch, "Energy Detection Using Estimated Noise Variance for Spectrum Sensing in Cognitive Radio Networks," In *IEEE Wireless Communications and Networking Conference, WCNC 2008* pp. 711-716, Las Vegas, Nevada, 31 March - 3 April, 2008.

[37] M. P. Oliveri, G. Barnett, A. Lackpour, A. Davis, and P. Ngo "A Scalable Dynamic Spectrum Allocation System with Interference Mitigation For Teams Of Spectrally Agile Software Defined Radios," In *New Frontiers in Dynamic Spectrum Access Networks, (DySPAN 2005),* pp. 170-179, Baltimore, Maryland, U.S.A., Nov. 2005.

[38] D. Datla, A.M. Wyglinski, G.J. Minden, "A Spectrum Surveying Framework for Dynamic Spectrum Access Networks," In *IEEE Transactions on Vehicular Technology,* vol. 58, no. 8, pp. 4158-4168, 2009.

[39] A. Tonmukayakul, M. B. H. Weiss, "Secondary Use of Radio Spectrum: A Feasibility Analysis," In *Proc. of TPRC Conference,* Qarter Hill Road, VA, Aug. 2004.

[40] Z. Tian, G.B. Giannakis, "A Wavelet Approach to Wideband Spectrum Sensing for Cognitive Radios," In *IEEE 1st International Conference on Cognitive Radio Oriented Wireless Networks and Communications, CrownCom 2006,* pp. 1-5, Mykonos Island, Greece, 8-10 June, 2006.

[41] Z. Tian, G.B. Giannakis, "Compressed Sensing for Wideband Cognitive Radios," In *IEEE International Conference on Acoustics, Speech and Signal Processing, 2007. ICASSP 2007,* pp. 13571360, Honolulu, HI, U.S.A., 15-20 April, 2007.

[42] M. Sezgin, B. Sankur, "A Survey over Image Thresholding Techniques and Quantitative Performance Evaluation," In *J. Electron. Imag.,* vol.13, no.1, pp. 146-165, Jan. 2004.

[43] A. Gorcin, "RSSI Based Location Awareness for Public Safety Cognitive Radio," In *IEEE Wireless Vitae Conference,* Aalborg, Denmark, May 2009 (Invited Paper)

[44] A. Gorcin, H. Celebi, K. A. Qaraqe, H. Arslan, "A Framework on Wideband Sensing and Direction Finding for Location Aware Public Safety Cognitive Radio," In *IEEE Wamicon Conference,* Clearwater, USA, April 2011.

[45] Effariza Hanafi, Philippa A. Martin, Peter J. Smith, and Alan J. Coulson, "Extension of Quickest Spectrum Sensing to Multiple Antennas and Rayleigh Channels," In *IEEE Communications Letters,* vol. 17, no. 4, pp. 625-628, 2013.

[46] Karsten Husby, Arne Lie, and Jan-Erik Hkegrd, "Efficiency of Opportunistic Spectrum Sensing by Sequential Change Detection in Cognitive Radio," In *The Third International Conference on Advances in Cognitive Radio,* pp. 7-11, Venice, Italy, April 21-26, 2013.

[47] M.L.D. Wong, and A.K. Nandi, "Efficacies of Selected Blind Modulation Type Detection Methods for Adaptive OFDM Systems," In *Proc. Int. Conf. on Signal Processing and Communication Systems (ICSPCS 2007),* Australia, Gold Coast, 17-19 December 2007

[48] A. Swami, and B.M. Sadler, "Hierarchical Digital Modulation Classification Using Cumulants," In *IEEE Transactions on Communications,* vol. 48, no. 3, pp. 416-429, Mar 2000.

[49] D. Grimaldi, S. Rapuano, and L. De Vito , "An Automatic Digital Modulation Classifier for Measurement on Telecommunication Networks", In*IEEE Transactions on Instrumentation and Measurement,* vol. 56, no. 5, pp. 1711-1720, 2007.

[50] M. Shi, A. Laufer, Y. Bar-Ness, and W. Su, "Fourth Order Cumulants in Distinguishing Single Carrier from OFDM Signals," In *Proc. IEEE Military Communications Conference (MILCOM 2008),* San Diego, CA, U.S.A., 16-19 Nov. 2008 , pp. 1-6

[51] W. Liu, J. Wang, S.u Li, "Blind Detection and Estimation of OFDM Signals in Cognitive Radio Contexts," In *2nd International Conference on Signal Processing Systems (ICSPS 2010),* Dalian, China, 5-7 July 2010, pp. 347-351

[52] K. Ulovec, 'Recognition of OFDM Modulation Method," In *Journal of Radioengineering,* vol. 17, no. 1, pp. 50-55, April 2008.

[53] H. Wang, B. Li, and Y. Wang, "Modulation Identification for OFDM in Multipath Circumstance Based on Support Vector Machine," In *Proc. 11th IEEE Singapore International Conference on Communication Systems (ICCS 2008),* Guangzhou, China, 19-21 Nov. 2008, pp. 1349-1353

[54] Wei Dai, Y. Wang, J. Wang "Joint Power Estimation and Modulation Classification Using Second- and Higher Statistics", In*Proc. IEEE Wireless Communications and Networking Conference (WCNC2002),* vol. 1, Orlando, Florida, U.S.A., 17-21 Mar 2002, pp. 155-158

[55] Bin Wang, Lindong Ge, "Blind Identification of OFDM Signal in Rayleigh Channel", In*Proc. IEEE 5th International Conference on Information, Communications and Signal Processing,* Bangkok, Thailand, 6-9 Dec. 2005, pp. 950-954

[56] J. Leinonen, and M. Juntti, "Modulation Classification in Adaptive OFDM Systems," In *Proc. IEEE 59th Vehicular Technology Conference (VTC 2004-Spring),* vol.3, Milan, Italy, 17-19 May 2004, pp. 1554-1558

[57] F. Wang, and B. Li, "A New Method for Modulation Classification Based on Bootstrap Technique," In *Proc. IEEE International Symposium on Computer Science and Computational Technology (ISCSCT'08),* vol. 2, Shanghai, China, 20-22 Dec. 2008, pp. 11-14

[58] J. Zhang, and B. Li, "A New Modulation Identification Scheme for OFDM in Multipath Rayleigh Fading Channel," In *Proc. IEEE International Symposium on Computer Science and Computational Technology (ISCSCT'08),* vol. 1, Shanghai, China, 20-22 Dec. 2008, pp. 793-796

[59] K.N. Haq, A. Mansour, S. Nordholm, "Classification of Digital Modulated Signals Based on Time Frequency Representation," In *2nd International Conference on Signal Processing Systems (ICSPS 2010),* Dalian, China, 5-7 July 2010, pp. 1-5

[60] A. Punchihewa, O.A. Dobre, S. Rajan, and R. Inkol, "Cyclostationarity-based Algorithm for Blind Recognition of OFDM and Single Carrier Linear Digital Modulations," In *Proc. IEEE 18th International Symposium on Personal, Indoor and Mobile Radio Communications (PIMRC 2007),* Athens, Greece, 3-7 Sept. 2007, pp. 1-5

[61] A. Bouzegzi, P. Ciblat, P.Jallon, "New Algorithms for Blind Recognition of OFDM Based Systems", In *Elsevier Signal Processing Journal,* vol. 90, no. 3, pp. 900-913, 2010.

[62] H. Li, Y. Bar-Ness, A. Abdi, O.S. Somekh, and W. Su, "OFDM Modulation Classification and Parameters Extraction," In *Proc. IEEE 1st International Conference on Cognitive Radio Oriented Wireless Networks and Communications,* Mykonos Island, Greece, 8-10 June 2006, pp. 1-6

[63] G. B. Giannakis, M. K. Tsatsanis, "Time-domain Tests for Gaussianity and Time-reversibility", In *IEEE Trans. Signal Processing,* vol. 42, pp. 3460-3472, Dec. 1994.

[64] W. Akmouche,"Detection of Multicarrier Modulations Using 4th-order Cumulants", In*Proc. IEEE Military Communications Conference (MILCOM 1999),* vol.1, Atlantic City, NJ, U.S.A., 31 Oct 1999 - 03 Nov 1999, pp. 432-436

[65] A. Gorcin, H. Arslan,"Identification of OFDM Signals Under Multipath Fading Channels", In*Proc. IEEE Military Communications Conference (MILCOM 2012),* Orlando, USA, 29 October 1 November 2012.

[66] D. Brillinger, "Time Series, Data Analysis and Theory," San Francisco: Holden day, 1981.

[67] D. Brillinger and M. Rosenblatt, "Computation and Interpretation of kth-order Spectra," In *Spectral Analysis of Time Series,* B. Harris, Ed. New York: Wiley, 1967, pp.189-232.

[68] G. B. Giannakis, M. K. Tsatsanis, "A Unifying Maximum-Likelihood View of Cumulant and Polyspectral Measures for non-Gaussian Signal Classification and Estimation", In *IEEE Trans. Inform. Theory,* vol. 38, pp. 386-406, Mar. 1992.

[69] C. Le Martret, D. Boiteau,"Modulation Classification by Mean of Different Orders Statistical Moments", In*Proc. IEEE Military Communications Conference (MILCOM 1997),* vol.3, Monterey, CA , U.S.A. , 02 - 05 Nov 1997, pp. 1387-1391

[70] E.L. Lehmann, "Theory of Point Estimation," New York: Wiley, 1983, ch.5.

[71] A. V. Dandawate, G. B. Giannakis, "Asymptotic Theory of Mixed Time Averages and kth-order Cyclic-moment and Cumulant Statistics", In *IEEE Transactions on Information Theory,* vol. 41, no.1, pp. 216-232, Jan 1995.

[72] A. Kanazawa, H. Tsuji, H. Ogawa, Y. Nakagawa, and T. Fukagawa, "An Experimental Study of DOA Estimation in Multipath Environment Using an Adaptive Array Antenna Equipment," In *Proc. IEEE of the Asia-Pacific Microwave Conference,* Sydney, Australia, December 2000, pp. 804-807

[73] Antonis Kalis, and Theodore Antonakopoulos,"Relative Direction Determination in Mobile Computing Networks", In *Proc. of 18th IEEE Instrumentation and Measurement Technology Conference, IMTC 2001,* vol.3, Budapest, Hungary, 21-23 May, 2001, pp. 1479-1484

[74] Iqbal Jami and Richard F. Ormondroyd,"Joint Angle of Arrival and Angle-spread Estimation of Multiple Users Using an Antenna Array and a Modified MUSIC Algorithm", In *Proc. of IEEE 53rd Vehicular Technology Conference (VTC 2001-Spring),* vol.1, Rhodes, Greece, 06 - 09 May, 2001, pp. 48-52

[75] Khalid AlMidfa, George V. Tsoulos, and Andy Nix, "Performance evaluation of direction-of-arrival (DOA) estimation algorithms for mobile communication systems," In *Proc. IEEE 51st Vehicular Technology Conference (VTC 2000-Spring),* vol.2, Tokyo, Japan, 15-18 May 2000, pp. 1055-1059

[76] L. Bigler, H. P. Lin, S. S. Jeng, and G. Xu,"Experimental Direction of Arrival and Spatial Signature Measurements at 900 MHz for Smart Antenna Systems", In *Proc. of IEEE 45th Vehicular Technology Conference,* vol.1, Chicago, IL, USA, 25-28 Jul 1995, pp. 55-58

[77] Lal Chand Godara, "Application of Antenna Arrays to Mobile Communications, II: Beam-forming and Direction-of-arrival Considerations", In *Proceedings of the IEEE,* vol. 85, no.8, pp. 1195-1245, 1997.

[78] Nicholas Cianos, "Low-cost, High-performance DF and Intercept Systems," In *Proc. IEEE Wescon Conference,* San Francisco, California, USA, 28-30 Sep 1993, pp. 372-376, 1993.

[79] David Peavey, and T. Ogumfunmi, "The Single Channel Interferometer Using a Pseudo-doppler Direction Finding System," In *Proc. IEEE Trans. on Acoust., Speech, Signal Processing,* pp. 41294132, 1997.

[80] Ugur Sarac, F. K. Harmanci, and Tayfun Akgul, "Experimental Analysis of Detection and Localization of Multiple Emitters in Multipath Environments", In *IEEE Trans. on Antennas and Propagation,* vol. 50, no. 5, pp. 61-70, 2008.

[81] R. Schmidt, and R. Franks, "Multiple Source DF Signal Processing: An Experimental System", In *IEEE Trans. on Antennas and Propagation,* vol. 34, no. 3, pp. 281-290, 1986

[82] M. Uthansakul, P. Uthansakul, N. Sangmanee, and S. Sangpradittara,"Low profile DOA Finder at 2.4 GHz", In *Microwave and Optical Technology Letters,* vol. 51, no. 1, pp. 252-256, 2009.

[83] Boaz Porat, and Benjamin Friedlander, "Analysis of the Asymptotic Relative Efficiency of the MUSIC Algorithm," In *IEEE Transactions on Acoustics, Speech and Signal Processing,* vol. 36, no. 4, pp. 532-544, 1988.

[84] R. L. Johnson, and G. E. Miner, "Comparison of Superresolution Algorithms for Radio Direction Finding," In *Proc. IEEE Transactions on Aerospace and Electronic Systems,* vol. 4, pp. 432-442, 1986.

[85] Petre Stoica, and Arye Nehorai, "Performance Comparison of Subspace Rotation and MUSIC Methods for Direction Estimation", In *IEEE Trans. on Signal Processing,* vol. 39 no. 2, pp. 446-453, 1991.

[86] Raymond J. Weber, and Yikun Huang, "Analysis for Capon and MUSIC DOA Estimation Algorithms," In *Proc. IEEE Antennas and Propagation Society International Symposium,* Charleston, SC, USA, 1-5 June 2009, pp. 1 - 4

[87] Hinrich Mewes, Franz Wolf, and Jan Luiken ter Haseborg, "High Resolution Direction Finding Algorithms-applications in the HF Band," In *Proc. IEEE Antennas and Propagation Society International Symposium,* vol.2, Baltimore, MD, USA, 1 - 26 Jul 1996, pp. 1344 - 1347

[88] K. R.Srinivas, and V. U. Reddy, "Finite Data Performance of MUSIC and Minimum Norm Methods," In *Proc. IEEE Transactions on Aerospace and Electronic Systems,* vol. 30, no. 1, pp. 161-174, 1994

[89] S.C. Swales, and M.A. Beach, "Direction Finding in the Cellular Land Mobile Radio Environment," In *Proc. Fifth International Conference on Radio Receivers and Associated Systems,* University of Cambridge, England, 23rd - 27th July 1990, pp. 192-196.

[90] Zhongfu Ye, and Chao Liu, "On the Resiliency of MUSIC Direction Finding Against Antenna Sensor Coupling," In *Proc. IEEE Transactions on Antennas and Propagation,* vol. 56, no. 2, pp. 371-380, 2008.

[91] Anne Ferreol, Pascal Larzabal, and Mats Viberg, "On the Asymptotic Performance Analysis of Subspace DOA Estimation in the Presence of Modeling Errors: Case of MUSIC", In *IEEE Transactions on Signal Processing,* vol. 54, no. 3, pp. 907-9203, 2006.

107

[92] Benjamin Friedlander, 'Sensitivity Analysis of the Maximum Likelihood Direction-finding Algorithm," In *IEEE Transactions on Aerospace and Electronic Systems,* vol. 26, no. 6, pp. 953-961, 1990.

[93] Stephanie L. Preston, David V. Thiel, Trevor A. Smith, Steven G. O'Keefe, and Jun Wei Lu, "Base-station Tracking in Mobile Communications Using a Switched Parasitic Antenna Array", In *IEEE Trans. on Antennas and Propagation,* vol. 46, no. 6, pp. 841-844, 1998.

[94] Thomas Svantesson and Mattias Wennstrom, "High-resolution Direction Finding Using a Switched Parasitic Antenna," In *Proc. of the 11th IEEE Signal Processing Workshop on Statistical Signal Processing,* Singapore, 06 - 08 Aug 2001, pp. 508-511.

[95] A. Hirata, E. Taillefer, H. Yamada, and T. Ohira, "Handheld direction of arrival finder with electronically steerable parasitic array radiator using the reactancedomain MUltiple SIgnal Classification algorithm", In *IET Microwaves, Antennas & Propagation,* vol. 1, no. 4, pp. 815-821, 2007.

[96] Jacob Sheinvald, and Mati Wax, "Direction Finding with Fewer receivers via Time-varying Preprocessing", In *IEEE Transactions on Signal Processing,* vol. 47, no. 1, pp. 2-9, 1999.

[97] E. Fishler and H. Messer, "Multiple Source Direction Finding with an Array of M Sensors Using Two Receivers," In *Proc. IEEE Signal Processing Workshop on Statistical Signal and Array Processing,* pp. 86-89, Pennsylvania, August 14-16, 2000

[98] Moon-Sik Lee, Vladimir Katkovnik, Yong-Hoon Kim, "System Modeling and Signal Processing for a Switch Antenna Array Radar," In *Proc. IEEE Transactions on Signal Processing,* vol. 52, no. 6, pp. 1513-1523, 2004

[99] J. Qu, J. Zhang, and Z. You, "Direction Finding Based on Single Receiving Channel," In *Proc. 8th International Conference on Signal Processing,* vol. 1, Beijing, China, 16-20 Nov. 2006.

[100] Van Yem Vu and Nguyen Huu Thanh, "Single Channel All Digital Direction Finding System," In *Proc. 6th International Symposium on Wireless Communication Systems (ISWCS 2009),* Siena, Italy, September 7 - 10 2009, pp. 696 - 699.

[101] Hao Xin, and Jun Ding, "An Improved Two-Antenna Direction of Arrival (DOA) Technique Inspired by Human Ears," In *Proc. Antennas and Propagation Society International Symposium,* San Diego, California, USA, 5-11 July 2008, pp. 1-4.

[102] Marcello Ascione, Aniello Buonanno, Michele D'Urso, Leopoldo Angrisani, and R. Schiano Lo Moriello, "A New Measurement Method Based on Music Algorithm for Through-the-Wall Detection of Life Signs," In *Proc. IEEE Transactions on Instrumentation and Measurement,* vol. 62, no. 1, pp. 13-25, 2013.

[103] Benjamin Friedlander, 'A Sensitivity Analysis of the MUSIC Algorithm," In *IEEE Transactions on Acoustics, Speech and Signal Processing,* vol. 38, no. 10, pp. 1740-1751, 1990.

[104] David Asztely, and Bjorn Ottersten, "The Effects of Local Scattering on Direction of Arrival Estimation with MUSIC", In *IEEE Transactions on Signal Processing,* vol. 47, no. 12, pp. 3220-3234, 1999.

[105] J. E. Evans, J. R. Johnson, and D. F. Sunt, "High Resolution Angular Spectrum Estimation Techniques for Terrain Scattering Analysis and Angle of Arrival Estimation," In *Proc. Proc. 1st ASSP Workshop Spectral Estimation,* pp. 134-139., Hamilton, Ontario, Canada, 1981.

[106] M. Zoltowski, and F. Haber, "A Vector Space Approach to Direction Finding in a Coherent Multipath Environment", In *IEEE Trans. on Antennas and Propagation,* vol.34, no. 9, pp. 1069-1079, 1986.

[107] Tie-Jun Shan, Mati Wax, and Thomas Kailat, "On Spatial Smoothing for Direction-of-arrival Estimation of Coherent Signals," In *Proc. IEEE Trans. on Acoust., Speech, Signal Processing,* vol. 33, no.4, pp. 806-811, 1985.

[108] A. Gorcin, H. Celebi, K. A. Qaraqe, H. Arslan, "An Autoregressive Approach for Spectrum Occupancy Modeling and Prediction based on Synchronous Measurements," In *Proc. IEEE 22nd International Symposium on Personal Indoor and Mobile Radio Communications (PIMRC 2011),* Toronto, Canada, September 2011, pp. 705-709.

[109] Anritsu Co., "Guide to Spectrum Analyzers Document," 2013.

[110] [Online Available]:[www.parallax.com/]

[111] [Online Available]:[www.minicircuits.com/pdfs/ZSWA-4-30DR.pdf]

[112] [Online Available]:[www.home.agilent.com/en/pd-1000004297]

[113] F. Wang, T. Lo, J. Litva, and W. Read, "VHF Antenna Array Processing: High Accuracy Direction Finding and Performance Evaluation with Real Data", In *IEE Proceedings Radar, Sonar and Navigation,* vol. 141, no. 3, pp. 137-143, 1994.

[114] Franz A. de Leon, and J. J. S. Marciano, "Source Localization using MUSIC in a Multipath Environment," In *Proc. The IEEE 9th International Conference on Advanced Communication Technology,* vol. 2, Phoenix Park, Korea, 12-14 February 2007, pp. 1327-1329.

[115] M. Kossor, "A Doppler Radio-Direction Finder", In*Proc. American Radio Relay League,* vol. 83, p.p. 35 - 40, Qst Newington, 1999.

[116] M. Wellens, Riihijarvi, J., and P. Mahonen,"Empirical Time and Frequency Domain Models of Spectrum Use," In *Elsevier Physical Communication,* vol. 2, number 1-2, pp. 10-32, 2009

[117] C. Song, D.Chen, Q. Zhang, "Understand the Predictability of Wireless Spectrum: A Large-scale Empirical Study", In *Proc. IEEE International Conference on Communications (ICC 2010),* pp. 1-5, Cape Town, South Africa, 23 - 27 May 2010.

[118] Z. Sun, J.N. Laneman, G.J. Bradford, "Sequence Detection Algorithms for Dynamic Spectrum Access Networks", In *Proc. IEEE Symposium on New Frontiers in Dynamic Spectrum,* pp. 1-9, Singapore, 6-9 April 2010.

[119] Y. Xing, R. Chandramouli, S. Mangold, "Dynamic Spectrum Access in Open Spectrum Wireless Networks," In *IEEE Journal on Selected Areas in Communications,* vol. 24, number 3, pp. 626-637, 2006

[120] S. Geirhofer, L. Tong, B.M. Sadler, "A Measurement-based Model for Dynamic Spectrum Access in WLAN Channels," In *IEEE Military Communications Conference (MILCOM 2006),* pp. 1 - 7, Washington, DC, USA, 23-25 Oct. 2006

[121] Q. Zhao, S. Geirhofer, L. Tong, B.M. Sadler, "Opportunistic Spectrum Access via Periodic Channel Sensing," In *IEEE Transactions on Signal Processing,* vol. 56, number 2, pp. 785-796, 2008

[122] Q. Zhao, K. Liu, "Detecting, Tracking, and Exploiting Spectrum Opportunities in Unslotted Primary Systems," In *IEEE Radio and Wireless Symposium,* pp. 491 - 494, Orlando, FL, USA, 22-24 Jan. 2008

[123] M. Wellens, A. de Baynast, and P. Mahonen,"Performance of Dynamic Spectrum Access Based on Spectrum Occupancy Statistics," In *IET Communications,* vol. 2, number 6, pp. 772-782, 2008

[124] L. Stabellini, "Quantifying and Modeling Spectrum Opportunities in a Real Wireless Environment", In *Proc. IEEE Wireless Communications and Networking Conference (WCNC 2010),* pp. 1-6, Sydney, Australia, 18-21 April 2010.

109

[125] A.S. Zahmati, X. Fernando, A. Grami, "Steady-state Markov Chain Analysis for Heterogeneous Cognitive Radio Networks", In *Proc. IEEE Sarnoff Symposium,* pp. 1-5, Princeton, NJ, USA, Nov. 12-14 April 2010.

[126] A. Alaya-Feki, B. Sayrac, E. Moulines, A. Le Cornec, "Opportunistic Spectrum Access: Online Search of Optimality", In *Proc. IEEE Global Telecommunications Conference (GLOBECOM 2008),* pp. 1-5, New Orleans, LO, USA, Nov. 30 2008-Dec. 4 2008.

[127] L. Yang, L. Cao,H. Zheng, "Proactive Channel Access in Dynamic Spectrum Networks," In *Elsevier Physical Communication,* vol. 1, number 2, pp. 103-111, 2008

[128] C. Ghosh, S. Pagadarai, D. Agrawal, A. Wyglinski, "A Framework for Statistical Wireless Spectrum Occupancy Modeling," In *IEEE Transactions on Wireless Communications,* vol. 9, number 1, pp. 38-44, 2010

[129] V.K. Tumuluru, P. Wang, D. Niyato, "A Neural Network Based Spectrum Prediction Scheme for Cognitive Radio", In *Proc. IEEE International Conference on Communications (ICC 2010),* pp. 1-5, Cape Town, South Africa, 23 - 27 May 2010.

[130] P.F. Marshall, "Closed-form Analysis of Spectrum Characteristics for Cognitive Radio Performance Analysis," In *IEEE 3rd Symposium on New Frontiers in Dynamic Spectrum Access Networks (DySPAN 2008),* pp. 1 - 12, Chicago, IL, USA, 14-17 Oct. 2008

[131] C.T. Chou, S. Shankar, H. Kim, K.G. Shin, "What and How Much to Gain by Spectrum Agility?," In *IEEE Journal on Selected Areas in Communications,* vol. 25, number 3, pp. 576-588, 2007

[132] C. Ghosh, S. Roy, M.B. Rao, D.P. Agrawal, "Spectrum Occupancy Validation and Modeling Using Real-time Measurements", In *Proc. Proceedings of the 2010 ACM Workshop on Cognitive Radio Networks (CoRoNet '10),* pp. 25-30, Chicago, Illinois, USA, 20 September 2010.

[133] R.J. Matheson, "Strategies for Spectrum Usage Measurements", In *Proc. IEEE International Symposium on Electromagnetic Compatibility,* vol.5, pp. 235-241, Seattle, WA , USA, 02 - 04 Aug 1988.

[134] S. Pagadarai, A.M. Wyglinski, "A Linear Mixed-effects Model of Wireless Spectrum Occupancy," In *EURASIP Journal on Wireless Communications and Networking,* vol. 2010, Article ID 203178, 7 pages, 2010. doi:10.1155/2010/203178

[135] S. Yin, D. Chen, Q. Zhang, M. Liu, S. Li, "Mining Spectrum Usage Data: a Large-Scale Spectrum Measurement Study," In *IEEE Transactions on Mobile Computing,* vol. 99, pp. 1-14, 2011

[136] Z. Wen, T. Luo, W. Xiang, S. Majhi, Y. Ma, "Autoregressive Spectrum Hole Prediction Model for Cognitive Radio Systems", In *Proc. IEEE International Conference on Communications Workshops (ICC Workshops 2008),* pp. 154-157, Beijing, China, 19-23 May 2008

[137] S. Kaneko, S. Nomoto, T. Ueda, S. Nomura, K. Takeuchi, "Predicting Radio Resource Availability in Cognitive Radio-an Experimental Examination," In *IEEE 3rd International Conference on Cognitive Radio Oriented Wireless Networks and Communications, (CrownCom 2008),* pp. 1 - 6, Singapore, 15-17 May 2008

[138] K. A. Qaraqe, ,H. Celebi, A. Gorcin, A. El-Saigh, H. Arslan, and M.-S. Alouini, "Empirical Results for Wideband Multidimensional Spectrum Usage," In *IEEE 20th International Symposium on Personal, Indoor and Mobile Radio Communications(PIMRC 2009),* pp. 1262 - 1266, Tokyo, Japan, 13-16 Sept. 2009.

[139] S.Yarkan, H. Arslan,"Binary Time Series Approach to Spectrum Prediction for Cognitive Radio", In*Proc. IEEE 66th Vehicular Technology Conference (VTC-2007 Fall),* vol.1, Baltimore, MD, U.S.A., 30 Sept. - 3 Oct. 2007, pp. 1563-1567

[140] V. Blaschke, H. Jaekel, T. Renk, C. Kloeck, F.K. Jondral, "Occupation Measurements Supporting Dynamic Spectrum Allocation for Cognitive Radio Design," In *IEEE 2nd International Conference on Cognitive Radio Oriented Wireless Networks and Communications, (CrownCom 2007),* pp. 50 - 57, Orlando, FL, USA, 1-3 Aug. 2007

[141] B. Kedem and K. Fokianos, *Regression Models for Time Series Analysis*, 1st ed., ser. Wiley Series in Probability and Statistics. John Wiley And Sons, Inc., 2002.

[142] H. Lütkepohl, *Introduction to Multiple Time Series Analysis*, 2nd ed. Springer–Verlag, 1993.

[143] T. Adali, "Why a nonlinear solution for a linear problem?" in *Proceedings of the IEEE Signal Processing Society Workshop, Neural Networks for Signal Processing IX*, Aug. 23–25, 1999, pp. 157–165.

[144] H. Hytti, R. Takalo, and H. Ihalainen, "Tutorial on Multivariate Autoregressive Modelling," *Journal of Clinical Monitoring and Computing*, vol. 20, no. 2, pp. 101–108, 2006.

[145] "Federal Communications Commission, Tech. Rep.," In *Et docket no. 03-322. Notice of Proposed Rule Making and Order,* Washington, DC , December 2003

[146] D. Cabric, S. M. Mishra, and R. W. Brodersen, "Implementation issues in spectrum sensing for cognitive radios," In *Proc. IEEE Asilomar Conf. on Signals, Syst., Computers, vol. 1,* pp. 772-776, Pacific Grove, CA, U.S.A., Nov. 2004

[147] H.S. Chen, W. Gao, D.G. Daut, "Signature Based Spectrum Sensing Algorithms for IEEE 802.22 WRAN," In *Proc. IEEE International Conference on Communications (ICC'07),* pp. 6487-6492, Glasgow, U.K., 24 - 28 June 2007

[148] S.J. Shellhammer, "Spectrum Sensing in IEEE 802.22," In *Proc. IAPR Wksp. Cognitive Info. Processing,* June 2008

[149] A.I. Perez-Neira, M.A. Lagunas, M.A. Rojas, P. Stoica, "Correlation Matching Approach for Spectrum Sensing in Open Spectrum Communications," In *IEEE Transactions on Signal Processing,* vol. 57, number 12, pp. 4823-4836, 2009

[150] J. Font-Segura, G. Vazquez, J. Riba, "Compressed Correlation-Matching for Spectrum Sensing in Sparse Wideband Regimes," In *Proc. IEEE International Conference on Communications (ICC'11),* pp. 1-5, 5-9 June 2011

[151] G. Vazquez-Vilar, R. Lopez-Valcarce, J. Sala, "Multiantenna Spectrum Sensing Exploiting Spectral a priori," In *IEEE Transactions on Wireless Communications,* vol. 10, number 11, pp. 4345-4355, 2011

[152] Eva Lagunas, Montse Najar, "Sparse Correlation Matching-based Spectrum Sensing for Open Spectrum Communications," In *EURASIP Journal on Advances in Signal Processing,* vol. 2012, number 1, pp. 31, 2012

[153] Z. Quan, S.J. Shellhammer, W. Zhang, A.H. Sayed, "Spectrum Sensing by Cognitive Radios at Very Low SNR," In *Proc. IEEE Global Telecommunications Conference (GLOBECOM 2009),* pp. 1-6, Honolulu, HI, U.S.A., Nov. 30 - Dec. 4 2009

[154] H. Wang, W. Jouini, R. Hachemani, J. Palicot, LS Cardoso, M. Debbah, "Blind Bandwidth Shape Recognition for Standard Identification Using USRP Platforms and SDR4all Tools," In *Proc. Sixth Advanced International Conference on Telecommunications (AICT 2010),* pp. 147-152, Barcelona, Spain, 9 - 15 May 2010.

[155] A. Gorcin, H. Arslan,"Template Matching for Signal Identification in Cognitive Radio Systems", In*Proc. IEEE Military Communications Conference (MILCOM 2012),* Orlando, USA, 29 October 1 November 2012.

111

[156] R. O. Duda, P. E. Hart, David G. Stork, "Pattern Classification," Wiley-Interscience; 2nd edition, November 9, 2000.

[157] W. K. Pratt, "Digital Image Processing," New York: Wiley, February 9, 2007.

[158] A. K. Jain, "Fundamental of Digital Image Processing," Englewood Cliffs, New Jersey: Prentice-Hall, 1989

[159] D. H. Friedman, "Detection of Signals by Template Matching," Baltimore: Johns Hopkins Press, 1969

[160] H. V. Poor, "An introduction to signal detection and estimation," 2nd ed., Springer, 1994.

[161] G.J. Vanderbrug, A. Rosenfeld, "Two Stage Template Matching," In *IEEE Transactions on Computers 26,* pp. 384393, 1977.

[162] A. Rosenfeld, G.J. Vanderbrug "Coarse Fine Template Matching," In *IEEE Transactions on Systems, Man and Cybernetics 7,*pp. 104-107, 1977.

[163] Arif Mahmood, and Sohaib Khan, "Correlation-coefficient-based Fast Template Matching Through Partial Elimination," In *IEEE Transactions on Image Processing,* vol. 21, no. 4, pp. 2099-2108, 2012

[164] Jonathan Weber, and Salvatore Tabbone, "Symbol Spotting for Technical Documents: An Efficient Template-Matching Approach," In *Proc. IEEE 21st International Conference on Pattern Recognition (ICPR),* pp. 669-672, Tsukuba, Ibaraki, Japan, 11-15 Nov. 2012.

[165] 3GPP TS 25.101 V9.2.0, "Technical Specification Group Radio Access Network; User Equipment (UE) radio transmission and reception (FDD)," December 2009

[166] 3GPP2 C.S0002-E V1.0, "Physical Layer Standard for cdma2000 Spread Spectrum Systems," September 2009

APPENDICES

113

Appendix A : Covariance Estimates for Fourth Order Cumulants of OFDM Signals

The asymptotic covariances of sample cumulants can be estimated based on the straightforward asymptotic covariance expression for the cumulant orders up to $k = 3$ [68]. However, the covariance estimation becomes a complex procedure for $k > 3$ due to the combinations of products of the second and fourth order moments. The estimate of the 4-th order cumulants can be written in terms of moments as [63]

$$\hat{c}_{4y}(i_1, i_2, i_3) = \hat{m}_{4y}(i_1, i_2, i_3) - \hat{m}_{2y}(i_1)\hat{m}_{2y}(i_2 - i_3)$$
$$- \hat{m}_{2y}(i_2)\hat{m}_{2y}(i_3 - i_1) - \hat{m}_{2y}(i_3)\hat{m}_{2y}(i_1 - i_2) \quad (A.1)$$

where

$$\hat{m}_{ky}(i_k) \triangleq \frac{1}{N} \sum_{t=0}^{T-1} y(t)y(t + i_1)y(t + i_2)\dots y(t + i_{k-1}), \quad (A.2)$$

and $i_k \triangleq (i_1, i_2, \dots, i_{k-1})$. The computation of each entry $cov\{\hat{c}_{4y}(i_1, i_2, i_3), \hat{c}_{4y}(j_1, j_2, j_3)\}$ of the Σ_c becomes a computationally consuming process under I_4^N. However the computation of the diagonal entries defined by I_4^M is sufficient for OFDM signals. If $\lambda = i_1 = i_2, \beta = j_1 = j_2, i_3 = j_3 = 0$ and $0 \le \beta \le M$, the open for of covariance of $\hat{c}_{4y}$ can be given in three parts and the first part is consists of covariances of two fourth order moments as

$$c_1 = cov\{\hat{m}_{4y}(\lambda, \lambda, 0), \hat{m}_{4y}(\beta, \beta, 0)\}, \quad (A.3a)$$

and the second part will be consist of various combinations of covariances of fourth order and second order moments. The open expression of these terms are given by

$$c_2 = cov\{\hat{m}_{4y}(\lambda, \lambda, 0), \hat{m}_{2y}(\beta)\hat{m}_{2y}(\beta)\} \quad (A.3b1)$$

$$+ cov\{\hat{m}_{4y}(\lambda, \lambda, 0), \hat{m}_{2y}(\beta)\hat{m}_{2y}(-\beta)\} \quad (A.3b2)$$

$$+ cov\{\hat{m}_{4y}(\lambda, \lambda, 0), \hat{m}_{2y}(0)\hat{m}_{2y}(0)\} \quad (A.3b3)$$

$$+ cov\{\hat{m}_{4y}(\beta, \beta, 0), \hat{m}_{2y}(\lambda)\hat{m}_{2y}(\lambda)\} \quad (A.3b4)$$

$$+ cov\{\hat{m}_{4y}(\beta, \beta, 0), \hat{m}_{2y}(\lambda)\hat{m}_{2y}(-\lambda)\} \quad (A.3b5)$$

$$+ cov\{\hat{m}_{4y}(\beta, \beta, 0), \hat{m}_{2y}(0)\hat{m}_{2y}(0)\}, \quad (A.3b6)$$

114

and finally the third term will be constituted by the covariances of all possible second order moments of the estimated cumulants as

$$c_3 = cov\{\hat{m}_{2y}(\lambda)\hat{m}_{2y}(\lambda), \hat{m}_{2y}(\beta)\hat{m}_{2y}(\beta)\} \tag{A.3c1}$$

$$+ cov\{\hat{m}_{2y}(\lambda)\hat{m}_{2y}(\lambda), \hat{m}_{2y}(\beta)\hat{m}_{2y}(-\beta)\} \tag{A.3c2}$$

$$+ cov\{\hat{m}_{2y}(\lambda)\hat{m}_{2y}(\lambda), \hat{m}_{2y}(0)\hat{m}_{2y}(0)\} \tag{A.3c3}$$

$$+ cov\{\hat{m}_{2y}(\lambda)\hat{m}_{2y}(-\lambda), \hat{m}_{2y}(\beta)\hat{m}_{2y}(\beta)\} \tag{A.3c4}$$

$$+ cov\{\hat{m}_{2y}(\lambda)\hat{m}_{2y}(-\lambda), \hat{m}_{2y}(\beta)\hat{m}_{2y}(-\beta)\} \tag{A.3c5}$$

$$+ cov\{\hat{m}_{2y}(\lambda)\hat{m}_{2y}(-\lambda), \hat{m}_{2y}(0)\hat{m}_{2y}(0)\} \tag{A.3c6}$$

$$+ cov\{\hat{m}_{2y}(0)\hat{m}_{2y}(0), \hat{m}_{2y}(\beta)\hat{m}_{2y}(\beta)\} \tag{A.3c7}$$

$$+ cov\{\hat{m}_{2y}(0)\hat{m}_{2y}(0), \hat{m}_{2y}(\beta)\hat{m}_{2y}(-\beta)\} \tag{A.3c8}$$

$$+ cov\{\hat{m}_{2y}(0)\hat{m}_{2y}(0), \hat{m}_{2y}(0)\hat{m}_{2y}(0)\}. \tag{A.3c9}$$

Therefore the covariance of $\hat{c}_{4y}$ is given by

$$cov\{\hat{c}_{4y}(\lambda, \lambda, 0), \hat{c}_{4y}(\beta, \beta, 0)\} = c_1 + c_2 + c_3. \tag{A.3d}$$

The derivation of these three groups can be based on the computable sample approximations of the asymptotic covariances established in [71] for the mixing discrete-time stationary processes such as defined in (2.9). The covariance of the moments is defined as

$$\lim_{N \to \infty} Ncov\{\hat{m}_{ky}(i_k), \hat{m}_{ky}(j_l)\} = \sum_{-\infty}^{\infty} cov\{y(0)y(i_1)\dots y(i_{k-1}),$$

$$y(\tau)y(\tau + j_1)\dots y(\tau + j_{l-1})\}. \tag{A.4}$$

115

Appendix A (Continued)

Following $cov\{ab\} = E\{ab\} - E\{a\}E\{b\}$ based on (A.4) and replacing the moments with their estimates as defined in (A.2), (A.3a) can be written as

$$c_1 = cov\{\hat{m}_{4y}(\lambda, \lambda, 0), \hat{m}_{4y}(\beta, \beta, 0)\}$$

$$\approx \frac{1}{N} \sum_{\tau=-K_N}^{K_N} [\hat{m}_{8y}(\lambda, \lambda, 0, \tau, \tau + \beta, \tau + \beta, \tau) - \hat{m}_{4y}(\lambda, \lambda, 0)\hat{m}_{4y}(\beta, \beta, 0)] \tag{A.5}$$

Note that limits of the sum in the (A.5) should satisfy $K_N \to \infty$ as $N \to \infty$ and $K_N/N \to 0$ as $N \to \infty$. In practice, for OFDM systems K_N can be selected as $K_N > \tau$ where $\hat{c}_{2x_m}(\tau) \approx 0$ [63]. The second group of sample estimates include the covariances of the multiplications of the moment terms and theorem 2.3.2 in [66] expresses such terms in the form of

$$cov\{a, bc\} = cov\{b\}cov\{a, c\} + cov\{c\}cov\{a, b\} \tag{A.6}$$

and (A.3a) can be written as

$$cov\{\hat{m}_{4y}(\lambda, \lambda, 0), \hat{m}_{2y}(\beta)\hat{m}_{2y}(\beta)\}$$

$$= E\{\hat{m}_{2y}(\beta)\}cov\{\hat{m}_{4y}(\lambda, \lambda, 0), \hat{m}_{2y}(\beta)\}$$

$$+ E\{\hat{m}_{2y}(\beta)\}cov\{\hat{m}_{4y}(\lambda, \lambda, 0), \hat{m}_{2y}(\beta)\}$$

$$= 2\Big[E\{\hat{m}_{2y}(\beta)\}cov\{\hat{m}_{4y}(\lambda, \lambda, 0), \hat{m}_{2y}(\beta)\}\Big]. \tag{A.7}$$

Depending on the estimator given in (A.2) and covariance definition in (A.4), similar to (A.5), the covariances in (A.7) can be expressed in terms of moments as

$$cov\{\hat{m}_{4y}(\lambda, \lambda, 0), \hat{m}_{2y}(\beta)\hat{m}_{2y}(\beta)\}$$

$$= 2[\hat{m}_{2y}(\beta) \sum_{\tau=-K_N}^{K_N} [\hat{m}_{6y}(\lambda, \lambda, 0, \tau, \tau + \beta) - \hat{m}_{4y}(\lambda, \lambda, 0)\hat{m}_{2y}(\beta)]]. \tag{A.8}$$

116

When the same derivations are applied to the rest of the equations and after some simplifications (A.3a - A.3b6) can be written as

$$c_2 = 2\Big(\Omega(2\hat{m}_{2y}(\beta) + \hat{m}_{2y}(-\beta)) + \Phi\hat{m}_{2y}(\beta) + 2\Psi\hat{m}_{2y}(0)\Big), \tag{A.9}$$

where

$$\Omega = \frac{1}{N} \sum_{\tau=-K_N}^{K_N} [\hat{m}_{6y}(\lambda, \lambda, 0, \tau, \tau + \beta) - \hat{m}_{4y}(\lambda, \lambda, 0)\hat{m}_{2y}(\beta)], \tag{A.10}$$

$$\Phi = \frac{1}{N} \sum_{\tau=-K_N}^{K_N} [\hat{m}_{6y}(\lambda, \lambda, 0, \tau, \tau - \beta) - \hat{m}_{4y}(\lambda, \lambda, 0)\hat{m}_{2y}(-\beta)], \tag{A.11}$$

and

$$\Psi = \frac{1}{N} \sum_{\tau=-K_N}^{K_N} [\hat{m}_{6y}(\lambda, \lambda, 0, \tau, \tau) - \hat{m}_{4y}(\lambda, \lambda, 0)\hat{m}_{2y}(0)]. \tag{A.12}$$

Note that the I_4^M leads to symmetric Σ_c therefore for each Σ_c entry not all six terms of second groups should be processed, estimation of the first half would be sufficient and the following terms will be replicated as indicated in (A.9). Similar to the second group, covariances of multiplications of the estimate moments which consist the third group are in the form of $cov\{ab, cd\}$. According to eqn.(2.3.8) in [66] these terms can be expressed as

$$cov\{ab, cd\} = cov\{a, c\}cov\{b, d\} + cov\{a, d\}cov\{b, c\}, \tag{A.13}$$

then the (A.3b6) is given by

$$\begin{aligned}
cov\{\hat{m}_{2y}(\lambda)\hat{m}_{2y}(\lambda), \hat{m}_{2y}(\beta)\hat{m}_{2y}(\beta)\} \\
= cov\{\hat{m}_{2y}(\lambda), \hat{m}_{2y}(\beta)\}cov\{\hat{m}_{2y}(\lambda), \hat{m}_{2y}(\beta)\} \\
+ cov\{\hat{m}_{2y}(\lambda), \hat{m}_{2y}(\beta)\}cov\{\hat{m}_{2y}(\lambda), \hat{m}_{2y}(\beta)\}.
\end{aligned} \tag{A.14}$$

Appendix A (Continued)

After applying the conversion defined in (A.13) and rearranging all nine terms, (A.3b6 - A.3c9) can be written as

$$
\begin{aligned}
c_3 =&\, 2\Gamma^2 + 2\Gamma\Lambda + 2\Theta^2 + 2\Gamma cov\{\hat{m}_{2y}(\lambda), \hat{m}_{2y}(-\beta)\} \\
&+ \Delta(\Gamma + \Lambda) + 2\Theta cov\{\hat{m}_{2y}(-\lambda), \hat{m}_{2y}(0)\} + 2\Upsilon^2 \\
&+ 2\Upsilon cov\{\hat{m}_{2y}(0), \hat{m}_{2y}(-\beta)\} + 2[cov\{\hat{m}_{2y}(0), \hat{m}_{2y}(0)\}]^2,
\end{aligned} \tag{A.15}
$$

where

$$
\Gamma = \frac{1}{N} \sum_{\tau=-K_N}^{K_N} [\hat{m}_{4y}(\lambda, \tau, \tau + \beta) - \hat{m}_{2y}(\lambda)\hat{m}_{2y}(\beta)], \tag{A.16}
$$

$$
\Lambda = \frac{1}{N} \sum_{\tau=-K_N}^{K_N} [\hat{m}_{4y}(\lambda, \tau, \tau - \beta) - \hat{m}_{2y}(\lambda)\hat{m}_{2y}(-\beta)], \tag{A.17}
$$

$$
\Theta = \frac{1}{N} \sum_{\tau=-K_N}^{K_N} [\hat{m}_{4y}(\lambda, \tau, \tau) - \hat{m}_{2y}(\lambda)\hat{m}_{2y}(0)], \tag{A.18}
$$

$$
\Delta = \frac{1}{N} \sum_{\tau=-K_N}^{K_N} [\hat{m}_{4y}(-\lambda, \tau, \tau - \beta) - \hat{m}_{2y}(-\lambda)\hat{m}_{2y}(-\beta)], \tag{A.19}
$$

$$
\Upsilon = \frac{1}{N} \sum_{\tau=-K_N}^{K_N} [\hat{m}_{4y}(\lambda, \tau, \tau + \beta) - \hat{m}_{2y}(\lambda)\hat{m}_{2y}(\beta)], \tag{A.20}
$$

and

$$
\begin{aligned}
&cov\{\hat{m}_{2y}(-\lambda), \hat{m}_{2y}(\beta)\} \\
&= \frac{1}{N} \sum_{\tau=-K_N}^{K_N} [\hat{m}_{4y}(-\lambda, \tau, \tau + \beta) - \hat{m}_{2y}(-\lambda)\hat{m}_{2y}(\beta)],
\end{aligned} \tag{A.21}
$$

$$
cov\{\hat{m}_{2y}(-\lambda), \hat{m}_{2y}(0)\} = \frac{1}{N} \sum_{\tau=-K_N}^{K_N} [\hat{m}_{4y}(-\lambda, \tau, \tau) - \hat{m}_{2y}(-\lambda)\hat{m}_{2y}(0)], \tag{A.22}
$$

$$
cov\{\hat{m}_{2y}(0), \hat{m}_{2y}(-\beta)\} = \frac{1}{N} \sum_{\tau=-K_N}^{K_N} [\hat{m}_{4y}(0, \tau, \tau - \beta) - \hat{m}_{2y}(0)\hat{m}_{2y}(-\beta)], \tag{A.23}
$$

118

Appendix A (Continued)

$$cov\{\hat{m}_{2y}(0), \hat{m}_{2y}(0)\} = \frac{1}{N} \sum_{\tau=-K_N}^{K_N} [\hat{m}_{4y}(0, \tau, \tau) - \hat{m}_{2y}(0)\hat{m}_{2y}(0)]. \qquad (A.24)$$

Each entry of Σ_c now can be computed as the sum of (A.5), (A.9), and (A.15) under I_4^M.

119

Appendix B : Copyright Notice for Chapter 2

Appendix C : Copyright Notice for Chapter 4

www.manaraa.com

Appendix D : Copyright Notice for Chapter 5

Appendix E : Copyright Notice for Chapter 6 - 1

Appendix F : Copyright Notice for Chapter 6 - 2

Rightslink® by Copyright Clearance Center

RightsLink® — Copyright Clearance Center

https://s100.copyright.com/AppDispatchServlet#formTop[7/9/2013 1:44:18 PM]

124

www.manaraa.com

Appendix G : Copyright Notice for Chapter 6 - 3

https://s100.copyright.com/AppDispatchServlet#formTop[7/9/2013 1:43:34 PM]

ABOUT THE AUTHOR

Ali Görçin received B.Sc. degree from Istanbul Technical University (ITU) Electronics and Telecommunications Engineering Program and M.Sc. degree from the Information Technologies at Institute of Science and Technology of ITU while he was also working as a researcher at Turkish Science Foundation (Tübitak). His research interests are signal identification and parameter estimation for dynamic spectrum access for intelligent communications systems, statistical modeling of communications environment for cognitive radios, wireless signal direction of arrival estimation, and public safety cognitive radios.